TÉCNICO LISBOA

Evaluation of Train Communications Interference-Free Regions along Rail Tracks

Nuno Henrique Vicente da Silva

Thesis to obtain the Master of Science Degree in

Electrical and Computer Engineering

Supervisor: Prof. Luís Manuel De Jesus Sousa Correia

Examination Committee

Chairperson: Prof. José Eduardo Charters Ribeiro da Cunha Sanguino

Supervisor: Prof. Luís Manuel De Jesus Sousa Correia

Members of Committee: Prof. António José Castelo Branco Rodrigues

: Eng. Fernando Manuel Lopes Santana

October 2020

I declare that this document is an original work of my own authorship and that it fulfils all the requirements of the Code of Conduct and Good Practices of the *Universidade de Lisboa*.

To my loved ones

Acknowledgements

First of all, I would like to express my sincere gratitude to my thesis supervisor Prof. Luis M. Correia for allowing me to develop this work under his supervision and for giving me the opportunity to develop it in collaboration with a multinational company. It was a pleasure to work with such an amazing professor. The meetings that we had every single week, where valuable advice was given to me, highly contributed to the final result of this work and motivated me to do each time better and better. Also, the way of thinking of Prof. Luis M. Correia made me clearer about the critical mentality an engineer must have and will certainly be of value throughout my professional career. Thank you professor.

To Thales, namely to Eng. Fernando Santana and Eng. Nuno Frigolet, for their valuable insights that helped me not only to understand the problem under study but also to adapt this work in such a way to answer industry's needs. Also, all the data provided by them to me were essential to add even more practical value to this work. Thank you for the opportunity.

To all GROW members, especially to my colleagues Frederico Moura and Sérgio Marinheiro that accompanied me in all the meetings that we had, for all the support, advice, and time spent together.

To my friends, who accompanied me not only during this journey but also during my entire academic life, for all the good moments spent together and for the help that always gave me to overcome the adversities.

A special thanks to Margarida Costa, my girlfriend, for understanding the endless days that I spent developing this work, for all the support throughout this long journey, and for having motivated me to keep constantly pushing forward. Thank you for always being there for me in the hardest moments.

Finally, to my family, especially to my parents, my mother, Isabel Silva, my father, Jorge Silva, for all the love, support, and for making me the person I am today. Thank you for your investment in my education that, for sure, will be of value throughout my entire life. I hope to make you proud. Also, to my grandparents for showing me that everything is possible, the limits being imposed by ourselves.

Abstract

This thesis addresses the compatibility between railway telecommunications systems (GSM-R, LTE-R, and BBRS) and other cellular and wireless external systems that use adjacent frequencies. A model to analyse this compatibility was developed and implemented in MATLAB. An interference estimation (taking three interference types into account) is performed based on the distance from the interferer's transmitter to the victim's receiver. This estimation is then used for the calculation of both the maximum communication distance, useful for a proper deployment of railway base stations / wayside access points under interference scenarios, and the capacity loss that railway telecommunications systems already deployed may be subjected to. The interference sources considered for GSM-R and LTE-R analyses are public GSM and UMTS networks. The interference sources considered for the BBRS analysis are Wi-Fi devices. The results obtained for GSM-R allow one to conclude that distances between railway base stations lower than the usual deployments may be needed when an interfering base station is deployed closer than 1.5 km from the rail track. For LTE-R, reusing the masts of the GSM-R base stations, an interfering base station deployed closer than 2.2 km from the rail track can make throughput to drop below the values that the voice service requires. For BBRS, a Wi-Fi device being used at a distance lower than 65 m from a railway wayside access point can make throughput to drop below 12 Mbps, maximum communication distances lower than 300 m being needed in these cases.

Keywords

Railway Telecommunications Systems, Cellular and Wireless Systems, Interference, Adjacent Frequencies, Deployment Distances.

Resumo

Esta tese aborda a compatibilidade entre sistemas de telecomunicações ferroviárias (GSM-R, LTE-R e BBRS) e outros sistemas celulares e sem fios externos que utilizam frequências adjacentes. Um modelo para analisar esta compatibilidade foi desenvolvido e implementado em MATLAB. Uma estimativa de interferência (levando em consideração três tipos de interferência) é realizada com base na distância do transmissor do interferente ao recetor da vítima. Esta estimativa é depois utilizada tanto para o cálculo da distância máxima de comunicação, útil para uma implantação adequada de estações base / pontos de acesso ferroviários em cenários de interferência, como para o cálculo da queda no ritmo de transmissão a que sistemas de telecomunicações ferroviárias já instalados podem estar sujeitos. As fontes de interferência consideradas para as análises do GSM-R e do LTE-R são as redes públicas de GSM e UMTS. As fontes de interferência consideradas para a análise do BBRS são dispositivos Wi-Fi. Os resultados obtidos para o GSM-R permitem concluir que distâncias entre as estações base ferroviárias mais baixas do que as implantações usuais podem ser necessárias quando uma estação base interferente está a menos de 1.5 km da via férrea. Para o LTE-R, fazendo-se o reuso dos mastros das estações base do GSM-R, uma estação base interferente instalada a menos de 2.2 km da via férrea pode fazer com que o ritmo de transmissão caia abaixo dos valores que o serviço de voz requer. Para o BBRS, um dispositivo Wi-Fi emitindo a uma distância inferior a 65 m de um ponto de acesso ferroviário pode fazer com que o ritmo de transmissão caia abaixo de 12 Mbps e distâncias máximas de comunicação inferiores a 300 m são necessárias nestes casos.

Palavras-chave

Sistemas de Telecomunicações Ferroviárias, Sistemas Celulares e Sem Fios, Interferência, Frequências Adjacentes, Distâncias de Implementação.

Table of Contents

List of Figures

List of Tables

List of Acronyms

1G	First Generation of Mobile Communications Systems
2G	Second Generation of Mobile Communications Systems
3G	Third Generation of Mobile Communications Systems
3GPP	Third Generation Partnership Project
4G	Fourth Generation of Mobile Communications Systems
5G	Fifth Generation of Mobile Communications Systems
ACI	Adjacent-channel Interference
ACLR	Adjacent Channel Leakage Ratio
ACS	Adjacent Channel Selectivity
AMC	Adaptive Modulation and Coding
AP	Access Point
ASCI	Advanced Speech Call Items
AuC	Authentication Centre
BBI	Blocking-based Interference
BBRS	Broad Band Radio System
BCC	Backup Control Centre
BPSK	Binary Phase Shift Keying
BS	Base Station
BSC	Base Station Controller
BSS	Base Station Subsystem
BTM	Balise Transmission Module
BTS	Base Transceiver Station
CBTC	Communications-based Train Control
CC	Control Centre
CCAP	Central Controller Access Point
CCI	Co-channel Interference
CCTV	Closed-circuit Television
CEPT	European Conference of Postal and Telecommunications
CS	Circuit Switch
CSD	Circuit Switched Data
CW	Continuous Wave

DL	Downlink
DMI	Driver Machine Interface
E-UTRAN	Evolved Universal Terrestrial Radio Access Network
ECC	Electronic Communications Committee
EDOR	European Train Control System Data Only Radio
EIR	Equipment Identity Register
EIRENE	European Integrated Radio Enhanced Network
EIRP	Effective Isotropic Radiated Power
eMLPP	enhanced-Multilevel Precedence and Pre-emption
EPC	Evolved Packet Core
ER-GSM	Extended Railway-GSM
ERTMS	European Rail Traffic Management System
ETCS	European Train Control System
EU	European Union
EVC	Euro Vital Computer
FA	Functional Addressing
FDD	Frequency Division Duplex
FRMCS	Future Railway Mobile Communication System
GGSN	Gateway General Packet Radio Service Support Node
GMSC	Gateway Mobile-services Switching Centre
GMSK	Gaussian Minimum Shift Keying
GPH	General Purpose Handled
GPRS	General Packet Radio Service
GSM	Global System for Mobile Communications
GSM-R	Global System for Mobile Communications-Railway
HDTV	High-definition Television
HLR	Home Location Register
HSR	High-speed Railway
HSS	Home Subscriber Service
IBI	Intermodulation-based Interference
IEEE	Institute of Electrical and Electronics Engineers
IF	Intermediate Frequency
IIP3	Input Third-order Intercept Point
IMEI	International Mobile Equipment Identity
IMP	Intermodulation Product
IMSI	International Mobile Subscriber Identity
INR	Interference-to-noise Ratio

IP	Internet Protocol
IP3	Third-order Intercept Point
IXL	Interlocking
JRU	Juridical Recording Unit
KPI	Key Performance Indicator
LdA	Location-dependent Addressing
LEU	Lineside Electronic Unit
LNA	Low Noise Amplifier
LoS	Line of Sight
LSE	Lineside Equipment
LTE	Long Term Evolution
LTE-R	Long Term Evolution-Railway
MA	Movement Authority
MCL	Minimum Coupling Loss
MCS	Modulation and Coding Scheme
MD	Mobile Device
MDC	Multiple Driver Communication
MFCN	Mobile Fixed Communication Network
MIMO	Multiple-input and Multiple-output
MME	Mobility Management Entity
MORANE	Mobile Radio for Railway Networks in Europe
MSC	Mobile-services Switching Centre
MT	Mobile Terminal
NMS	Network Management System
NSS	Network and Switching Subsystem
NR	New Radio
OBE	Onboard Equipment
OCC	Operation Control Centre
ODO	Odometer
OFDM	Orthogonal Frequency Division Multiplexing
OFDMA	Orthogonal Frequency Division Multiple Access
OIP3	Output Third-order Intercept Point
OMC	Operations and Maintenance Centre
OOBI	Out-of-band Interference
OPH	Operational Purpose Handled
OPS	Operational Purpose Shunting-handled
PCRF	Policy and Charging Resource Function

PDN-GW	Packet Data Network Gateway
PS	Packet Switch
PSTN	Public Switched Telephone Network
QAM	Quadrature Amplitude Modulation
QoS	Quality of Service
QPSK	Quadrature Phase Shift Keying
R-GSM	Railway-GSM
RB	Resource Block
RBC	Radio Block Centre
REC	Railway Emergency Call
RF	Radio Frequency
RFFE	Radio Frequency Front-end
S-GW	Serving Gateway
SC-FDMA	Single-carrier Frequency Division Multiple Access
SEM	Spectrum Emission Mask
SGSN	Serving General Packet Radio Service Support Node
SISO	Single-input and Single-output
SM	Shunting Mode
SMSC	Short Message Service Centre
SNIR	Signal-to-noise-plus-interference Ratio
SNR	Signal-to-noise Ratio
TDMA	Time Division Multiple Access
TIS	Train Integrity System
TIU	Train Interface Unit
UIC	Union Internationale des Chemins de Fer
UL	Uplink
UMTS	Universal Mobile Telecommunications System
USIM	Universal Subscribers Identity Module
VBS	Voice Broadcast Service
VGCS	Voice Group Call Service
VLR	Visitor Location Register

List of Symbols

Δf^{int}	Channel bandwidth of the interferer
Δf^{vic}	Channel bandwidth of the victim
β_{IN}	Interference-to-noise ratio
ρ_N	Signal-to-noise ratio
ρ_{NI}	Signal-to-noise-plus-interference ratio
A_{mask}	Spectrum emission mask attenuation
$A_{RFfilter}$	RF filter attenuation
A_{sel}	Selectivity attenuation
a_l	Coefficients of the low noise amplifier
c_f	Okumura-Hata model correction factor
D	Desensitisation
d	Propagation distance
d_{bp}	Breakpoint distance
$d_{free-region}$	Interference-free region distance
$d_{interference}$	Interference distance
d_{max}	Maximum communication distance
F	Noise figure
$f_{1,2}$	Frequency of the interfering tones
f_c^{int}	Centre frequency of the interferer
f_c^{vic}	Centre frequency of the victim
f_{IMP}	Frequency of the third-order intermodulation product
G_r	Receiver antenna gain
G_t^{int}	Transmitter antenna gain of the interferer
G_t^{vic}	Transmitter antenna gain of the victim
H_{mu}	Okumura-Hata model parameter
h_{bs}	Height of the base station
h_{ms}	Height of the mobile station
I	Interference power
I_{BBI}	Blocking-based interference power
I_{IBI}	Intermodulation-based interference power

I_{IMP}^{in}	Third-order intermodulation product input interference power
I_{OOBI}	Out-of-band interference power
$K_{a,b,c,d}$	Winner II model parameters
L_p^{int}	Path loss of the interfering signal
L_p^{vic}	Path loss of the desired signal
L_r	Receiver losses
L_t^{int}	Transmitter losses of the interferer
L_t^{vic}	Transmitter losses of the victim
M_I	Interference margin
M_S	System margin
N	Noise power
n_{IMP}	Number of third-order IMPs that lie within the IF passband
n_{RB}^{aloc}	Number of resource blocks allocated to the user
n_{sc}^{aloc}	Number of subcarriers allocated to the user
n_{sc}^{tot}	Number of subcarriers that compose the victim channel
n_{sc}^{tran}	Number of subcarriers being transmitted
n_{tones}	Number of equally spaced interfering tones
P_{block}	Blocking power
P_{EIRP}^{int}	Effective isotropic radiated power of the interferer
P_{EIRP}^{vic}	Effective isotropic radiated power of the victim
$P_{EIRP/tone}^{int}$	Effective isotropic radiated power per interfering tone
P_{IIP3}	Input third-order intercept point power
P_{mask}	Out-of-band emission mask power
P_r	Desired signal power
P_{req}	Required power
$P_{r\,min}$	Receiver sensitivity
P_{rtone}^{in}	Power of each received interfering tone
P_t^{int}	Transmission power of the interferer
P_t^{vic}	Transmission power of the victim
$P_{t/sc}$	Transmission power of the victim per allocated subcarriers
R_b	Throughput
r	Coding rate
U	Amplitude of the continuous waves
x_{in}	Input signal of the Taylor series
x_{out}	Output signal of the Taylor series

List of Software

Draw.io	Flowchart editor
MATLAB R2015a	Numerical computing
Microsoft Word	Text editing
Microsoft Paint	Image editing

Chapter 1

Introduction

This chapter starts by giving an overview of the historical facts, main concepts, and future perspectives related to railway telecommunications systems. Then, in the problem statement section, one introduces the problem under study and the objectives of this thesis. The structure of this thesis together with the content covered in each chapter are described at the end.

1.1 Overview

The usage of trains has been increasing over the last years motivated by various reasons, namely, to avoid road congestion, to save money, and to have the possibility to work on the go, as mentioned by many passengers. This growth in the number of passengers, in the case of the European Union (EU) countries, is presented in Figure 1.1; in addition to passenger transportation, trains are also widely used for freight transportation, which also has registered an increase in Europe [EUSE19a]. These increases in the flux of passengers and freight transportation bring the need for a highly reliable and high-performance infrastructure. A continuous reform on trains' equipment, carriages, rail tracks, stations, control and signalling systems, and railway telecommunications systems is needed to cope with this tendency.

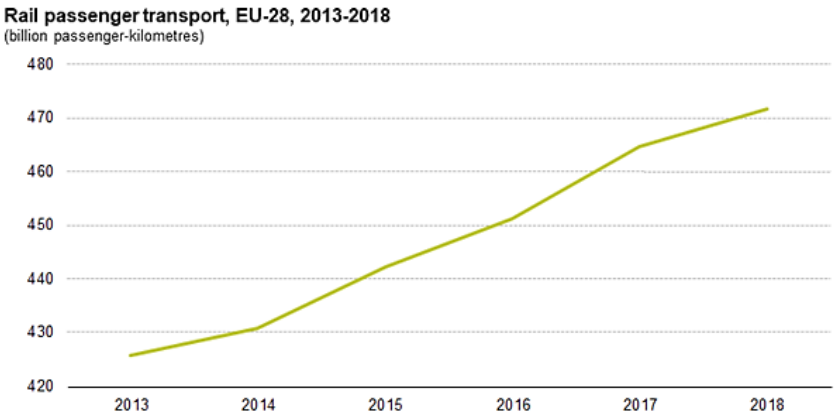

Figure 1.1 – Number of rail passengers in the EU over the last years (adapted from [EUSE19b]).

Railway telecommunications systems play a key role in maintaining a safe operation of the train itself, today being even responsible for the operation of the control and signalling systems. Continuous investment in this area has been made over the last years. The first railway telecommunications systems were based on analogue First Generation of Mobile Communications Systems (1G) technology. The limited functionality, the difficulty in finding replacement parts, the increasing price of maintenance, and the world movement to digital communication technologies determined that these systems had to be replaced. There were over 35 different railway analogue systems operating at the same time in Europe at the end of the last century [GSMR19].

The already mentioned reasons, plus the ambition of a single and cross-border interoperable system, led to the launch of a project in 1992, called European Integrated Radio Enhanced Network (EIRENE), resulting from a collaboration among the Union Internationale des Chemins de Fer (UIC), the European Commission, and European railway companies [UICG19]. The EIRENE project had the aim to specify the requirements of a telecommunications system that fulfilled the needs of the railway environment. To validate that these requirements could be implemented into telecommunications technologies, a new project was born in 1996, called Mobile Radio for Railway Networks in Europe (MORANE). The two

projects led to the creation of Global System for Mobile Communications – Railway (GSM-R), which saw its full specifications finalised in 2000 [UICG19]. GSM-R is a digital railway telecommunications system built upon the narrowband Global System for Mobile Communications (GSM) standard, a Second Generation of Mobile Communications Systems (2G) technology, providing voice and data communication to the railway environment in both Circuit Switch (CS) and Packet Switch (PS) (with General Packet Radio Service (GPRS) option) modes. GSM-R has additional functionalities compared to the public GSM, guarantees performance at train speeds up to 500 km/h with no communication losses, and provides throughputs up to 172 kbps [HAWG16].

To complement the work of these projects, and also because in Europe there were more than 15 different control and signalling systems [Ghaz14], the UIC launched another project called European Rail Traffic Management System (ERTMS), intending to harmonise all the control and signalling systems into a single one. It is possible to observe in Figure 1.2 the different planned corridors to be equipped with ERTMS in Europe. ERTMS has two components: the European Train Control System (ETCS) and the GSM-R itself [GSMR19]. ETCS is a dedicated system for the control and signalling of the train and GSM-R aims to provide the data transmission needed (via Circuit Switched Data (CSD) mode) to ETCS to operate. Other countries around the world adopted ERTMS, like China, Turkey, Saudi Arabia, Australia, Algeria, South Korea, Taiwan [ERTM19].

Figure 1.2 – The planned corridors to be equipped with ERTMS in Europe (extracted from [RGIN19]).

The adoption and implementation, by the countries in the EU, of GSM-R and ETCS, still is a gradual process. Member countries and associates that have not adopted GSM-R yet, must do it under the Control-Command Signalling Technical Specifications for Interoperability [Smit17]. As in the EU, other countries around the world launched their analogue radio replacement programmes, which are still ongoing. However, one problem arises: while, on the one hand, one is reaching a new decade and public mobile communications are making the transition from Long Term Evolution (LTE), which is a Fourth Generation of Mobile Communications Systems (4G) technology, to New Radio (NR), which is the new

Fifth Generation of Mobile Communications Systems (5G) technology, on the other hand, GSM-R is still a 2G based system, obsolete in what performance is concerned. Suppliers commit to provide GSM-R equipment only until 2030 [Smit17], hence, after this date, it will be very difficult to attend infrastructure's replacement needs and, therefore, its Quality of Service (QoS). Thus, it is time to work on a successor.

Since 2012, a UIC project known as Future Railway Mobile Communication System (FRMCS) has started to assess what is the best way forward [UICF19]. The successor must meet many requirements, such as high data rates, low latencies, and the possibility to coexist with GSM-R for a long period of time. The preference is to select an already mature system and to add specific railway features to it, hence, a solution seems to go through LTE – Railway (LTE-R), a system based on LTE.

LTE-R is an Internet Protocol (IP)-based broadband railway telecommunications system that provides voice and high-speed data transmission, and has advanced specific features dedicated to the railway environment. It aims to provide throughputs up to 100 Mbps in the Downlink (DL) and up to 50 Mbps in the Uplink (UL) without communication losses at train speeds up to 500 km/h [HAWG16]. LTE-R is not fully standardised yet, but there is already an implementation of LTE-R in a 120 km High-speed Railway (HSR) in South Korea, Figure 1.3. The implementation was performed with an eye on the Winter Olympics 2018. The adoption of LTE-R as the next main railway telecommunications system implies to jump over Universal Mobile Telecommunications System (UMTS), a Third Generation of Mobile Communications Systems (3G) technology: since LTE has a simpler and flat architecture, providing higher data rates and lower latencies, and being on the market for almost 10 years, it seems the proper choice.

Figure 1.3 – LTE-R's implementation in a HSR in South Korea (extracted from [SAMS19]).

In addition to GSM-R and LTE-R, based on mobile cellular communications technologies, other railway telecommunications systems based on Wi-Fi are also widely used nowadays for railway communications, Broad Band Radio System (BBRS) being one of these systems, deployed by Thales, based on IP data packet transmission. It offers throughputs between 70 Mbps and 125 Mbps and supports train speeds of up to 250 km/h, serving the needs of systems asking for real-time information (mainly non-critical safety applications). According to [BBRS17], the deployment of this system is mainly outside Europe, with implementations in India, Saudi Arabia, Canada, and Qatar.

1.2 Problem Statement

One should be aware that the frequency spectrum is scarce, and so, each telecommunications system is assigned with frequency bands adjacent to each other or, even, with frequency bands that are shared by other systems. The three introduced railway telecommunications systems (GSM-R, LTE-R, and BBRS) may be subject to interference problems because their frequency bands are adjacent to bands used by telecommunications systems external to the railway usage. It is possible to see in Figure 1.4 a representation of these portions of the radio spectrum and the sources likely to cause interference. If these external telecommunications systems are deployed too close to the rail tracks, they can interfere with the operation of the railway telecommunications systems.

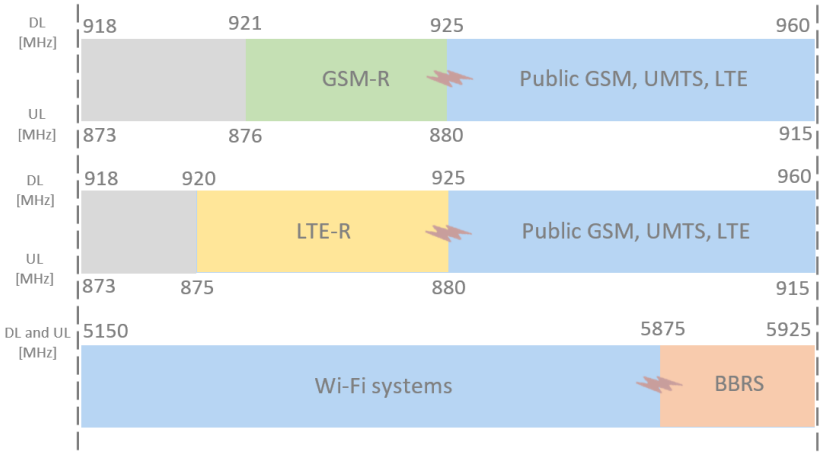

Figure 1.4 – Frequency bands commonly used by the three railway communications systems.

In Europe, the frequency band assigned to GSM-R is adjacent, in both UL and DL, to the E-GSM-900 one, which is used by Mobile Fixed Communication Networks (MFCNs) such as public GSM, UMTS, and LTE [CEPT19a], Figure 1.4, and many interference cases have been reported [CEPT11]. The frequency band of LTE-R is not standardised yet, but it is expected that LTE-R will coexist with GSM-R in the same frequency band in a first stage of the transition and, then, it will end up using the whole band used today by GSM-R when the transition is completed [ETSI19], Figure 1.4. Therefore, it is necessary to study the susceptibility of LTE-R to interference from the MFCNs working in the E-GSM-900 band as well. BBRS, contrary to GSM-R and LTE-R, is mainly deployed outside Europe (also there is some BBRS projects in Europe) and, depending on its use and country, the frequency bands can vary. BBRS can make use of both licensed and unlicensed bands [BBRS17]. The case of adjacent interference to the licensed band of BBRS is represented in Figure 1.4, but the adjacent interference case can be also applied when BBRS is using the 5 GHz unlicensed band, worldwide used by Wi-Fi.

According to [CEPT11], the reported cases of interference to GSM-R are mainly in its DL operation, that is, the emissions from the public Base Stations (BSs) of the MFCNs interfere with the reception of the desired signal on GSM-R Mobile Terminals (MTs). For LTE-R, the DL interference scenario is also expected to be the most demanding one. BBRS uses the same band for both UL and DL, and Access Points (APs) are used on both ends, so the interference to both its DL and UL operation needs to be considered; Figure 1.5 shows a physical representation of the interference problems.

The objective of this thesis is to analyse the compatibility between the three mentioned railway telecommunications systems (GSM-R, LTE-R, and BBRS) and other telecommunications systems external to railway usage that use adjacent frequencies. The majority of the works performed in this matter cover only one interference type and focus only on interference having the handover point of the railway telecommunications systems as the reference one (which is the worst-case scenario, but does not allow to cover the cases where an interfering source is deployed close to other points of the rail tracks).

In this work, one develops a model for interference estimation (taking three interference types into account) and evaluation of interference-free regions along rail tracks in various deployment scenarios. The interference estimation is then used for both a proper deployment of railway BSs / wayside APs under interference scenarios (deployment guidelines) and to analyse the capacity loss that already deployed railway telecommunications systems may be subject to.

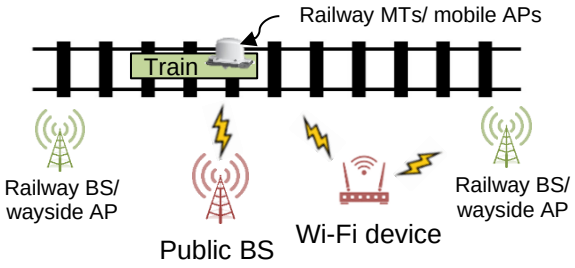

Figure 1.5 – Physical representation of the interference problems.

1.3 Contents

This thesis is composed of 5 chapters, followed by 9 annexes where additional data is provided.

Chapter 1, the present one, describes the historical evolution of railway telecommunications systems, presenting some important milestones, and giving future perspectives. The problem under study and the objective of this thesis are explained. The structure of the whole thesis is described. Chapter 2 gives a detailed description of GSM-R, LTE-R, and BBRS, presenting their network architectures and radio interfaces. The services and applications that these railway telecommunications systems aim to provide are presented as well as their requirements and the usual scenarios where railway communications can take place. Performance parameters are overviewed and the interference types that the three railway telecommunications systems may be subject to are explained. The state of the art is also presented. Chapter 3 presents the model developed to deal with the problem under study, explaining its inputs, outputs, and all the equations that compose it. The implementation of the various equations in MATLAB is explained. The assessment of the model is performed by comparison with results from other authors. Chapter 4 describes the scenarios chosen for the interference analysis, the obtained results are presented and their analysis is performed. Chapter 5 presents the conclusions of this work and the main points that may be analysed in future works to complement this thesis.

Chapter 2

Fundamental Concepts and State of the Art

This chapter starts by giving an overview of the network architectures and radio interfaces of GSM-R, LTE-R, and BBRS. Then, the applications and services of railway communications, their requirements, and some scenarios where they can take place are presented. Performance parameters are stated, and a deeper analysis of the interference parameter is performed where the interference types are introduced. Some works from other authors are mentioned in the state of the art.

2.1 GSM-R

The current section describes the network architecture of GSM-R, its useful characteristics for railway communications compared to public GSM and its radio interface.

2.1.1 Network Architecture

GSM-R has basically the same network architecture as public GSM, which is represented in Figure 2.1. Five different main categories can be defined: the MTs, the Base Station Subsystem (BSS), the Network and Switching Subsystem (NSS), the Operations and Maintenance Centre (OMC), and the public networks.

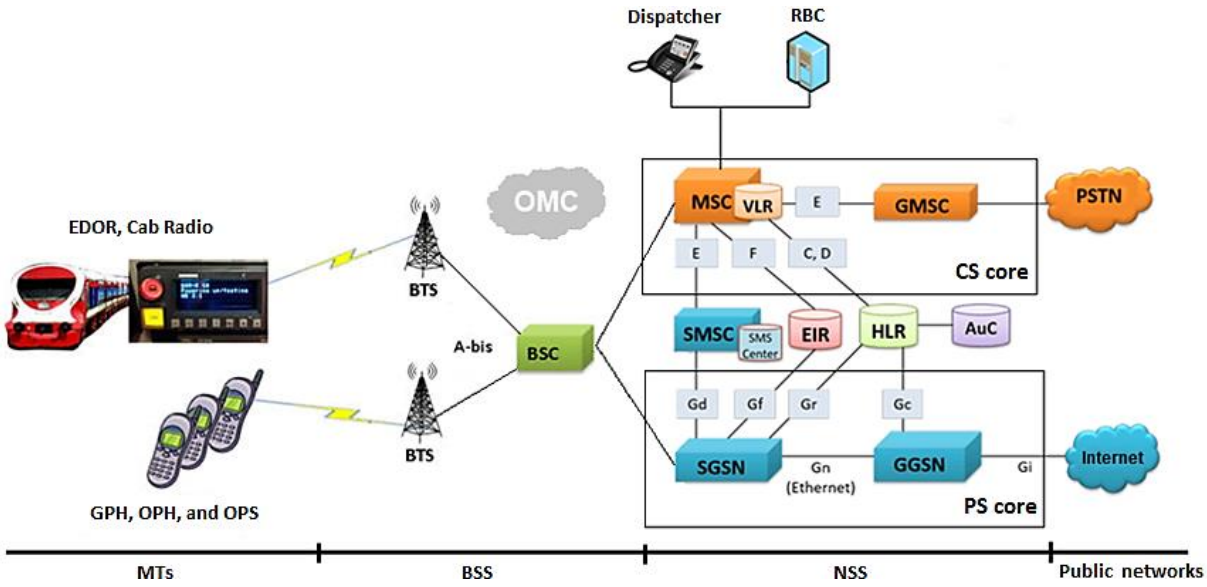

Figure 2.1 – GSM-R's network architecture (adapted from [GLCI19]).

The MTs represent the group of in-movement terminals, several types being specified for railway communications, [PuTa09]: the Cab Radio, the European Train Control System Data Only Radio (EDOR), the General Purpose Handled (GPH), the Operational Purpose Handled (OPH) and the Operational Purpose Shunting-handled (OPS). The Cab Radio and the EDOR are the MTs installed inside the train. Each MT is identified by its International Mobile Equipment Identity (IMEI) number and has its own Universal Subscribers Identity Module (USIM) card, which carries the International Mobile Subscriber Identity (IMSI) number, used for user identification in the network.

The BSS is responsible for handling all functionalities related to radio transmission and reception. It contains the Base Transceiver Stations (BTSs) (also commonly known as BSs) and the Base Station Controllers (BSCs). The BSs contain the antennas, transceivers, amplifiers, and other transmission/receiving equipment. The network's area is divided into different cells, each cell having a BS assuring MTs

communications within it. The BSCs control the BSs equipment, performing power control and handover decisions, among others; it is up to the BSCs to decide when to perform handovers and these decisions strongly influence network capacity [PuTa09].

The NSS is divided into two cores: the CS core and the PS core. The CS core contains the Mobile-services Switching Centres (MSCs) and the Gateway Mobile-services Switching Centres (GMSCs). The MSCs are responsible for traffic management control among BSs, and the GMSCs are responsible for forwarding traffic between the MSCs and the public networks. There is a Visitor Location Register (VLR) attached to each MSC that contains temporary information about the users of a designated area of the network. The PS core contains the Serving General Packet Radio Service Support Nodes (SGSNs) and the Gateway General Packet Radio Service Support Nodes (GGSNs), which perform a similar function to the MSCs and the GMSCs, respectively, but for packets' traffic. The NSS contains also, shared by the CS core and by PS core, the Home Location Registers (HLRs), the Authentication Centres (AuCs), the Equipment Identity Registers (EIRs) and the Short Message Service Centres (SMSCs). The first three are databases that hold permanent user's profile and location information, security information, and equipment information, respectively. The SMSCs are responsible for storing and forwarding short messages between two points.

The OMC is responsible for the monitoring of the entire GSM-R's network, ensuring its proper functioning. It is where the centralised control of the network (BSCs, databases, MSCs, SGSNs, etc) is being performed.

The public networks represent the interconnection of GSM-R's network to the public domain. The CS core is connected to the Public Switched Telephone Network (PSTN), and the PS one to the public internet.

The only differences to the public GSM's network architecture are the inclusion of the dispatcher terminals and of the Radio Block Centres (RBCs), both exclusive for railway usage. The dispatcher terminals are the fixed terminals in the Control Centres (CCs) used to communicate with the MTs mentioned above (except with the EDORs). The RBCs are railway specific equipment exclusive for the functioning of ETCS and they communicate with the EDORs for that purpose. This latter connection is a data one and is exclusively assured by the CS core, via CSD [PuTa09]. The RBCs are covered in Section 2.4, where the functioning of ETCS is explained.

GSM-R provides to the MTs various additional dedicated services and features compared to public GSM, namely related to voice applications, to attend railways' specific needs [UICG19]. These services and features are divided into two groups as presented in Table 2.1: Advanced Speech Call Items (ASCI) services and EIRENE features.

For the former, one has Voice Group Call Service (VGCS), Voice Broadcast Service (VBS) and enhanced-Multilevel Precedence and Pre-emption (eMLPP), while for the latter it has Functional Addressing (FA), Location-dependent Addressing (LdA), Shunting Mode (SM), Multiple Driver Communication (MDC) within the same train and Railway Emergency Call (REC).

Table 2.1 – Description of ASCI services/EIRENE features (based on [GSMR15a] and [GSMR15b]).

	Service/ feature	Description
ASCI services	VGCS	A service that allows MTs with permission for that to make group speech conversation. This service requires MTs that support it.
	VBS	A service used to make announcements and to broadcast recorded messages to and from the trains in a push-to-talk manner. Only the users requesting the service can speak, the others being listeners.
	eMLPP	A service used to classify calls at different priority levels, allowing critical MTs to work in an emergency situation, where everybody is trying to use their devices.
EIRENE features	FA	A function that simplifies the making of a call. Instead of tapping a whole phone number, a single number identifies the user.
	LdA	A function used to route calls to a destination number that is within a certain location. This feature is used when the driver wants to communicate with the dispatcher of a certain region.
	SM	A dedicated mode of MTs to perform shunting operations.
	MDC	A function that allows communication between drivers of the same train.
	REC	A special type of VGCS call with the highest priority possible set up when an emergency situation is detected. This type of call is made to a specific region and the trains within that region are who take the call.

2.1.2 Radio Interface

GSM-R works in slightly different frequency bands depending on the country. In Europe, GSM-R has a standardised band around the 900 MHz assigned to it, which can be seen, in Figure 2.2, with the respective standardised frequency band commonly named as Railway-GSM (R-GSM) band. This band ranges from 876 MHz to 880 MHz for UL and from 921 MHz to 925 MHz for DL (4 MHz for each). Both the upper and lower parts of these bands include a 100 kHz guard band, so there is only 3.8 MHz left for communications [PuTa09]. One carrier has 200 kHz of bandwidth and there is no space between adjacent carriers, so there are 19 carriers available in the R-GSM band. The 3 MHz bands represented in Figure 2.2, in both UL and DL, stand for Extended Railway-GSM (ER-GSM) and are used in some countries to increase the number of carriers of GSM-R to allow more traffic.

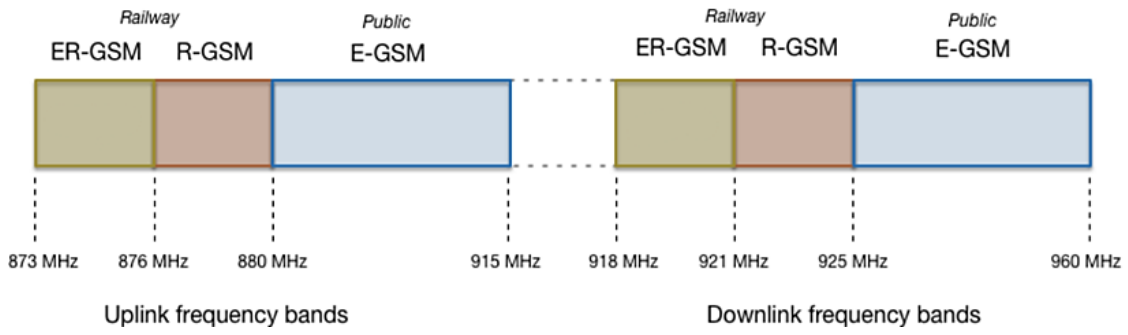

Figure 2.2 – GSM-R's standardised frequency band (adapted from [Wolf18]).

The centre frequency of each carrier, for both UL and DL, is given by:

$$f_c{}^{UL}{}_{[\mathrm{MHz}]} = 876 + k \times 0.2\,, \qquad k = 1, \ldots, 19 \tag{2.1}$$

$$f_c{}^{DL}{}_{[\mathrm{MHz}]} = 921 + k \times 0.2\,, \qquad k = 1, \ldots, 19 \tag{2.2}$$

Because spectrum is limited, one must use it in the most effective manner, allowing for bidirectional transmission of data. GSM-R combines Frequency Division Duplex (FDD) and Time Division Multiple Access (TDMA) [Corr18]: FDD states that different frequency bands are used for UL and DL, as one can see in Figure 2.2, and TDMA, represented in Figure 2.3, states that each user has access to the whole available band, being the division (among users) made in time, in time-frames, each time-frame containing 8 time-slots.

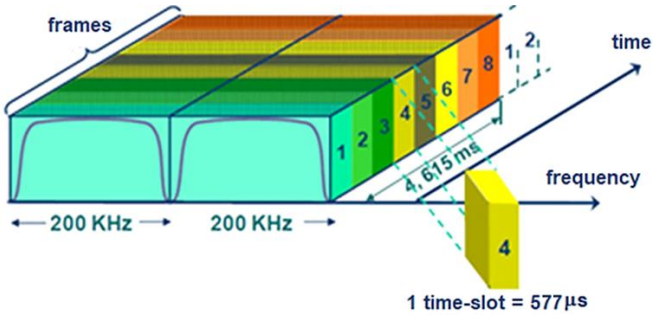

Figure 2.3 – Overview of TDMA (adapted from [Sour13]).

The transmission of a time-frame is done in bursts and has a duration of 4.615 ms, while a time-slot has a total duration of 577 μs and is 156.25 bits long, these being the physical channels [Corr18]. TDMA leads to a limited number of time-slots at a given time, which can lead to call drops and overall quality decrease of connections, depending on traffic. GSM-R uses Gaussian Minimum Shift Keying (GMSK) as the modulation method [SnSo12]. The previous information applies to both PS and CS, except in the part of time-slots allocation. The number of time-slots allocated per user in the PS mode can be different between UL and DL (dynamically assigned) allowing for higher data rates.

2.2 LTE-R

The current section describes LTE-R's network architecture and radio interface. LTE-R's additional railway features are not yet fully specified but a list of expected features can be seen in [CMAF13].

2.2.1 Network Architecture

LTE-R has basically the same network architecture as public LTE, as represented in Figure 2.4. It is divided into four main groups: the MTs, the Evolved Universal Terrestrial Radio Access Network (E-UTRAN), the Evolved Packet Core (EPC), and the public networks.

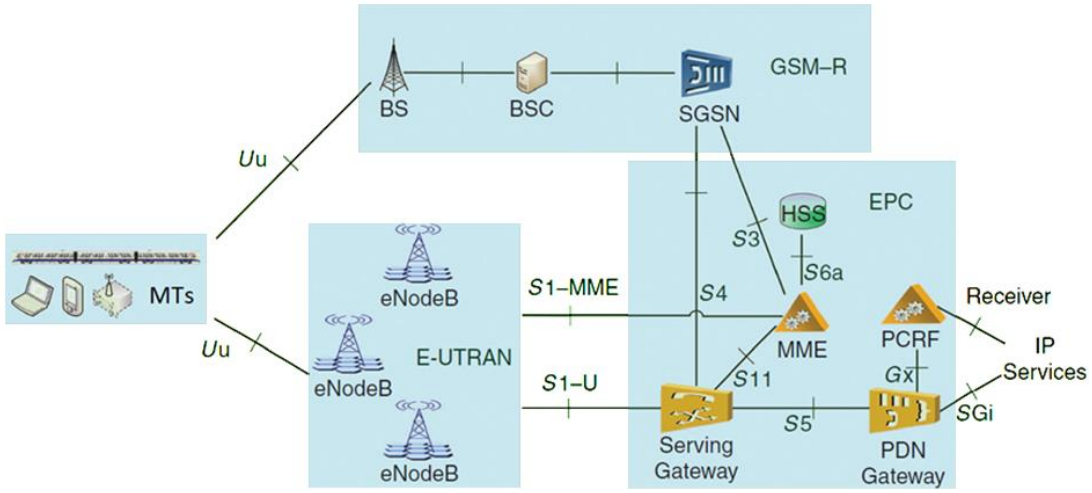

Figure 2.4 – LTE-R's network architecture (adapted from [HAWG16]).

The MTs represent, as in GSM-R, the group of in-movement terminals.

E-UTRAN contains nodes called eNodesB [HAWG16], which are autonomous BSs that are designed to cope with all the work that BSs and BSCs have in GSM-R's network architecture. The intention is to replace the BS-to-BSC dependency, leading to a flat network where there are fewer nodes, thus leading to lower latency of radio interface operations and to better overall network performance. The E-UTRAN is responsible for radio resources management, security of communications, and connectivity between the MTs and the EPC.

The EPC contains the Serving Gateways (S-GWs), the Packet Data Network Gateways (PDN-GWs), the Mobility Management Entities (MMEs), the Home Subscriber Services (HSSs), and the Policy and Charging Resource Functions (PCRFs). The S-GWs are responsible for forwarding user data packets while also acting as an anchor for MTs handover between eNodesB. The PDN-GWs are the points of entry and exit of traffic. The PCRFs are software nodes that search for information to and from the network, in real-time, to determine network policy rules and then make policy decisions based on them for each MT. The HSSs are databases, based on the HLRs and on the AuCs databases from GSM-R, that deal with user authentication, access authorisation, and subscription-related information. The MMEs are responsible for initiating paging and authentication of the MTs in the HSSs, saving their locations, and selecting the appropriate S-GW [HAWG16].

The public networks represent the interconnection of LTE-R's network to the public domain. In this case, because LTE-R is based only on PS, this connection is via IP services (public internet).

In the case where GSM-R is already deployed in a rail track, LTE-R is prepared to be installed in a coexistence scenario, as represented in Figure 2.4. In that case, the connection to the various MTs may be shared between the two systems. Because LTE-R is not widely deployed yet, this network architecture is basically the public LTE one. The connections to the RBCs and to the dispatcher terminals are not represented in Figure 2.4, but in case of a coexistence scenario between GSM-R and LTE-R, these connections can be shared by the two systems.

2.2.2 Radio Interface

LTE-R is not standardised yet regarding frequency bands allocation, but the R-GSM frequency band represented in Figure 2.2 is the most probable contender for this system; the problem is that even considering the ER-GSM and the R-GSM bands together, there are only 7 MHz available in total. In the future, higher bandwidths may be needed to extract all the potential from LTE-R and assigning parts of the public LTE bands to LTE-R can be also a future reality. In Europe, public LTE can use various frequency bands, presented in Table 2.2, and the E-GSM 900 band, beyond the frequency bands given in Table 2.2, can also be used for public LTE.

Table 2.2 – LTE's frequency bands used in Europe (based on [CEPT19a]).

Frequency bands	Downlink [MHz]	Uplink [MHz]
800	791 – 821	832 – 862
1800	1 805 – 1 880	1 710 – 1 785
2600	2 620 – 2 690	2 500 – 2 570

LTE uses FDD and different multiple access techniques for both UL and DL [Corr18]: Orthogonal Frequency Division Multiple Access (OFDMA) for DL and Single-carrier Frequency Division Multiple Access (SC-FDMA) for UL. In OFDMA, represented in Figure 2.5, the available band is divided into orthogonal (in time and frequency) subcarriers of 15 kHz, and sets of these subcarriers are allocated to the user. LTE radio channels have variable bandwidths depending on the number of allocated subcarriers. There is an overlap between adjacent subcarriers but not causing interference because these adjacent subcarriers are orthogonal to each other. The physical channels allocated to users are called Resource Blocks (RBs), each one corresponding to a set of 12 subcarriers with a duration of 0.5 ms, corresponding to 7 symbols. OFDMA is exclusively used for DL due to MTs' power limitations.

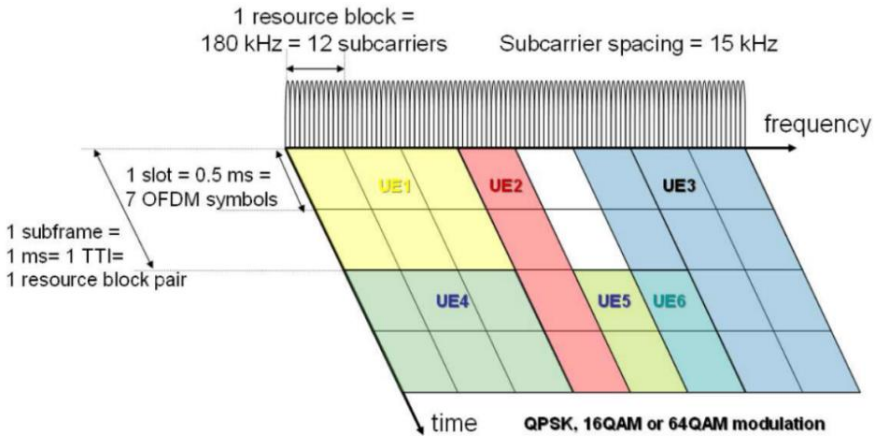

Figure 2.5 – Overview of OFDMA (extracted from [GeRK12]).

In SC-FDMA, instead of sets of subcarriers, the entire available channel's bandwidth is used by a single user at a time. Beyond that, the symbols' duration of this transmission method is much shorter providing better power behaviour and allowing MTs to save battery life.

LTE can make use of three different modulation methods: Quadrature Phase Shift Keying (QPSK), 16-Quadrature Amplitude Modulation (QAM), and 64-QAM.

2.3 BBRS

The current section describes BBRS' network architecture and radio interface.

2.3.1 Network Architecture

One can divide BBRS' network architecture, represented in Figure 2.6, into four main groups: the Operation Control Centre (OCC), the Backup Control Centre (BCC), the wayside APs and the mobile APs.

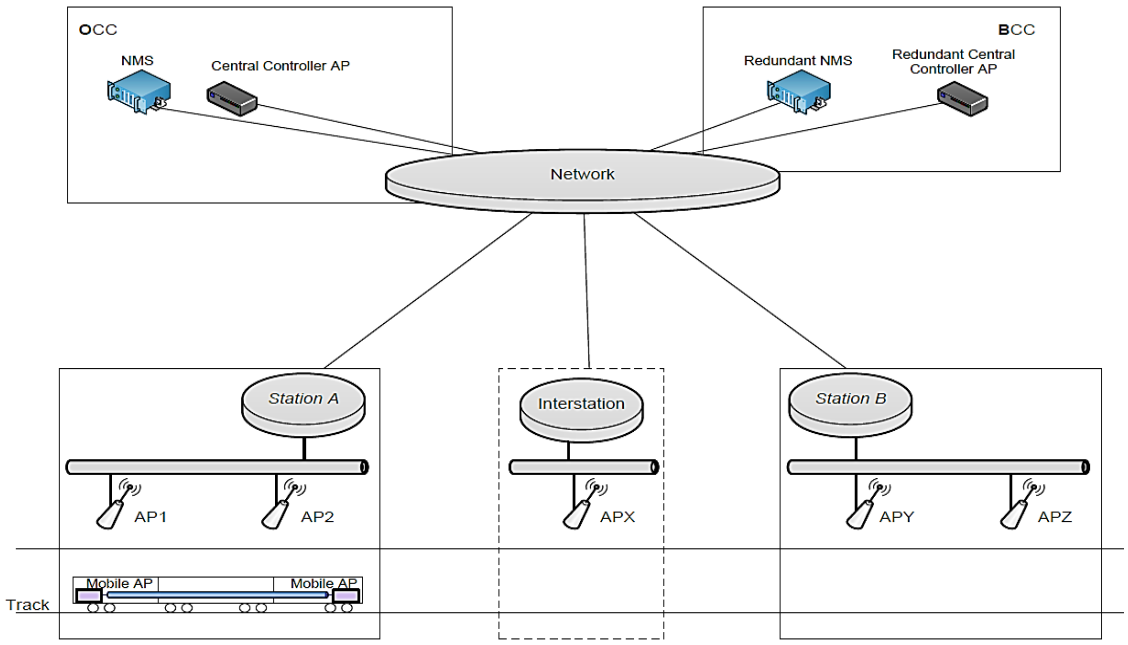

Figure 2.6 – BBRS' network architecture (extracted from [BBRS17]).

The mobile APs are the radios devices installed onboard the trains. Each carriage has normally 2 antennas on the roof to communicate with the wayside APs, which are cable-connected through the mobile APs that have the aim to spread the signal over the respective carriage. This two-hop transmission is used to avoid the penetration losses that a direct connection would cause.

The wayside APs consist of several APs installed along the rail track, providing radio coverage to the mobile APs. The connection of wayside APs to the network is performed via optical fibre.

The OCC includes the Network Management System (NMS) and the Central Controller Access Points (CCAPs). The NMS is composed of control servers on technical rooms responsible for real-time monitoring, configuration and performance analysis of the entire network. The functions of the NMS are to identify handovers, to detect errors, to access network configurations and to execute security procedures. The CCAPs are responsible for maintaining the well-behaviour of the network, for controlling the wayside APs radio power levels and for routing traffic to the destination. The BCC is a backup copy of the OCC, providing additional redundancy to guarantee network reliability in case a problem occurs.

2.3.2 Radio Interface

BBRS makes use of Wi-Fi as already mentioned, being based on the Institute of Electrical and Electronics Engineers' (IEEE) 802.11n 2x2 standard [BBRS17], which employs several techniques to improve throughput and reliability of the wireless network: Multiple-input and Multiple-output (MIMO) technology, channel bonding and packet aggregation.

BBRS can work in various frequency bands: one around 2.4 GHz and three others around 5 GHz, Table 2.3. The recommended frequency band is the licensed one from the 5 GHz available bands, as represented in Figure 1.4, which allows having more flexibility in managing interference, providing a more secure, reliable and dedicated link; the same band is used for both UL and DL.

Table 2.3 – BBRS' frequency bands (based on [BBRS17]).

Type	Frequency bands [GHz]
Standard non-license	2.405 – 2.495 5.150 – 5.825
Non-Standard non-license	5.825 – 5.875
Non-Standard licensed (recommended)	5.875 – 5.925

The transmission method of the 802.11n standard is Orthogonal Frequency Division Multiplexing (OFDM), [MERA07], represented in Figure 2.7, which is very similar to the already presented OFDMA, but less efficient. OFDMA divides the available band into sets of subcarriers and each user is assigned with some sets per time-slot, while OFDM allocates all the subcarriers of a channel to a specific user during a time-slot, therefore, not allowing the radio resources to be used as efficient as in OFDMA. The modulation methods available are Binary Phase Shift Keying (BPSK), QPSK, 16-QAM and 64-QAM.

MIMO is a technique in which the communicating APs use multiple antennas to transmit and to receive, [CISC07]. Multipath propagation implies that the transmitted signals reach the receiver with different delays, decreasing the overall received signal strength, but with MIMO, multiple signals are transmitted and advanced signal processing techniques are employed at the receiver to combine them. This standard is a 2x2, so it uses 2 transmitting and 2 receiving antennas.

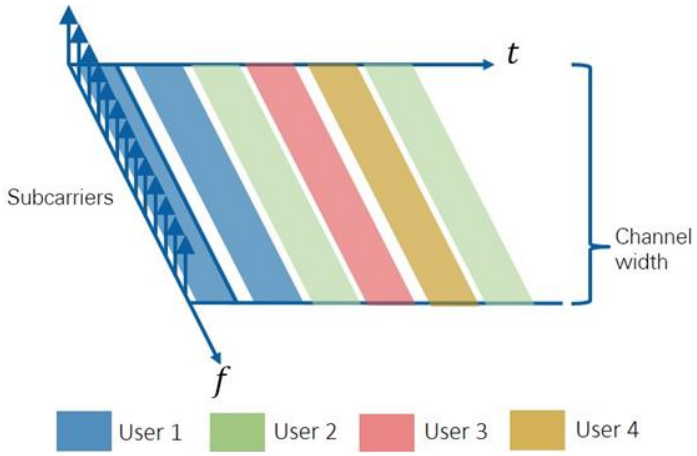

Figure 2.7 – Overview of OFDM (adapted from [NAIN19]).

The channels can be 20 MHz (64 subcarriers) or 40 MHz (128 subcarriers) wide: the 40 MHz ones are the result of channel bonding, which combines two adjacent 20 MHz channels doubling the bandwidth and the throughput. Another technique used to increase throughput is packet aggregation, where multiple packets of data are aggregated into a single transmission frame, reducing the number of transmitted frames, and, consequently, the time needed for the transmission.

2.4 Railway Communications

The current section overviews the services and applications of railway communications and defines their requirements. Some scenarios where railway communications can take place are also presented.

2.4.1 Services and Applications

The various applications of railway communications can be rearranged into four main classes of services: voice, non-safety critical data, control and signalling data, and video and other broadband services. To better understand the following overview, it is important to state which services are provided by each railway telecommunications system (GSM-R, LTE-R, BBRS): GSM-R aims to provide voice, non-safety critical data, and control and signalling data services; LTE-R aims to cover all the previous four classes of services; BBRS aims to provide video and other broadband services. The following analysis of voice, non-safety critical data, and control and signalling data services mentions GSM-R only because as already explained LTE-R is not yet fully standardised and GSM-R is the system in use.

Voice

One can divide the voice service into five types of sub-services [GSMR15b]: point-to-point calls, public emergency calls, broadcast calls, group calls, and multi-party calls. Public emergency calls are used to call external entities in case of an emergency, like ambulances, while broadcast and group calls are assured by VBS and VGCS services (ASCI services), respectively, already mentioned in Table 2.1.

A general representation of the parties that can make use of the voice service is represented in Figure 2.8. All these mentioned sub-services can be used in applications such as dispatching, shunting or maintenance. A description of each of these applications is given in Table 2.4. The voice service, beyond the use of ASCI services, makes also use of the EIRENE features, also mentioned in Table 2.1. For example, the REC feature, an EIRENE one, is represented in Figure 2.8.

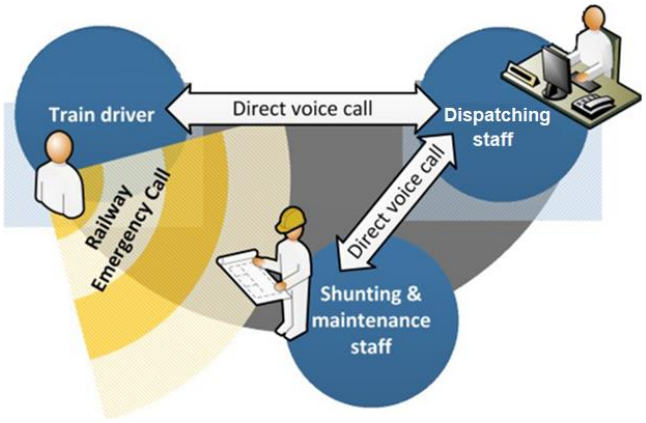

Figure 2.8 – Representation of the calls' parties (adapted from [SnSo12]).

Table 2.4 – Description of the main applications of the voice service (based on [HUAW12]).

Application	Description
Dispatching	Communication between the train drivers (via the cab radios) and the dispatching staff (via the fixed terminals in the CCs) to guarantee the correct operation of the train.
Shunting	Communication between the train drivers and the shunting staff to perform shunting operations. Shunting is the process where carriages are manoeuvred to form complete trains or the opposite.
Maintenance	Communication between the rail track workers (via the handled terminals) and the dispatching staff (via the fixed terminals in the CCs) to perform works on the line, etc.

Non-safety Critical Data

One can divide the data service into four sub-services [GSMR15b], three of them being considered to be non-safety-critical data ones, which are text messages, general data applications and automatic fax. The parties and applications are basically the same that one defines for the voice service.

Control and Signalling Data

The fourth data sub-service mentioned in [GSMR15b] has to do with train control and signalling related applications, and so, it is classified as safety critical data. ERTMS is the system responsible for this matter, which comprises ETCS as the component used for control and signalling, and GSM-R as the component offering the needed data transmission. The ETCS' equipment is connected to the Interlockings (IXLs), which are respectively connected to the CCs [ECMT19a], Figure 2.9. The CCs and the IXLs

belong to the national railway implementation: the CCs are the rooms where the real-time monitoring of train circulation and signalling equipment information is performed, and the IXLs are line management systems that create maps of the train's location, sending this information to the CCs where it is displayed.

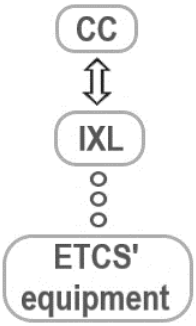

Figure 2.9 – Connection of the national railway implementation to the ETCS' equipment.

The ETCS component is divided into four main functional levels [Palu13]: Level 0 to Level 3. The ETCS' equipment can be divided into Lineside Equipment (LSE) and Onboard Equipment (OBE). The OBE is presented at the end of this subsection. The LSE varies from functional level to functional level, hence being important to overview the different functional levels. To better understand the different levels, one should introduce two concepts first: blocks and Movement Authorities (MAs). Blocks are how the rail tracks are divided, to ensure that trains do not collide, with only a train being allowed at a block at a time. MAs are the permissions gave to a train to cross these blocks.

Level 0 is characterised by a train equipped with ETCS' OBE using a rail track equipped with LSE that does not belong to ETCS. In practice, this level is not considered to be an ETCS level, because the MAs given to the driver are given by a signalling system external to ETCS, in this case by trackside signals from the previous existing signalling system, having only limited monitoring tasks, like speed monitoring.

Level 1, represented in Figure 2.10, is the first level equipped with both ETCS' OBE and ETCS' LSE, having the possibility of superimposition to the already existent signalling system (trackside signals), in a complementary scenario. The LSE of this level are Eurobalises and Lineside Electronic Units (LEUs). Eurobalises are passive devices installed between the rails of a railway that store and transmit data as pre-formatted telegrams (MAs given by the trackside signals, speed limits, etc.); they are passive devices because they do not need an energy supply, being activated when they receive signals from the antenna beneath the train. These Eurobalises can be fixed or switchable: fixed ones transmit the same data every time and are not connected to any equipment, while switchable ones are connected to the LEUs and send data based on trackside signals. LEUs make the data connection between the switchable Eurobalises, the trackside signals and the IXLs. The IXLs control the trackside signals according to the information sent by detection beacons placed along the rail track. When a train crosses one Eurobalise, the pre-formatted telegrams are sent to the OBE via the antenna beneath the train, then, the OBE monitors the speed and calculates braking curves from these data to be able to slow down and collect the next Eurobalises' data. It is also possible to implement Euroloops, which are extensions of Eurobalises over a particular distance, over cable or radio, that allow continuous transmission of data.

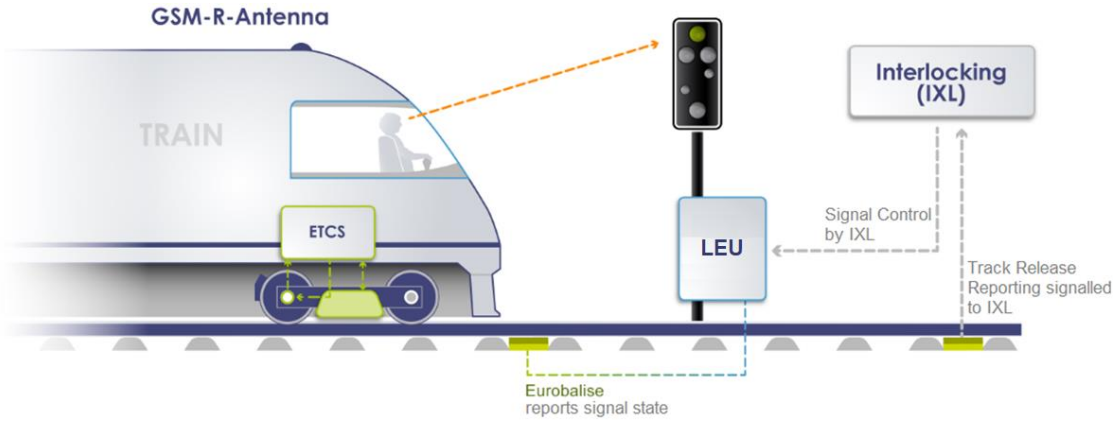

Figure 2.10 – Level 1 operation diagram (adapted from [THAL19]).

Level 2, represented in Figure 2.11, is a digital radio-based level making use of GSM-R. It is also equipped with both ETCS' OBE and ETCS' LSE. The LSE of Level 2 are Eurobalises and RBCs. The RBCs are computing devices that receive train detection information from the IXLs and, based on that information, generate MAs and transmit them to the trains. The train detection information is sent to the IXLs by the same detection beacons one has in Level 1. In this level, the Eurobalises do not transmit MAs anymore, being now only responsible for reporting train position information to the train itself, and acting as reference points for correcting distance measurement errors. The transmission of data (MAs generated by RBCs, train position given by Eurobalises, speed limits, etc.) between the train and the RBCs is made continuously via GSM-R and in full-duplex mode (both ways). The RBC is connected by cable to the GSM-R's network as one can see in Figure 2.1 where the GSM-R's network architecture is represented. The driver only has to pay attention to the OBE.

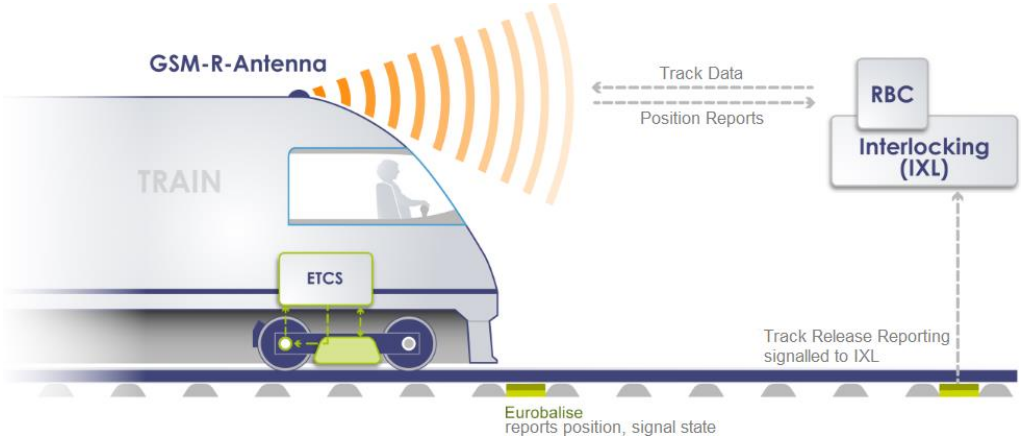

Figure 2.11 – Level 2 operation diagram (extracted from [THAL19]).

Level 3, represented in Figure 2.12, is the more advanced level. The LSE of this level is the same that one has in Level 2, the train position being transmitted to the train itself in the same way that in Level 2, via Eurobalises. The main difference is that rail tracks are no longer divided into fixed blocks: the train is equipped with a system that is responsible for monitoring its integrity, integrity data being sent along with the train location data to the RBCs, and the RBCs calculating the safe distance between two trains, generating MAs and transmitting them to the train. This two-way transmission between the trains and the RBCs, as in Level 2, is made via GSM-R in full-duplex mode. This type of operation, that one can

call moving blocks, ensures greater exploitation of the rail track capacity, allowing to achieve a continuous rail-clear authorisation. The IXLs are no longer connected to detection beacons in the rail track.

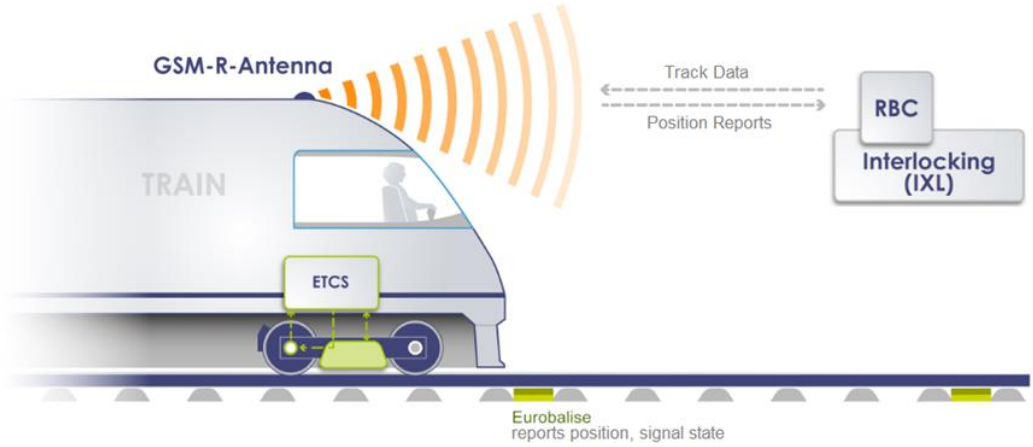

Figure 2.12 – Level 3 operation diagram (adapted from [THAL19]).

Finally, represented in Figure 2.13, one has the ETCS' OBE. The Euro Vital Computer (EVC) is the core unit [ECMT19b]. The Driver Machine Interface (DMI) is the interface that the driver uses to operate the train. The EDOR is the radio device responsible for processing the data received via the GSM-R antenna, and a type of MT described in the GSM-R's network architecture subsection. The Juridical Recording Unit (JRU) is like the "black box". The Train Interface Unit (TIU) is an interface responsible for applying ETCS' control commands to the brakes. The Balise Transmission Module (BTM) is the interface responsible for processing the data received by the Eurobalises. The Odometer (ODO) is a subsystem composed of wheel sensors, radars, accelerometers. The Train Integrity System (TIS) is the system to check for train integrity. All the equipment is transversal to every functional level mentioned above, except the EDOR and the TIS. The EDOR is only used in Level 2 and in Level 3 where GSM-R is used. The TIS is available in Level 3 only.

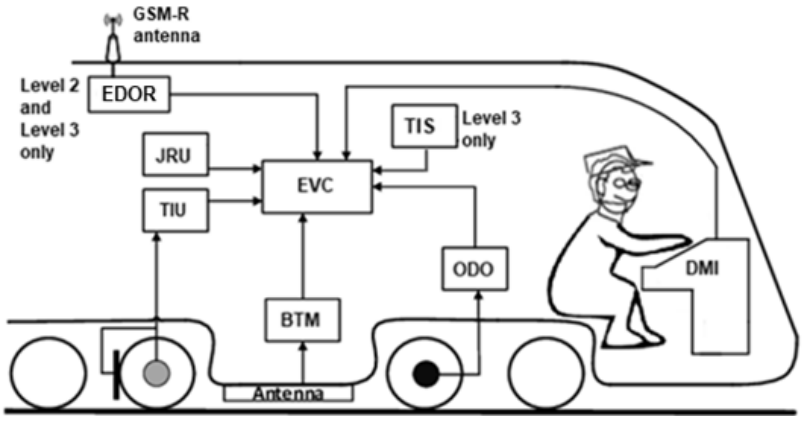

Figure 2.13 – ETCS' OBE (adapted from [FICS12]).

Video and other Broadband Services

Finally, in Table 2.5, one presents some of the broadband services of railway communications, which aim to provide applications related to infotainment and security of the passenger.

Table 2.5 – Description of the broadband services (based on [HUAW12] and [BBRS17]).

Type of service	Description
High-definition Television (HDTV)	Onboard television for infotainment applications.
Closed-circuit Television (CCTV)	Live video stream and record of onboard cameras.
Public address	Announcements via an advanced IP system.
Platform cameras	Live video stream of station platform cameras to the drivers' cab.
Passenger information	Multimedia messages appearing in cab and platform monitors.
Help points	Infotainment equipment for passengers to interact with.
Equipment management	Real-time monitoring of onboard equipment.
High-speed internet access	High-speed internet access for passengers.

2.4.2 Requirements

The four classes of services mentioned in the previous subsection have some requirements. The maximum allowable delay and average required throughput, as well as the peak throughput offered by each of the mentioned railway telecommunications systems, are given in Table 2.6.

Table 2.6 – Delay/throughput requirements of each service class and peak offered throughput by each railway telecommunications system (based on [PALA15], [FrFC17], and [Corr18]).

Service	Maximum allowable delay [ms]	Average required throughput [kbps]	Peak offered throughput		
			GSM-R [kbps]	BBRS [Mbps]	LTE-R [Mbps]
Voice	100	~ 22	171.2 (GPRS)	–	100 (DL) 50 (UL)
Non-safety Critical Data	best effort	best effort	171.2 (GPRS)	–	
Control and Signalling Data (ETCS levels 2/3)	500	~ 1	9.6 (CSD)	–	
Video and other Broadband Services	100	~ 4 000	–	125 (UL and DL)	

One can observe in Table 2.6 that for the non-safety critical data service, the employed method, for both the allowable delay and required throughput, is the “best effort”. This means that the non-safety critical data sub-services, because they are not based on real-time connections, are only served when possible. The same does not apply to the other service types, and stricter requirements exist.

GSM-R offers different peak throughputs depending on the service type: the peak offered throughput to both voice and non-safety critical data services refers to transmission by the PS core, via GPRS. As already said, the control and signalling data are transmitted over CSD, and so, the peak offered throughput is much lower. For LTE-R and BBRS, because the transmission is always via PS, the peak offered throughput is represented as the same to all the service types that they aim to serve.

Because GSM-R's voice calls can be classified into different priority levels via the eMLPP ASCI service, different call set-up time requirements for the different types of calls are defined. These different call set-up times are given in Table 2.7. The RECs are the calls with the highest priority possible as already stated, and so, their call set-up time is the lowest one.

Table 2.7 – GSM-R's specific voice requirements (extracted from [GSMR15b]).

Call type	Call set-up time [s]
Railway emergency calls	4
High priority group calls	5
All operational and high priority mobile-to-fixed calls not covered by the above	5
All operational and high priority fixed-to-mobile calls not covered by the above	7
All operational mobile-to-mobile calls not covered by the above	10
All other calls	10

The control and signalling data service is assured by ETCS. Some additional requirements need to be defined because safety-critical data is involved, which are given in Table 2.8, being defined for a certain percentage of connections (95%, 99% or 100%).

Table 2.8 – ETCS' specific requirements (control and signalling data) (extracted from [FrFC17]).

Parameter	Value
Maximum connection establishment delay [s]	<8.5 (95%); <10 (100%)
Connection establishment error ratio	$<10^{-2}$ (100%)
Connection loss rate [/h]	$<10^{-2}$ (100%)
End-to-end transfer delay [s]	≤0.5 (99%)
Transmission interference period [s]	<0.8 (95%); <1 (99%)
Error-free period [s]	>20 (95%); >7 (99%)
Network registration delay [s]	≤30 (95%); ≤35 (99%); ≤40 (100%)

GSM-R has specific coverage requirements, which are given in Table 2.9, being defined for the ER-GSM frequency band. The coverage probability means that with the mentioned probability (in this case 95%) the received signal level should be equal or above the receiver sensitivity. The data given in Table 2.9 take a margin of 6 dB into account to guarantee that the received signal is always above the receiver sensitivity.

Table 2.9 – GSM-R's specific coverage requirements (based on [GSMR15a]).

Service	Coverage [%]	Speed [km/h]	Receiver sensitivity [dBm]
Voice and Non-safety Critical Data	95	–	-98
Control and Signalling Data (ETCS levels 2/3)	95	≤220 [220, 280] ≥280	-95 [-92, -95] -92

Lastly, the interference related requirements, are defined by a certain Signal-to-noise-plus-interference Ratio (SNIR), i.e., the minimum difference between the power of the desired signal and the sum of the powers of the interfering signals with noise. The minimum SNIR for GSM is fixed (only uses one data modulation method) and it can be considered as 9 dB [Corr18], to be able to offer the voice service., while for LTE (LTE-R) and Wi-Fi (BBRS), because they use Adaptive Modulation and Coding (AMC), unlike GSM, it has no fixed value and depends on the required throughput.

2.4.3 Scenarios

It is important to define the different types of railway scenarios where communications can take place. This importance relies on the fact that different environments cause completely different behaviours in the propagation of the signals (both desired and interfering ones). One provides in Table 2.10 four different types of rail tracks and their characteristics.

Table 2.10 – Characteristics of different types of rail tracks (based on [FrFC17]).

Characteristics	Urban	Urban/Inter-City	Inter-City	High-Speed
Maximum speed [km/h]	≤70	]70; 160]	]160, 250[	≥250
Line length [km]	≤20	]20, 100[	[100, 250[	≥250
Parallel tracks [units]	1	2	3	4
Rolling stock	Single	Similar	Mixed	Very mixed
Stock types	1	[2, 4]	[5, 8]	≥9
Train stations	[1, 5]	[6, 20]	[21, 50]	≥51
Operators	1	2	[3, 5]	≥6
Passengers [/km of line]	<10k	[100k, 200k[	[200k, 500k[	≥500k
Range of services	Single	Small diversity	Multiple variances	Extremely varied

The various scenarios/structures that one can encounter along rail tracks are, for example, urban, sub-urban, rural, viaduct, cutting, tunnel, railway station, mountain, desert, water, and combination scenarios (groups of tunnels or cuttings). Examples of a viaduct and a cutting, two of the most common railway scenarios/structures, are represented in Figure 2.14.

a) Viaduct. b) Cutting.

Figure 2.14 – Two common railway scenarios (extracted from [AHZG12]).

All the mentioned scenarios/structures introduce multipath effects resulting in fading and channel time dispersion. It is therefore important to be aware of the effects of multipath in what concerns path loss, taking path loss exponent, standard deviation caused by shadowing and the distribution used to characterise fast fading into account. An analysis of these parameters for different scenarios/structures (for 930 MHz) is given in Table 2.11. Different frequencies may lead to different values, but this analysis is important for one to be aware of the order of magnitude that one is dealing with.

Table 2.11 – Some characteristics of the different railway scenarios/structures (based on [AHZG12]).

Scenario/ structure	Path loss exponent	Standard deviation of shadowing [dB]	Fast fading distribution
Urban	4-7	3-5	Rice
Suburban	3-5	2-3	Rice
Rural	2-5	2-3	Rice
Viaduct	2–4	2-4	Rice
Cutting	2.5-4	3-5	Rice
Tunnel	1.8-3	5-8	Rice
Railway station	2-5	2-5	Rice/Rayleigh
Mountain	3-7	2-6	Rice/Rayleigh
Desert	2-4	2-3	Rice
Water	2-4	2-3	Rice
Group of tunnels	1.5-5	3-5	Rice/Rayleigh
Group of cuttings	5-8	4-7	Rayleigh

Railway communications can be divided into mobile-to-infrastructure, inter-carriage, and infrastructure-to-infrastructure communications [FrFC17]. This thesis considers only mobile-to-infrastructure communications, i.e., between onboard railway MTs / mobile APs and railway BSs / wayside APs.

2.5 Performance Parameters

In this section, one overviews important performance parameters, and, after that, because interference is the most important parameter for the problem under study, various interference types are presented.

2.5.1 Overview

It is necessary to clarify some of the main parameters and respective Key Performance Indicators (KPIs) to be taken as metrics for the interference analysis. The main parameters are coverage, capacity, and interference. The importance of these parameters' clarification lies in the fact that they are inter-correlated and vary dynamically with each other. The aim is to maximise coverage and capacity, minimise interference, and to offer the best QoS possible (above the requirements defined for each service type in subsection 2.4.2). Each of the mentioned parameters and the respective KPIs can be defined as follows [Isab14], [Corr18]:

- **Coverage:** the range within which a wireless network can communicate with the MTs, which depends essentially on the link budget, which in turn depends on the system and corresponding frequencies being used. The coverage area is defined as the area within which MTs achieve a certain minimum received power, denoted as receiver sensitivity (coverage-based KPI), usually expressed in dBm. Because in wireless networks one cannot say "the MT is covered", the receiver sensitivity is defined for a certain probability of the MT being covered.
- **Capacity:** a measure of how much data one can transmit in a wireless channel for certain conditions, being usually defined either for a single user or for the whole available channel's bandwidth. It can be measured in terms of throughput (capacity-based KPI), expressed in bps. The throughput a system can offer to each user depends strongly on the number of users using the network, on the system being used and on the available bandwidth.
- **Interference:** disturbance that affects the reception of the desired signal by various means. One should be aware of the difference between noise and interference: an interfering signal is a type of noise signal, but a noise signal not always causes interference; in this last case, it is just considered random noise. If the interfering signal has a power high enough to reduce the SNIR (interference-based KPI), expressed in dB, present at the receiver, it can affect the reception of the desired signal**.** The interference influence depends on the quality of the equipment being used (transmitters and receivers), on the frequencies being used, on the propagation environment, etc.

A good trade-off between coverage, capacity, and interference is crucial to be achieved in the cellular planning phase. According to [Corr18], cellular planning consists of placing BSs (railway BSs and wayside APs in the railway environment) and establishing coverage, in performing optimum management of radio resources, and in minimising interference.

Cellular planning accomplishment is essentially based on the implementation scenario and on the used propagation models, these last ones being essential for the calculation of the maximum path loss, which is important for the estimation of the cell range. A signal undergoes two types of fading: slow and fast. Slow fading, or shadowing, depends on the distance from the MT to the BS and follows a Log-Normal Distribution, while fast fading depends on the terminal movement and follows a Rice or a Rayleigh Distribution as one can see in Table 2.11 for different railway scenarios/structures. Cellular planning is also performed based on user profiles and traffic models [Corr18].

Regarding the cells' shape, railway cells are different from the public network ones. In these last ones, the BSs antennas create, in general, the concept of "circular cell" because an MT can be anywhere around. On the other hand, the location of the rail tracks is fixed, and the railway MTs / mobile APs are always located around them, enabling the antennas of the railway BSs / wayside APs to radiate to a narrower area, leading to linear cells. The concepts of circular and linear cells, as well as the corresponding gain in coverage when using a linear cell configuration (for frequencies of 450 MHz and 1.8 GHz as an example in this case), are represented in Figure 2.15.

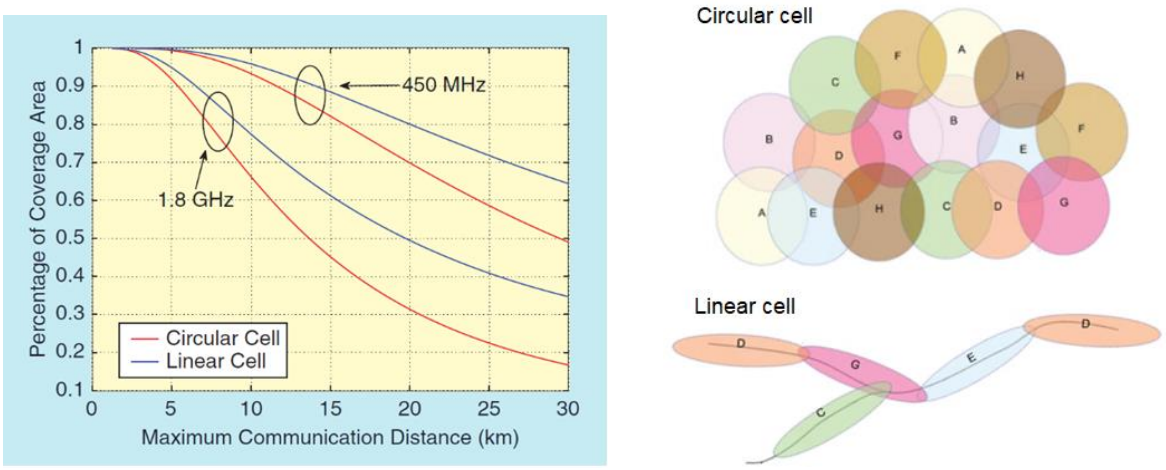

a) Coverage performance comparison. b) Cell type comparison.

Figure 2.15 – Comparison between circular and linear cells (extracted from [HAWG16] and [Sarf08]).

2.5.2 Interference Types

This thesis intends to focus only on types of interference related to the radio interface, where one can consider a division in noise signals that can cause interference in the railway environment: transient noise and permanent noise [HSDR09]. Transient noise signals are associated with signals without information and they are generated by the poor contact between the pantograph and the catenary (structures for the electric operation of the train itself); transient noise is out of the scope of this thesis. Permanent noise is the type that one analyses here, being signals containing information transmitted by telecommunications systems external to the railway usage, and capable of interfering, by various means, with the reception of the desired signal transmitted by the railway telecommunications systems.

To understand how interfering signals can degrade the performance of a system, it is important to have in mind the hardware architecture of a typical receiver, because it is where the degradation takes place. All the signals that reach the receiver antenna are filtered out by a Radio Frequency (RF) filter, which aims to pre-filter the signals in frequencies different from the desired ones. The signals are then amplified by a Low Noise Amplifier (LNA), because the desired signals that reach the receiver have usually low power due to the propagation losses, after which the signals pass through a set of operations that aim to convert them into the corresponding bitstream. The processes up to the Intermediate Frequency (IF) stage are performed by the Radio Frequency Front-end (RFFE), to which the antenna is connected,

being usually used simultaneously for transmission and reception. A general RFFE's hardware architecture is represented in Figure 2.16; the RF filter is not always used due to its cost and size, and not using an RF filter to pre-filter the incoming signals can be a source of interference problems, being a key element for the interference analysis.

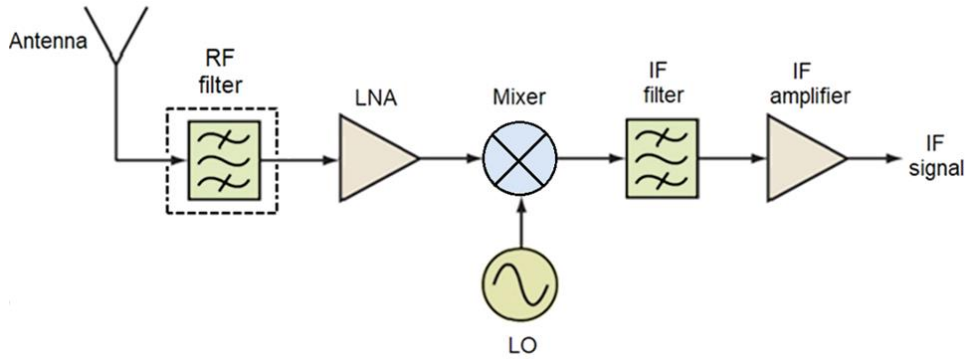

Figure 2.16 – Hardware architecture of a Radio Frequency Front-end (adapted from [PaGG14]).

Next, one presents some important interference types [EuCO16]:

- **Co-channel Interference (CCI):** the interference generated by systems that use the same frequency channel that is used by the victim system (when one refers to the victim system, one is referring to the system being interfered). The interfering signals are not filtered out, because they fall within the reception band of the victim's receiver. This type of interference can be caused by an adjacent cell of the same system, because of the reuse of the same frequency channels in adjacent cells or by an external system when both systems use unlicensed frequencies and so both systems can use the same frequency channels. When the interference comes from an adjacent cell of the system, it can be managed during the cellular planning phase using sectorised cells, down-tilting the main lobe of the antenna, or performing power control [Corr18].
- **Out-of-band Interference (OOBI):** the interference generated by systems that use transmission frequencies adjacent to those used by the victim system, some energy of the transmission being leaked to adjacent frequencies due to the poor performance of the interferer's transmitter. The interfering signals are not filtered out, because they fall within the reception band of the victim's receiver, and so, they can affect the reception of the desired signal. This type of interference can be caused either by an adjacent cell of the same system (in that case commonly named Adjacent-channel Interference (ACI)) or by an external system using adjacent frequencies. Only emissions that fall right after the transmission band of the interferer are considered, and spurious emissions are not considered as OOBI, because they fall far away in frequency from the transmission band of the interferer compared to out-of-band emissions. The power of spurious emissions is also much lower than out-of-band ones.
- **Blocking-based Interference (BBI):** the interference generated by systems that impose high power interfering signals at the RFFE of the victim's receiver, which can cause problems in the reception of the desired signal, even if falling outside of the reception band of the victim's receiver, due to insufficient selectivity of the filters present in the RFFE of the victim's receiver. These high-power signals are perceived as in-band interference because they are captured by

these filters. If the interfering signals are not blocked they can mask the desired ones.

- **Intermodulation-based Interference (IBI):** the interference indirectly generated by emissions from interfering systems due to the non-linearities of the LNAs/mixers of the victim's receiver. The interfering signals, even falling outside the reception band of the victim's receiver, can still reach the LNAs/mixers with a high power if they are not correctly filtered out. The LNAs/mixers, due to their non-linearities, mix various interfering signals or various spectral components of a single interfering signal (wideband signal) and generate other signals at frequencies that are not just harmonic frequencies but sums and differences of two of these frequency components, which are called Intermodulation Products (IMPs), and if they fall within the reception band of the victim's receiver they can affect the reception of the desired signal. The more common IMPs to cause interference are the third-order ones. IMPs can be also of second or higher orders, but these orders do not lead to interference into rightly adjacent frequencies, because these products fall far away from the transmission band of the interferer.

Because the frequency bands of the three railway telecommunications systems being analysed are licensed ones, CCI can only be caused by an adjacent cell of the same system. CCI is not analysed in this thesis, because the problem under study is the adjacent compatibility between systems. The remaining three types of interference are analysed. An example of OOBI, BBI, and IBI is represented in Figure 2.17. In fact, OOBI and BBI are not two interference mechanisms but rather a single one, still this division into two different mechanisms is considered a good approximation [Vere18]. One can see also in Figure 2.17 that, contrary to OOBI and BBI, IBI can be considered a discrete type of interference. The reception band of the victim's receiver and the transmission band of the interferer's transmitter are also represented in Figure 2.17.

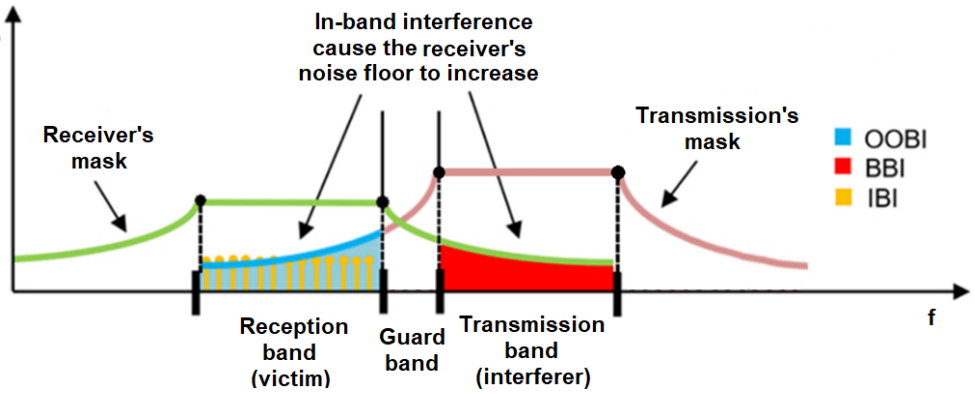

Figure 2.17 – Interference types to be analysed (based on [EuCO16]).

2.6 State of the Art

In this section, one mentions some works that have been performed around the problem under study, which is the adjacent compatibility between railway telecommunications systems (GSM-R, LTE-R, and BBRS) and systems external to the railway usage. The study of this problem is in different development

stages for each one of the mentioned railway telecommunications systems, GSM-R being the railway telecommunications system where the majority of the work has been performed.

A balance on the DL powers between the desired GSM-R signals and the interfering ones emitted by public GSM BSs is established in [HSDR09], the focus being on the powers of the signals received by the antenna above the train. A measurement campaign with a large number of data collected was performed onboard a moving train (at very low speed) between Schaerbeek and Herent, in Belgium, in a route equipped with GSM-R with about 24 km. The authors conclude that the last channel of GSM-R should not be used in geographical areas where public GSM BSs use the 925.2 MHz channel. This conclusion is based on the fact that the powers of the interfering signals can be higher than the GSM-R coverage level, but this conclusion cannot be used as a deployment guideline to a proper deployment of GSM-R BS under interference scenarios, since many other parameters are at stake.

The UIC Frequency Working Group shows the results of a fully accredited interference test campaign in [FMST12], intending to demonstrate the interference caused on GSM-R MTs by public UMTS and public LTE BSs. This test campaign was performed at the European Commission's Joint Research Centre in Ispra, Lago Maggiore, Italy. Four real ETSI compliant GSM-R MTs from various manufacturers were used. Instead of a GSM-R BS, a Rohde & Schwarz BS simulator was used, and, instead of a public UMTS/LTE BS, an Agilent signal generator was used. A spectrum analyser was used to analyse both signals reaching GSM-R MTs. This work concludes that the transmission powers of UMTS and LTE BSs need to be restricted to prevent the third-order intermodulation behaviour of GSM-R MTs and that raising the power of GSM-R signals is not a viable solution, hence, additional filtering must be used. This work does not consider OOBI, which also has to be taken into account.

Some works have been conducted by the Electronic Communications Committee (ECC) within European Conference of Postal and Telecommunications Administrations (CEPT) around the interference problem caused by MFCNs to GSM-R. Two methods are used in [CEPT07] to assess the impact of public UMTS on GSM-R DL operation: one is based on the Minimum Coupling Loss (MCL) and the other is based on Monte Carlo simulations. MCL calculations show that coordination between both systems is needed, but the calculations are only performed for some fixed distances; additionally, the interference types are studied separately and IBI is not taken into account. The interference caused by public GSM to GSM-R is studied in [CEPT10a] where minimum separation distances between the two systems are calculated. IBI is not taken into account nor are deployment guidelines provided. A study on the interference caused by LTE BSs to GSM-R MTs is performed in [CEPT10b], its conclusions being an extension of the study in [CEPT07], so, again, the combined effect of the three types of interference is not taken into account. Some interference mitigation techniques to attenuate the interference problems between MFCNs and GSM-R are mentioned in [CEPT11]. It is recommended to increase the GSM-R signal level received at the GSM-R MT to overcome interference problems, but this increase is not quantified. RF filtering is another proposed mitigation technique, but the effect of the introduction of a filter is not quantified. Frequency coordination between both systems is also proposed, but this effect is, again, not quantified. This thesis intends to provide deployment guidelines to overcome the interference caused

by MFCNs to GSM-R, while analysing various frequency offsets between both victim and interferer systems. The effect of the introduction of RF filtering is also analysed in this thesis. The report in [CEPT15] presents field tests performed to prove the improved filter capabilities of a new GSM-R module introduced in 2014. The implementation of these new GSM-R modules will take time and, in the meantime, a coordination method is needed.

The interference caused by MFCNs to GSM-R is overviewed in [SuMi15]. The causes of interference, the types of interference and its negative effects are stated. Known reported cases of interference all across Europe are mentioned. A case study is performed in Poland about the blocking problem suffered by Cab Radios and EDORs (both GSM-R MTs). The power of the interfering signals reaching the MTs is compared to the expected minimum received signal power level of GSM-R. The coexistence problem between MFCNs and GSM-R is overviewed in [Sumi16a], as in [SuMi15]. A model for risk assessment is developed based on the Okumura-Hata model and also on the free-space one. The model aims to measure the difference at the rail track level in signal powers between the signals emitted from both MFCN BSs and GSM-R BSs. Differently from [SuMi15], this model considers the propagation losses in the GSM-R link and not only the minimum received power level of GSM-R. A method for evaluating the area covered by the signals emitted by MFCNs that interfere with GSM-R handled MSs is presented in [Sumi16b]. While other works focus mainly on the Cab Radios, this work focus on interference to handled terminals like GPHs, OPHs, and OPSs, being then applied in a case study to evaluate its real performance. The area selected for the case study was around the 97th km of the railway line E-65 in Poland. These latter three works do not take the sum of various interference types into account.

BBRS is a system deployed by Thales and there is not public information about interference suffered by this system. Still, some works deal with interference caused by public Wi-Fi systems to a railway telecommunications system called Communications-based Train Control (CBTC), which, similar to BBRS, is based on Wi-Fi and uses frequencies in the 5 GHz band [CEPT19b]. This work studies the interference caused by Wi-Fi systems working in the same channel as CBTC and does not cover the adjacent compatibility in the 5 GHz band, which could also represent an interference problem.

In what concerns LTE-R, because it is supposed that it will use the same band as GSM-R in a first stage of the transition, some works study the compatibility of GSM-R and LTE-R to coexist in the same frequency band [LSTA16], [TrSK18]. These works do not cover the problem under study in this thesis, that is, the interference caused by MFCNs to LTE-R if in a second stage of the transition LTE-R starts using the whole frequency band assigned to GSM-R today.

Chapter 3

Model Development and Implementation

This chapter starts by giving a global overview of the model developed to perform the interference analysis. After that, the various equations that compose the model are presented, being related to desired signal power, interference criterion, interfering signal power, path loss and SNIR/throughput calculations. The steps to the implementation of the model in MATLAB are explained. A model assessment is performed comparing with results from other authors.

3.1 Model Overview

This section intends to give a high-level overview of the model developed to perform the interference analysis. The model configuration with its main inputs and outputs is represented in Figure 3.1.

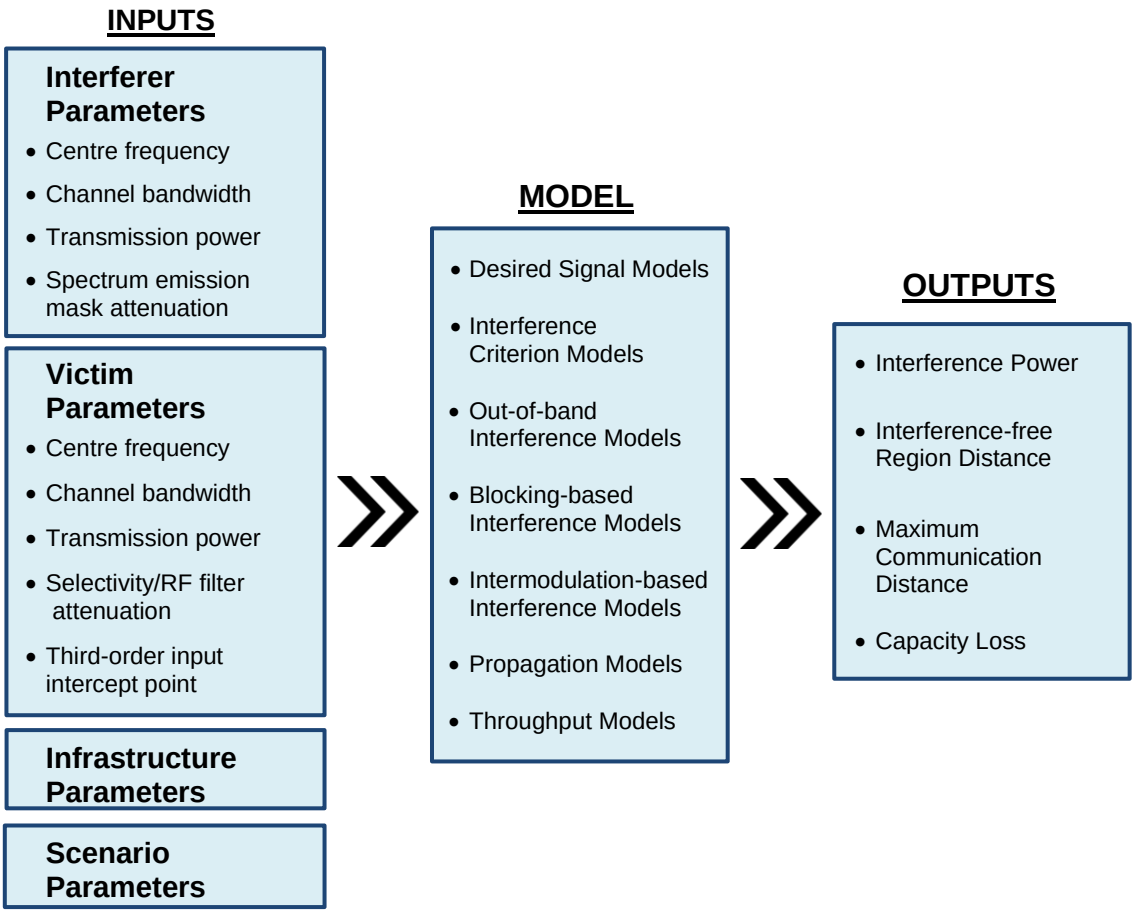

Figure 3.1 – Model configuration.

The model is composed of various "sub-models". The desired signal models define equations to calculate the desired signal power at the input of the victim's receiver. The interference criterion models define equations to calculate parameters related to the interference effect itself. OOBI, BBI and IBI models are used to calculate the power corresponding to the various interference types at the input of the victim's receiver. The propagation models are used to calculate the path loss of both the desired and interfering signals. The throughput models establish the relationship between throughput and SNIR.

In what concerns the model inputs, interferer parameters refer to the parameters of the interferer's transmitter. Victim parameters refer to the parameters of the victim's both transmitter and receiver. Infrastructure parameters refer to the heights of the infrastructures involved. Scenario parameters are related to corrections factors to apply to the propagation models.

The Spectrum Emission Mask (SEM) attenuation defines the out-of-band attenuation relative to the in-band power, at the frequency offset being considered, that a system's transmission must comply with. The selectivity and RF filter attenuations are applied by the filters of the victim's receiver at the frequency offset being considered. The Third-order Intercept Point (IP3) is a characteristic associated with the non-linearities of the victim's receiver components. Additional to the inputs represented in Figure 3.1, the gains of the antennas (both interferer and victim), the transmitter and receiver losses (e.g., cable losses), the receiver's noise figure, the system margin and the interference margin are also inputs.

The model has various outputs. The main four outputs are represented in Figure 3.1. The interference power, as already mentioned, calculated through OOBI, BBI and IBI models, refers to the power of the interfering signal at the input of the victim's receiver. The interference-free region distance is the one from which the interferer is not causing a non-acceptable interference case anymore and the interference can be classified as acceptable. When the interferer's transmitter is deployed at a distance from the victim's receiver (the distance in a straight line between the interferer's transmitter and the victim's receiver is named as interference distance) lower than the interference-free region distance, then the interference can be classified as non-acceptable depending on the power of the desired signal. In this last case, because the interference power is high, in order to maintain the required system performance, the required power (provided by the desired signal) has to increase and, consequently, the maximum communication distance between the transmitter and the receiver of the railway telecommunications system has to be lower than usual deployment distances. The maximum communication distance is another model output, which can be used as a deployment guideline to the deployment of railway BSs / wayside APs when interfering sources are already deployed within a certain area. The capacity loss is also a model output, aiming to simulate cases where the railway telecommunications systems are already deployed (fixed maximum communication distance) and interfering sources are causing a capacity degradation. The interference-free region distance and the maximum communication distance are represented in Figure 3.2 via two exemplification cases; the red BS and the red AP simulate, respectively, the interference sources that one mentioned in the problem statement section for GSM-R/LTE-R and BBRS.

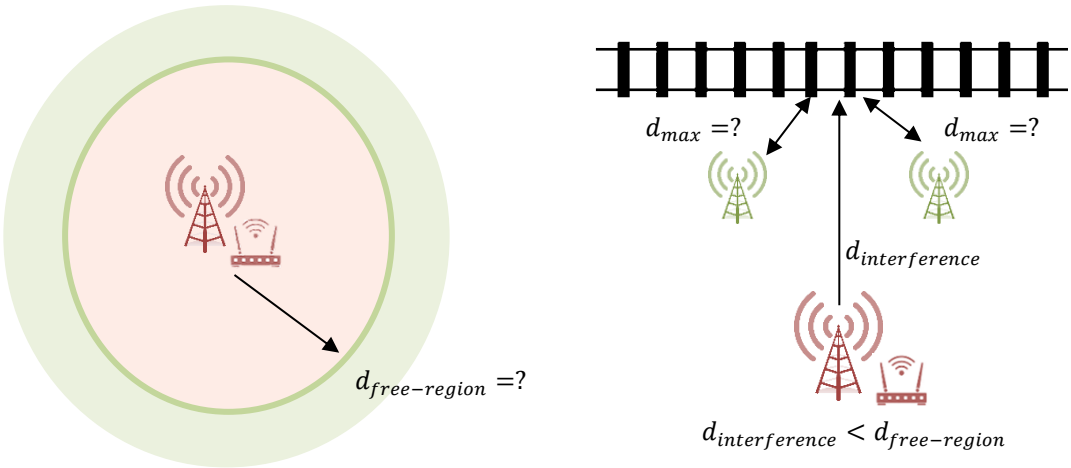

a) Interference-free region distance. b) Maximum communication distance.

Figure 3.2 – Model outputs exemplification.

3.2 Model Development

In this section, the various sub-models are explained and the equations are defined.

3.2.1 Desired Signal Models

The desired signal power at the input of the victim's receiver (whenever one mentions receiver's input is after the RF filter represented in Figure 2.16) can be calculated through simple link budgets equations, but these equations vary, depending on the system that one is analysing. For GSM-R and BBRS, because the full bandwidth is used for transmission, the equations can be considered as generic ones, and the Effective Isotropic Radiated Power (EIRP) of the victim can be calculated as follows [Corr18]:

$$P_{EIRP\,[\mathrm{dBm}]}^{vic\ (GSM-R,\,BBRS)} = P_{t\,[\mathrm{dBm}]}^{vic} - L_{t\,[\mathrm{dB}]}^{vic} + G_{t\,[\mathrm{dBi}]}^{vic} \tag{3.1}$$

where:

- P_t^{vic}: transmission power of the victim;
- L_t^{vic}: transmitter losses of the victim;
- G_t^{vic}: transmitter antenna gain of the victim.

For LTE-R and considering its DL operation according to the problem under study, because it uses OFDMA, the subcarriers are transmitted independently and the transmission power is divided per the number of transmitted subcarriers. In this case, one is only interested in the transmission power per the number of allocated subcarriers (channel) being interfered, which can be defined as follows [EuCO16]:

$$P_{t/sc} = \frac{n_{sc}^{aloc} \times P_t^{vic}}{n_{sc}^{tran}} \tag{3.2}$$

where:

- n_{sc}^{aloc}: number of subcarriers allocated to the user being interfered;
- n_{sc}^{tran}: number of subcarriers being transmitted;

hence, the EIRP is given by:

$$P_{EIRP\,[\mathrm{dBm}]}^{vic\ (LTE-R)} = P_{t/sc\,[\mathrm{dBm}]} - L_{t\,[\mathrm{dB}]}^{vic} + G_{t\,[\mathrm{dBi}]}^{vic} \tag{3.3}$$

In either of the two previous cases, the desired signal power at the input of the victim's receiver can be defined by [Corr18]:

$$P_{r\,[\mathrm{dBm}]} = P_{EIRP\,[\mathrm{dBm}]}^{vic} - L_{p\,[\mathrm{dB}]}^{vic} + G_{r\,[\mathrm{dBi}]} - L_{r\,[\mathrm{dB}]} \tag{3.4}$$

where:

- L_p^{vic}: path loss of the desired signal;
- G_r: receiver antenna gain;
- L_r: receiver losses.

3.2.2 Interference Criterion Models

The three types of interference (OOBI, BBI and IBI) are related to the increase in the noise floor of the victim's receiver. This effect is related to the interfering signals that are captured by the receiver's mask, and in order to properly capture it, it is necessary to define first some parameters and corresponding equations for their calculation. The first parameter one has to account for is the noise power, also referred to as noise floor, which depends on the channel's bandwidth and on the noise figure of the victim's receiver. The noise figure is a receiver parameter and represents the noise introduced by the components of the receiver's chain, hence, lower values of noise figure represent, therefore, a better receiver. The noise power can be defined as follows [Corr18]:

$$N_{[\mathrm{dBm}]} = -174 + 10\log\left(\Delta f^{vic}_{[\mathrm{Hz}]}\right) + F_{[\mathrm{dB}]} \tag{3.5}$$

where:

- Δf^{vic}: channel bandwidth of the victim;
- F: receiver's noise figure.

While for GSM-R and BBRS, one takes the system channel bandwidth, for LTE-R, since it uses OFDMA, the channel bandwidth varies with the number of allocated subcarriers [EuCO16], being given by:

$$\Delta f^{vic\ (LTE-R)}_{[\mathrm{kHz}]} = n_{sc}^{aloc} \times 15 \tag{3.6}$$

Another important parameter is the receiver sensitivity, which defines the minimum power at which the receiver must receive the desired signal so that a certain service can work properly. The receiver sensitivity depends on the already defined noise power and on the Signal-to-noise Ratio (SNR), which in turn depends on the system and on the services that the system aims to offer. Each service requires a different throughput, which is related to a required SNR. To account for variations on the signal level two margins are considered in the receiver sensitivity calculation: system and interference. The system margin accounts for moderate losses due to slow and fast fading, while the interference one is a safety margin against moderate interference, but they are not effective in severe interference or fading conditions. The receiver sensitivity can be defined as follows [Corr18]:

$$P_{r\ min\ [\mathrm{dBm}]} = N_{[\mathrm{dBm}]} + \rho_{N\ [\mathrm{dB}]} + M_{S\ [\mathrm{dB}]} + M_{I\ [\mathrm{dB}]} \tag{3.7}$$

where:

- ρ_N: signal-to-noise ratio;
- M_S: system margin;
- M_I: interference margin.

As stated above, the interference margin protects a system only against moderate interference and it is taken as a fixed value for a certain system's design. To understand how the interference margin protects a system against moderate interference, it is important to explain first the interference effect mentioned above and how it can be quantified.

The increase in the noise floor is literally the increase of the noise power that one calculates using (3.5). To quantify this effect, it is important to define first the Interference-to-noise Ratio (INR), which, is defined as follows [EuCO16]:

$$\beta_{IN} = \frac{I}{N} \tag{3.8}$$

where:

- I: interference power.

The increase in the noise floor, commonly named as desensitisation of the victim's receiver, can be calculated as follows [EuCO16]:

$$D = \beta_{IN} + 1 \tag{3.9}$$

All the parameters introduced above are represented in Figure 3.3, which helps to understand this effect, and in which the three different interference cases are represented: no interference, acceptable interference, and non-acceptable interference. The no interference case, on the left side of Figure 3.3, represents an ideal case, in practice never achievable. The no interference case is represented only for sake of comparison. It is possible to see that a system is designed according to (3.7) with a certain receiver sensitivity for a certain service to be able to work. The system margin is not represented in Figure 3.3 for a clearer explanation of the interference effect, but it has to be taken into account in the sensitivity calculation.

The two cases on the right of Figure 3.3 consider the realistic scenarios of interfering signals reaching the victim's receiver, leading to desensitisation. In the acceptable interference case, one represents an interfering signal reaching the victim's receiver with a power lower than the noise floor, which leads to a low desensitisation of the victim's receiver, lower than the interference margin accounted for in the system's design. A desensitisation lower than the interference margin is the criterion used to characterise acceptable interference. In this case, the receiver should be able to distinguish the desired signal from the unwanted ones. The interference-free region distance is calculated based on this criterion, that is, the desensitisation must be equal, at most, to the interference margin accounted for.

In Figure 3.3, the non-acceptable interference case represents an interfering signal reaching the victim's receiver well above the noise floor, which generates a high desensitisation of the victim's receiver, higher than the interference margin accounted for. In fact, when the interference power is well above the noise floor, the noise-plus-interference power is almost equal to the interference one. This interference case leads to a situation where the receiver sensitivity is no longer enough to offer the required SNR for the service to be able to work properly, therefore being required a received power (desired signal power) higher than the sensitivity level to overcome the interference problem and to provide the required SNR by a certain service. This higher desired signal power at the input of the victim's receiver can be achieved by a lower maximum communication distance (one of the model outputs). If the desired signal power is not increased, an SNR reduction occurs and, consequently, a capacity loss (one of the model outputs).

The required power at the input of the victim's receiver needed to overcome the non-acceptable interference case can be calculated, based on the sensitivity equation as follows [Corr18]:

$$P_{req\,[\mathrm{dBm}]} = N_{[\mathrm{dBm}]} + \rho_{NI\,[\mathrm{dB}]} + M_{S\,[\mathrm{dB}]} + D_{\,[\mathrm{dB}]} \tag{3.10}$$

where:

ρ_{NI}: signal-to-noise-plus-interference ratio.

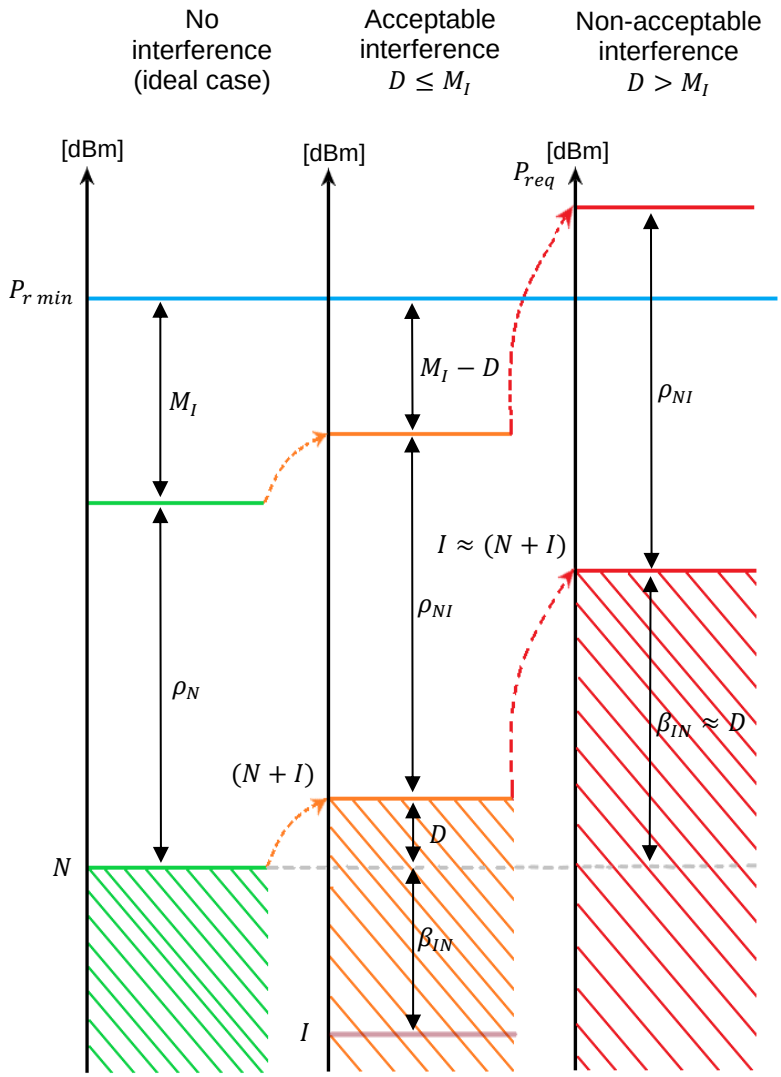

Figure 3.3 – Desensitisation of the victim's receiver (based on [EuCO16]).

Both in the acceptable interference case as in the non-acceptable one represented in Figure 3.3, SNIR is used instead of the SNR, just to clarify the reference being used. Because in these two cases one is dealing with interference, it makes total sense to take the noise floor together with the influence of interference into account in the calculation.

The criterion used to characterise acceptable and non-acceptable interferences is, as already mentioned and as represented in Figure 3.3, the desensitisation to be lower or higher than the interference margin, respectively.

3.2.3 Out-of-band Interference Models

The transmission band of a system can be defined as the bandwidth that contains 99% of the transmission power [Vere18]. In practice, the emissions of a system are not just restricted to its transmission band, because of the modulation process/insufficient filtering and consequently some energy is leaked to adjacent frequencies. The emissions that fall outside the transmission band, i.e., the out-of-band ones, can be calculated by various models. The two more common ways are based on the Adjacent Channel Leakage Ratio (ACLR) and on the SEM [EuCO16], both defining attenuations to be applied to the power contained within the transmission band of a system in order to reduce interference into systems using adjacent frequencies. The EIRP of the interferer, the power contained within the transmission band of the interferer, can be calculated by:

$$P_{EIRP\,[\mathrm{dBm}]}^{int} = P_{t\,[\mathrm{dBm}]}^{int} - L_{t\,[\mathrm{dB}]}^{int} + G_{t\,[\mathrm{dBi}]}^{int} \tag{3.11}$$

where:

- P_t^{int}: transmission power of the interferer;
- L_t^{int}: transmitter losses of the interferer;
- G_t^{int}: transmitter antenna gain of the interferer.

The ACLR approach defines attenuations based on channels adjacent to the channel used by the system itself. Because one is analysing (not only but also) interference scenarios between systems that use different channel bandwidths, this method cannot be applied, hence, one uses the SEM approach which specifies attenuations depending on the frequency offset between the interferer and the victim channels. The SEM or transmission's mask of the interferer and the SEM attenuation (for a certain frequency offset) concepts are represented in Figure 3.4.

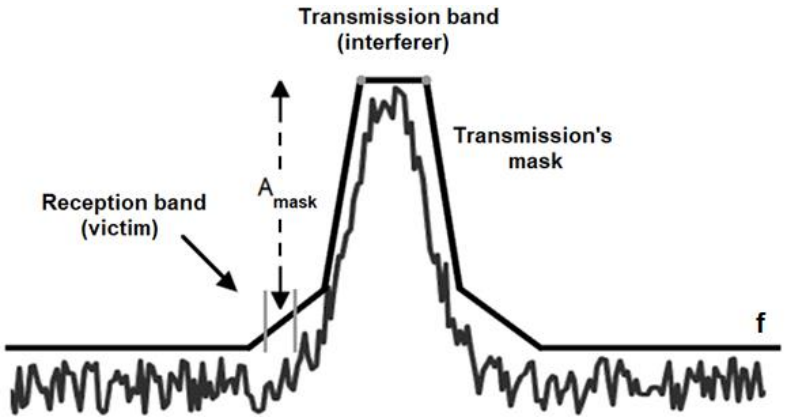

Figure 3.4 – Transmission's mask concept (adapted from [Vere18]).

The SEM attenuation is specified in different units by the specifications of the systems, depending on the system that one is dealing with [Vere18]. The SEM attenuation is specified normally in terms of relative power density, in dB/Hz, rather than in dB, but it can be also specified in terms of dB referenced to the whole channel's bandwidth of the interferer or in terms of dB referenced to the bandwidth of the spectrum analyser that is used to perform the measurement (to define the mask), for example. Considering that the SEM attenuation is provided in terms of dB referenced to the bandwidth of the spectrum

analyser, the SEM attenuation is defined for a set of frequency offset intervals and each interval can have its own reference bandwidth. In either of the previous cases, if the SEM attenuation is not defined in dB/Hz, it must be normalised.

Because one is dealing with power densities, the value of the SEM attenuation also depends on the channel's bandwidth of the victim. In practice, the SEM mask should be integrated over the channel's bandwidth of the victim to obtain the corresponding SEM attenuation because, as one can observe in Figure 3.4, the SEM presents a certain slope within the reception band of the victim. One does an approximation to get around the integral by picking the SEM attenuation corresponding to the centre of the reception band and by converting it to the channel's bandwidth of the victim, thus, one can conclude that a wider bandwidth absorbs more energy than a narrowband one. It is also worth mentioning that, according to [EuCO16], in the case of a victim system using OFDMA, the channel's bandwidth is given by (3.6), that is, only interference into the allocated subcarriers is considered. The out-of-band emission mask power, given the SEM attenuation, can be calculated by [Vere18]:

$$\begin{aligned} P_{mask\,[\mathrm{dBm}]} &= P^{int}_{EIRP\,[\mathrm{dBm}]} - A_{mask\,[\mathrm{dB/Hz}]} + 10\log\Delta f^{vic}_{[\mathrm{Hz}]} \\ &= P^{int}_{EIRP\,[\mathrm{dBm}]} - A_{mask\left[\mathrm{dB}/\Delta f^{vic}_{[\mathrm{Hz}]}\right]} \end{aligned} \tag{3.12}$$

where:

- A_{mask}: spectrum emission mask attenuation at the frequency offset being considered.

The OOBI power can be calculated by using the out-of-band emission mask power in a simple link budget calculation. No attenuation is applied by the victim's receiver, because interfering signals fall within the reception band. The reception band of the victim is covered in more detail in the next subsection. The OOBI power at the receiver's input can be calculated as follows [Vere18]:

$$I_{OOBI\,[\mathrm{dBm}]} = P_{mask\,[\mathrm{dBm}]} - L^{int}_{p\,[\mathrm{dB}]} + G_{r\,[\mathrm{dBi}]} - L_{r\,[\mathrm{dB}]} \tag{3.13}$$

where:

- L^{int}_{p}: path loss of the interfering signal.

3.2.4 Blocking-based Interference Models

While OOBI model deals with out-of-band emissions that fall within the reception band of the victim, the BBI one intends to address emissions within the transmission band of the interferer that do not fall within the reception band of the victim, but which are still captured due to insufficient selectivity attenuation of the victim's receiver. The key factor in this model is, therefore, the selectivity attenuation applied by the victim's receiver at the frequency offset being considered between the interferer and the victim channels, unlike in the OOBI model, where the key factor is the SEM attenuation. The selectivity attenuation is mainly determined by the IF filter of the victim's receiver [Vere18] and it is represented by the receiver's mask concept, Figure 3.5.

In the specifications of the systems, the selectivity attenuation can be given in terms of Adjacent Channel Selectivity (ACS) (usually for close frequency offsets), given in dB, or, it can be derived from the blocking

power (usually for interferers far away in frequency), expressed in dBm. The ACS defines an attenuation to be applied to an adjacent channel, considering that the channel's bandwidth of both the interferer and the victim systems are equal and that both systems use the same technology. The blocking power can be considered a relative definition of the selectivity attenuation [Vere18].

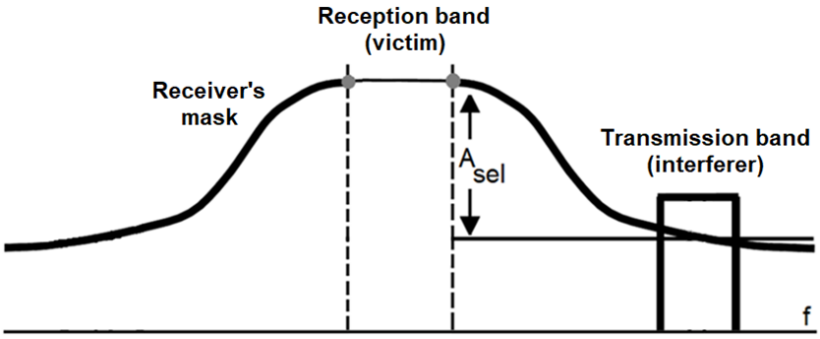

Figure 3.5 – Receiver's mask concept (adapted from [Vere18]).

The blocking power represents the level of the interfering signal, at the offset being considered between the interferer and the victim channels, causing a certain desensitisation of the victim's receiver. The blocking power is the result of a measurement test performed to assess the susceptibility of the receiver of being blocked by interfering signals, where the victim's receiver is fed with the desired signal with a power above the sensitivity of the receiver by a certain interval. The interfering signal is then increased until the receiver is desensitised. The blocking power is normally specified for Continuous Wave (CW) interfering signals in the specifications of the systems. The selectivity attenuation can be derived from the blocking power as follows [EuCO16], [CEPT11]:

$$A_{sel\,[\mathrm{dB}]} = P_{block\,[\mathrm{dBm}]} - N_{[\mathrm{dBm}]} - \beta_{IN\,[\mathrm{dB}]} \tag{3.14}$$

where:

- P_{block}: blocking power.

To simplify the problem, the selectivity attenuation is considered to be flat over the transmission band of the interferer, that is, the slope of the mask is neglected as represented in Figure 3.5, this approximation [Vere18] being in agreement with the fact that the selectivity attenuation is not defined as a power density.

When the interference is generated at the transmitter's side like in the OOBI model, the calculation of interference power is directly referred to the input of the victim's receiver. Here, the interference power is referred to the IF output (because the selectivity is mainly determined by the IF filter), but because one does not have access to the internal gains of the receiver, one assumes an equivalent power at the input of the victim's receiver. According to [Vere18], which also neglects the internal gains of the receiver, the BBI power can be calculated as follows for a generic victim system, being applicable to GSM-R and BBRS:

$$I_{BBI\,[\mathrm{dBm}]}^{(GSM-R,\,BBRS)} = P_{EIRP\,[\mathrm{dBm}]}^{int} - L_{p\,[\mathrm{dB}]}^{int} + G_{r\,[\mathrm{dBi}]} - L_{r\,[\mathrm{dB}]} - A_{sel\,[\mathrm{dB}]} \tag{3.15}$$

In case the victim uses OFDMA (LTE-R), the BBI power is considered to be equally divided among all the subcarriers that compose the victim channel, thus, the BBI power referred to the allocated subcarriers being interfered can be calculated as follows [EuCO16]:

$$I_{BBI\,[\mathrm{dBm}]}^{(LTE-R)} = P_{EIRP\,[\mathrm{dBm}]}^{int} - L_{p\,[\mathrm{dB}]}^{int} + G_{r\,[\mathrm{dBi}]} - L_{r\,[\mathrm{dB}]} - A_{sel\,[\mathrm{dB}]} + 10\log\left(\frac{n_{sc}^{aloc}}{n_{sc}^{tot}}\right) \quad (3.16)$$

where:

- n_{sc}^{tot}: number of subcarriers that compose the victim channel.

3.2.5 Intermodulation-based Interference Models

The interference calculations regarding IBI are not as straightforward as the calculations presented in the other two interference models. To simplify this analysis, one assumes that the third-order IMPs are generated at the LNA of the victim's receiver, [Vere18]. Some steps have to be followed:

- to calculate the power of each received interfering tone at the input of the LNA;
- to determine how many third-order IMPs fall within the IF passband of the victim's receiver;
- to calculate the power of each third-order IMP referred to the input of the LNA;
- to sum all the equivalent input powers of all the third-order IMPs that lie within the IF passband.

To study IBI, one divides an interfering signal into equally spaced frequency components that one calls tones, as represented in Figure 3.6. This procedure is based on the fact that the interfering signal is a wideband one, but it can be also adapted to narrowband interfering signals. In the case of narrowband interfering signals such as GSM, one can simulate IBI by assuming that each narrowband GSM signal corresponds to a single tone and that each GSM carrier is equally spaced.

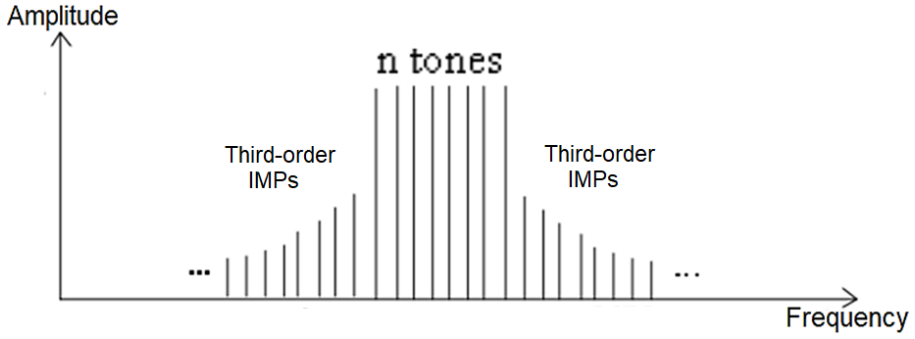

Figure 3.6 – Division of the interfering signal into equally spaced tones (extracted from [CaPe99]).

These tones mix together at the LNA and generate third-order IMPs. The EIRP of each tone can be calculated by linearly dividing the EIRP of the interfering signal (the linear sum of the EIRP of each GSM signal in the case of interfering GSM signals) by the number of equally spaced tones as follows:

$$P_{EIRP/tone}^{int} = \frac{P_{EIRP}^{int}}{n_{tones}} \quad (3.17)$$

where:

- n_{tones}: number of equally spaced interfering tones.

Next, one needs to calculate the power of each tone at the input of the LNA (after the RF filter), the first step mentioned above, for which one uses a simple link budget equation that takes the attenuation applied by the RF filter into account. The RF filter attenuation is applied instead of the IF filter attenuation because third-order IMPs are generated at the RF stage of the receiver (before the IF stage). These third-order IMPs can fall within the IF passband of the victim's receiver. The power of each tone at the input of the LNA after being filtered out by the RF filter, $A_{RFfilter}$, can be calculated as follows:

$$P^{in}_{rtone\,[\mathrm{dBm}]} = P^{int}_{EIRP/tone\,[\mathrm{dBm}]} - L^{int}_{p\,[\mathrm{dB}]} + G_{r\,[\mathrm{dBi}]} - L_{r\,[\mathrm{dB}]} - A_{RFfilter\,[\mathrm{dB}]} \tag{3.18}$$

The second step is to calculate the number of third-order IMPs that fall within the IF passband. In fact, not only these third-order IMPs can increase the noise floor of the receiver (all the third-order IMPs that are captured by the receiver's mask contribute to this effect, but one is neglecting the ones that are then filtered out by the IF filter). Despite that, it is a good approximation, because third-order IMPs suffering IF attenuation will have almost no contribution, as the approach taken in [ITUR07]. One considers, therefore, third-order IMPs that fulfil the condition:

$$f_c^{vic} - 0.5 \times \Delta f^{vic} \leq f_{IMP} \leq f_c^{vic} + 0.5 \times \Delta f^{vic} \tag{3.19}$$

In order to count the IMPs, one needs to know how they are generated. The non-linear behaviour of the LNA can be approximated by the Taylor series, which is defined as follows [Vere18]:

$$x_{out\,[\mathrm{V}]}(t) = \sum_{l=0}^{\infty} a_{l\,[V^{-(l-1)}]} {x_{in\,[\mathrm{V}]}}^{l}(t) \tag{3.20}$$

where:

- a_l: coefficients of the low noise amplifier;
- x_{in}: input signal of the Taylor series.

The Taylor series takes CWs as inputs. Although one assumes equally spaced tones with a certain bandwidth, one does now a second approximation by assuming that each tone is a CW. A two-tone test is usually used to evaluate the intermodulation behaviour, that is, the LNA generates third-order IMPs by mixing two tones, in this case, two CWs. The sum of two CWs with equal amplitude is therefore considered as input (phases are considered to be zero for simplicity of the calculations):

$$x_{in\,[\mathrm{V}]}(t) = U_{\,[\mathrm{V}]} \cos(2\pi f_1 t) + U_{\,[V]} \cos(2\pi f_2 t) \tag{3.21}$$

where:

- U: amplitude of the continuous waves;
- f_1: frequency of the first interfering tone;
- f_2: frequency of the second interfering tone.

One considers only the expansion of the Taylor series till the third order, because the resulting signals will be smaller for higher exponents. Additionally, one is only interested in IMPs that fall near the transmission band, the others being filtered out by the IF filter. Under these assumptions, the signal at the output of the LNA is given by [Vere18]:

$$x_{out\,[\mathrm{V}]}(t) \simeq \left(a_1 U_{[\mathrm{V}]} + \frac{9}{4} a_{3[V^{-2}]} {U_{[\mathrm{V}]}}^3\right)\cos(2\pi f_1 t) + \left(a_1 U_{[\mathrm{V}]} + \frac{9}{4} a_{3[V^{-2}]} {U_{[\mathrm{V}]}}^3\right)\cos(2\pi f_2 t) +$$

$$+\left(\frac{3}{4} a_{3[V^{-2}]} {U_{[\mathrm{V}]}}^3\right)\cos(2\pi(2f_1 - f_2)t) + \left(\frac{3}{4} a_{3[V^{-2}]} {U_{[\mathrm{V}]}}^3\right)\cos(2\pi(2f_2 - f_1)t) \quad (3.22)$$

The frequency of each generated third-order IMP can be, therefore, calculated by:

$$f_{IMP} = 2f_1 - f_2 \quad (3.23)$$

$$f_{IMP} = 2f_2 - f_1 \quad (3.24)$$

The third step is to calculate the power of third-order IMPs referred to the input of the LNA. For that, one could use (3.22), but the coefficients of the LNA are usually not known. One takes a different approach, based on IP3, a figure of merit of the LNAs, which represents the point where a certain power at the input of the LNA causes the tones and the third-order IMPs to have the same output power as represented in Figure 3.7. The Input Third-Order Intercept Point (IIP3) and the Output Third-order Intercept Point (OIP3) are, respectively, the input and output powers corresponding to this point. The OIP3 is, in practice, never reached, because the LNA will saturate/overload before that (in the saturation/overload state the gain of the LNA is reduced and the LNA starts compressing all the signals including the desired ones) as represented in Figure 3.7. A question could be raised concerning the non-linearity of the LNA, which comes from the fact that the region commonly considered as the linear region (in which the device is supposed to operate) is in fact not really linear [Vere18].

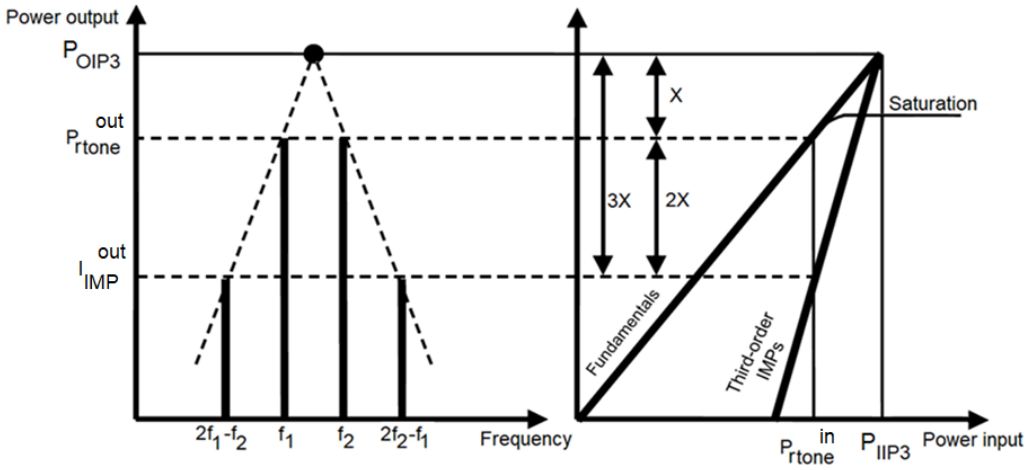

Figure 3.7 – Third-order intercept point concept (adapted from [Vere18]).

One can observe in Figure 3.7 the relationship between the input power and output power of both tones (represented as fundamentals) and the third-order IMPs: the fundamentals have a slope of 1 while the third-order IMPs have a slope of 3, which is the reason why one can define IP3. By using the relationship between the slopes, one can calculate the power of the IMPs (generated by two tones) referred to the input of the LNA as follows [Vere18], [ITUR07]:

$$I^{in}_{IMP\,[\mathrm{dBm}]} = 3\,P^{in}_{rtone\,[\mathrm{dBm}]} - 2\,P_{IIP3\,[\mathrm{dBm}]} \quad (3.25)$$

where:

- P_{IIP3}: input third-order intercept point power.

One calculates the power referred to the input of LNA not only because one does not have access to the gain of the LNA but also because OOBI and BBI powers are calculated taking the receiver's input as reference. For this approach, one uses the IIP3 in (3.25), where the IIP3 value can be obtained via datasheets of LNAs. Knowing the number of third-order IMPs that lie within the IF passband, n_{IMP}, one can calculate the IBI power (referred to the input of the LNA) as follows:

$$I_{IBI\ [\mathrm{mW}]} = \sum_{n_{IMP}} I_{IMP\ [\mathrm{mW}]}^{in} \tag{3.26}$$

3.2.6 Propagation Models

To calculate the path loss of both the desired and interfering signals one needs to define propagation models. The choice of the propagation models depends on the scenarios that one intends to analyse. For the analyses of GSM-R and LTE-R, rural, suburban, and urban scenarios are assumed. In this case, the same scenario is considered for both the desired and interfering signals. For the analysis of BBRS different scenarios are considered for the desired and interfering signals: for the desired BBRS signal, an outdoor Line of Sight (LoS) scenario is assumed, which is according to the low propagation distances at stake, while for the signal interfering with BBRS one considers two scenarios. The first scenario is the same as the one used for the desired signal, and the second one is an indoor scenario aiming to cover common cases where Wi-Fi devices (interference sources considered for BBRS analysis) are being used inside a building that is close to a rail track. Three propagation models are used:

- Free-space model [Corr18];
- Okumura-Hata model [Corr18];
- Winner II model [KMHZ07].

The free-space model gives the path loss assuming LoS between the transmitter and the receiver, and that the earth's surface does not affect signal propagation. The free-space model is very useful for the sake of performance comparison with other models, defining path loss as follows [Corr18]:

$$L_{p\ [\mathrm{dB}]}^{(FS)} = 32.44 + 20\log\left(d_{\ [\mathrm{km}]}\right) + 20\log\left(f_{c\ [\mathrm{MHz}]}\right) \tag{3.27}$$

where:

- d: propagation distance.

The Okumura-Hata model covers rural, suburban and urban scenarios, and is being widely used to study signal propagation in HSRs. It is valid for systems working in frequencies ranging from 150 MHz to 1500 MHz and for distances ranging from 1 km to 20 km. A parameter and a correction factor need to be applied to the general expression of this model, depending on the scenario that one intends to cover, because the general expression is based on an urban flat scenario. The general expression of the Okumura-Hata model can be defined as follows [Corr18]:

$$L_{p\ [\mathrm{dB}]}^{(OH)} = 69.55 + 26.16\log\left(f_{c\ [\mathrm{MHz}]}\right) - 13.82\log\left(h_{bs\ [\mathrm{m}]}\right) +$$

$$+\left[44.90 - 6.55\log\left(h_{bs\ [\mathrm{m}]}\right)\right]\log\left(d_{\ [\mathrm{km}]}\right) - H_{mu\ [\mathrm{dB}]}\left(h_{ms\ [\mathrm{m}]}, f_{c\ [\mathrm{MHz}]}\right) - \sum c_{f\ [\mathrm{dB}]} \tag{3.28}$$

where:

- h_{bs}: height of the base station;
- h_{ms}: height of the mobile station;
- H_{mu}: Okumura-Hata model parameter;
- c_f: Okumura-Hata model correction factor.

The Okumura-Hata model parameter is defined as follows:

$$H_{mu\,[\mathrm{dB}]} = \begin{cases} \left[1.10\log\left(f_{c\,[\mathrm{MHz}]}\right) - 0.70\right]h_{ms\,[\mathrm{m}]} - \left[1.56\log\left(f_{c\,[\mathrm{MHz}]}\right) - 0.80\right], & \text{rural and suburban} \\ 8.29\log^2\left(1.54\,h_{ms\,[\mathrm{m}]}\right) - 1.10, & f_c \leq 200\ \mathrm{MHz\ urban} \\ 3.20\log^2\left(11.75\,h_{ms\,[\mathrm{m}]}\right) - 4.97, & f_c \geq 400\ \mathrm{MHz\ urban} \end{cases} \quad (3.29)$$

The correction factor to apply to the general Okumura-Hata model expression can be calculated by (in case of an urban scenario there is no need to apply any correction factor):

$$c_{f\,[\mathrm{dB}]} = \begin{cases} 4.78\log^2\left(f_{c\,[\mathrm{MHz}]}\right) - 18.33\log\left(f_{c\,[\mathrm{MHz}]}\right) + 40.9, & \text{rural} \\ 2.00\log^2\left(\frac{f_{c\,[\mathrm{MHz}]}}{28}\right) + 5.40, & \text{suburban} \end{cases} \quad (3.30)$$

The Okumura-Hata model is valid for distances higher than 1 km, but one needs to cover also interfering sources close deployed to the rail track, hence, an extension to the Okumura-Hata model, the two-slope extension, is used [Rahn08]. This approach is based on the free-space model and it is used to better predict the signal behaviour for distances lower than 1 km taking a stronger LoS contribution into account, being defined as follows:

$$L_{p\,[\mathrm{dB}]}^{(OH\ near-site)} = L_{p\,[\mathrm{dB}]}^{(OH)}\left(d_{bp\,[\mathrm{km}]}^{(OH)}\right) + \\ + \left[\frac{L_{p\,[\mathrm{dB}]}^{(OH)}\left(d_{bp\,[\mathrm{km}]}^{(OH)}\right) - L_{p\,[\mathrm{dB}]}^{(FS)}(0.001)}{\log\left(d_{bp\,[\mathrm{km}]}^{(OH)}\right) - \log(0.001)}\right]\left[\log\left(d_{\,[\mathrm{km}]}\right) - \log\left(d_{bp\,[\mathrm{km}]}^{(OH)}\right)\right] \quad (3.31)$$

where:

- d_{bp}: breakpoint distance (distance at which the Okumura-Hata model becomes valid (1 km)).

The Winner II model can be applied to any wireless system with frequencies ranging from 2 GHz to 6 GHz with up to 100 MHz bandwidth, the “D2 – Moving Networks” scenario being suitable for railway communications, which assumes outdoor LoS conditions, being valid for distances up to 10 km and train speeds up to 350 km/h (taking the large Doppler variability that signals are subjected to into account). The general expression of the Winner II model can be defined as follows [KMHZ07]:

$$L_{p\,[\mathrm{dB}]}^{(WII)} = K_a\log\left(d_{\,[\mathrm{m}]}\right) + K_b + K_c\log\left(h_{bs\,[\mathrm{m}]}\right) + K_d\log\left(\frac{f_{c\,[\mathrm{GHz}]}}{5}\right) \quad (3.32)$$

where:

- $K_{a,b,c,d}$: Winner II model parameters, given in Table 3.1.

The Winner II model parameters depend on the propagation distance. The breakpoint distance makes the distinction between which parameters to use, being calculated as follows, [KMHZ07]:

$$d_{bp\,[\mathrm{m}]}^{(WII)} = \frac{4\, h_{bs\,[\mathrm{m}]}\, h_{ms\,[\mathrm{m}]}\, f_{c\,[\mathrm{MHz}]}}{300} \tag{3.33}$$

Table 3.1 – Winner II model parameters (extracted from [KMHZ07]).

Condition	K_a	K_b	K_c	K_d
$(10\ \mathrm{m} < d < d_{bp}^{WII})$	21.5	44.2	0	20
$(d_{bp}^{WII} < d < 10\ \mathrm{km})$	40	$10.5 - 18.5 \log h_{ms\,[\mathrm{m}]}$	−18.5	1.5

To cover the already mentioned indoor scenario, one sums an extra indoor attenuation of 17 dB to the Winner II model expressions, which can be assumed when buildings are considered as traditional (not thermally-efficient), [ITUR19].

3.2.7 Throughput Models

This section presents the equations that establish the relationship between throughput and SNIR. The throughput offered by each system depends on the Modulation and Coding Scheme (MCS) that the system is making use of. GSM-R, as already stated, makes use of GMSK as its modulation method, being considered that it can offer the voice service for an SNIR higher than 9 dB [CEPT07]. LTE-R and BBRS, on the other hand, make use of various MCSs.

Different MCSs offer different throughputs for the same SNIR. The objective is to use, at any instant, the MCS that offers the highest throughput (for a certain SNIR), which can be achieved with AMC. It is, therefore, necessary to define equations that establish the relationship between SNIR and throughput for each MCS. The following analysis will take models for LTE and Wi-Fi (which are LTE-R and BBRS counterparts) into account.

LTE-R, contrary to BBRS, uses OFDMA as already mentioned, hence, a user can be allocated with a different number of subcarriers at any time. The throughput depends on the number of allocated sub-carriers and this factor has to be accounted for in LTE's throughput models. The higher the number of allocated subcarriers, the higher number of RBs, and, consequently, the offered throughput (for the same SNIR).

The equations used here for establishing the relationship between throughput and SNIR for LTE-R were derived by Third Generation Partnership Project (3GPP) based on real throughput performance tests [3GPP11]. The tests were performed using 2x2 MIMO in DL and 50 RBs allocated to the user. Three expressions were deduced taking QPSK, 16-QAM, and 64-QAM into account. In order to account for single stream scenarios (which is the one considered in this thesis for the interference analysis) instead of MIMO, one adds a factor of 0.5 to the expressions.

The throughput offered by LTE-R can be calculated as follows:

$$R_{b\,[\mathrm{Mbps}]}^{(LTE-R)} = \frac{2.34201}{14.0051 + e^{-0.577897\rho_{NI\,[\mathrm{dB}]}}} \times n_{RB}^{aloc} \times 0.5, \qquad \text{for QPSK r} = 1/3 \tag{3.34}$$

$$R_{b\,[\mathrm{Mbps}]}^{(LTE-R)} = \frac{0.0476131}{0.0926275 + e^{-0.29583\rho_{NI\,[\mathrm{dB}]}}} \times n_{RB}^{aloc} \times 0.5, \qquad \text{for } 16-\text{QAM r} = 1/2 \tag{3.35}$$

$$R_{b\,[\mathrm{Mbps}]}^{(LTE-R)} = \frac{0.0264058}{0.0220186 + e^{-0.24491\rho_{NI\,[\mathrm{dB}]}}} \times n_{RB}^{aloc} \times 0.5, \qquad \text{for } 64-\text{QAM r} = 3/4 \tag{3.36}$$

where:

- n_{RB}^{aloc}: number of resource blocks allocated to the user.

The curves obtained with LTE's throughput equations for the case of a single stream scenario and 25 RBs in use, are represented in Figure 3.8. It is possible to see that the highest throughput is offered by different MCSs with the variation of the SNIR. This is where the use of AMC comes in, allowing to always extract the maximum throughput possible. AMC is represented with a dotted line in Figure 3.8.

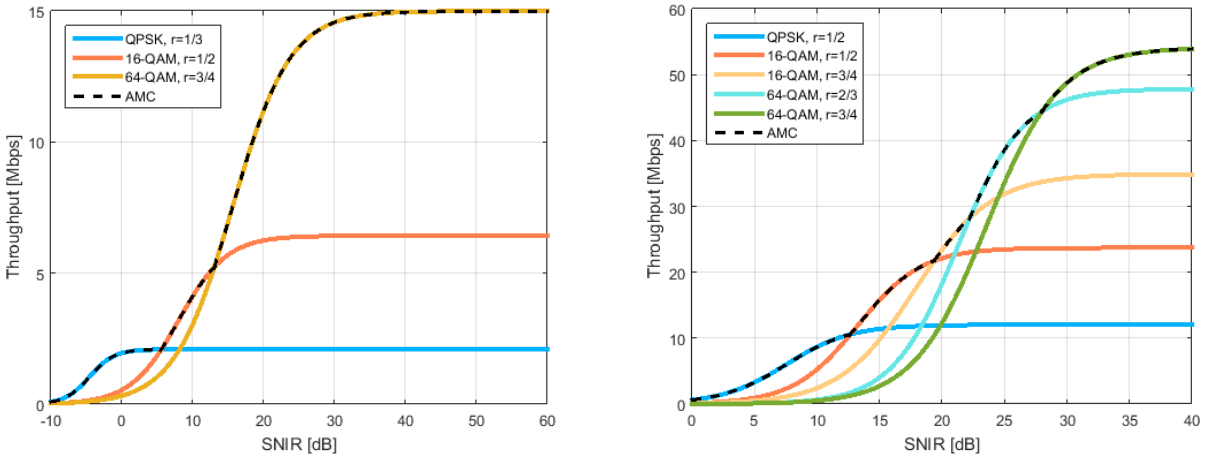

a) LTE (25 RBs allocated, single stream). b) Wi-Fi (20 MHz signal, single stream).

Figure 3.8 – Throughput offered by each MCS of each system.

The throughput models for BBRS, unlike LTE-R's, were not extracted but deduced by extrapolation from throughput curves specific for Wi-Fi given in [BJHS03]; the same approach is used also in [Delg18]. An example of the throughput offered by a real Wi-Fi system (20 MHz channel without MIMO) in a Rayleigh propagation channel is given in [BJHS03]. One extrapolates several points for several MCSs and fitting is performed through MATLAB to the same equation that served as the starting point for the models deducted by 3GPP for LTE. The equations presented below take therefore a 20 MHz signal and a Single-input and Single-output (SISO) scenario (which is the one considered in this thesis for the interference analysis) into account. Expressions are deducted for five MCSs.

The throughput offered by BBRS can be calculated as follows:

$$R_{b\,[\mathrm{Mbps}]}^{(BBRS)} = \frac{0.6505}{0.05409 + e^{-0.3865\rho_{NI\,[\mathrm{dB}]}}}, \qquad \text{for QPSK r} = 1/2 \tag{3.37}$$

$$R_{b\,[\text{Mbps}]}^{(BBRS)} = \frac{0.1384}{0.005836 + e^{-0.3887\rho_{NI\,[\text{dB}]}}}, \quad \text{for } 16-\text{QAM } r = 1/2 \tag{3.38}$$

$$R_{b\,[\text{Mbps}]}^{(BBRS)} = \frac{0.0958}{0.002745 + e^{-0.3302\rho_{NI\,[\text{dB}]}}}, \quad \text{for } 16-\text{QAM } r = 3/4 \tag{3.39}$$

$$R_{b\,[\text{Mbps}]}^{(BBRS)} = \frac{0.01433}{0.0002996 + e^{-0.3815\rho_{NI\,[\text{dB}]}}}, \quad \text{for } 64-\text{QAM } r = 2/3 \tag{3.40}$$

$$R_{b\,[\text{Mbps}]}^{(BBRS)} = \frac{0.016465}{0.0003045 + e^{-0.3437\rho_{NI\,[\text{dB}]}}}, \quad \text{for } 64-\text{QAM } r = 3/4 \tag{3.41}$$

The curves obtained with the Wi-Fi's throughput equations for the case of a single stream scenario are represented in Figure 3.8. As in LTE's case, the throughput offered through AMC for the BBRS case is represented in Figure 3.8 with a dotted line.

3.3 Model Implementation

In this section, one indicates how all previous equations were implemented together in MATLAB to calculate each one of the model outputs. The flowchart represented in Figure 3.9 helps in understanding how the interference power and the interference-free region distance are calculated. These interference estimation results are then used to calculate both the maximum communication distance and the capacity loss as represented in Figure 3.10.

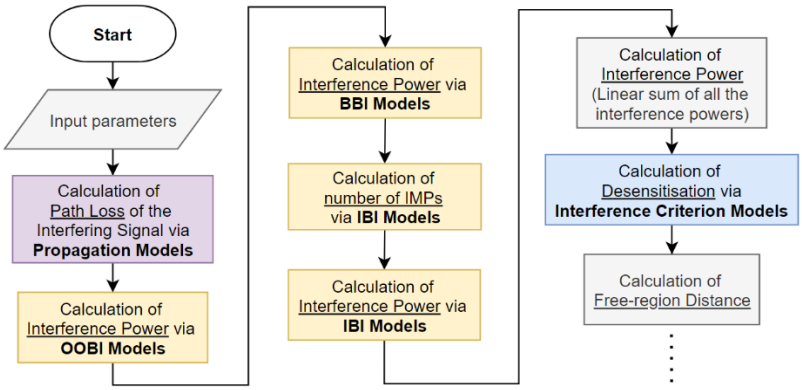

Figure 3.9 – Flowchart of the MATLAB's script used to calculate I and $d_{free-region}$.

First, the path loss of the interfering signal is computed for a vector of interference distances using the propagation models. Then, one calculates the interference powers corresponding to each interference type being studied (OOBI, BBI and IBI), again, for that same vector of interference distances, using OOBI, BBI and IBI models. One has to note that before the IBI power calculation, the intermodulation of the interfering signal is performed and the third-order IMPs that fall within the IF passband of the victim's receiver are counted. After that, all the interference powers are linearly summed (for each interference distance). Then, the total desensitisation is calculated using the interference criterion models and it is compared with the interference margin to obtain the interference-free region distance. Having computed

the total desensitisation, both the maximum communication distance and the capacity loss are calculated. An additional input to those shown in Figure 3.1 needs to be provided for the calculation of each one of these two outputs. For the maximum communication distance calculation, a fixed throughput is asked for input (in case of LTE-R or BBRS). For the capacity loss calculation, a fixed maximum communication distance is asked for input.

For the maximum communication distance calculation, first, the path loss of the desired signal is calculated for a vector of distances using the propagation models. Then, using the desired signal models, the desired signal power is calculated (for that same vector of distances). The next step is to calculate the required SNIR corresponding to the throughput that is asked for input. For that, the throughput models are used in case the system in study is either LTE-R or BBRS; otherwise, an SNIR of 9 dB is assumed for GSM-R. The total desensitisation (for each interference distance), calculated using the flowchart represented in Figure 3.9, is then compared with the interference margin. If the desensitisation is lower than the interference margin, a maximum communication distance that provides a power equal to the receiver sensitivity at the input of the victim's receiver is enough; otherwise, a power higher than the receiver sensitivity is required and, consequently, a lower maximum communication distance.

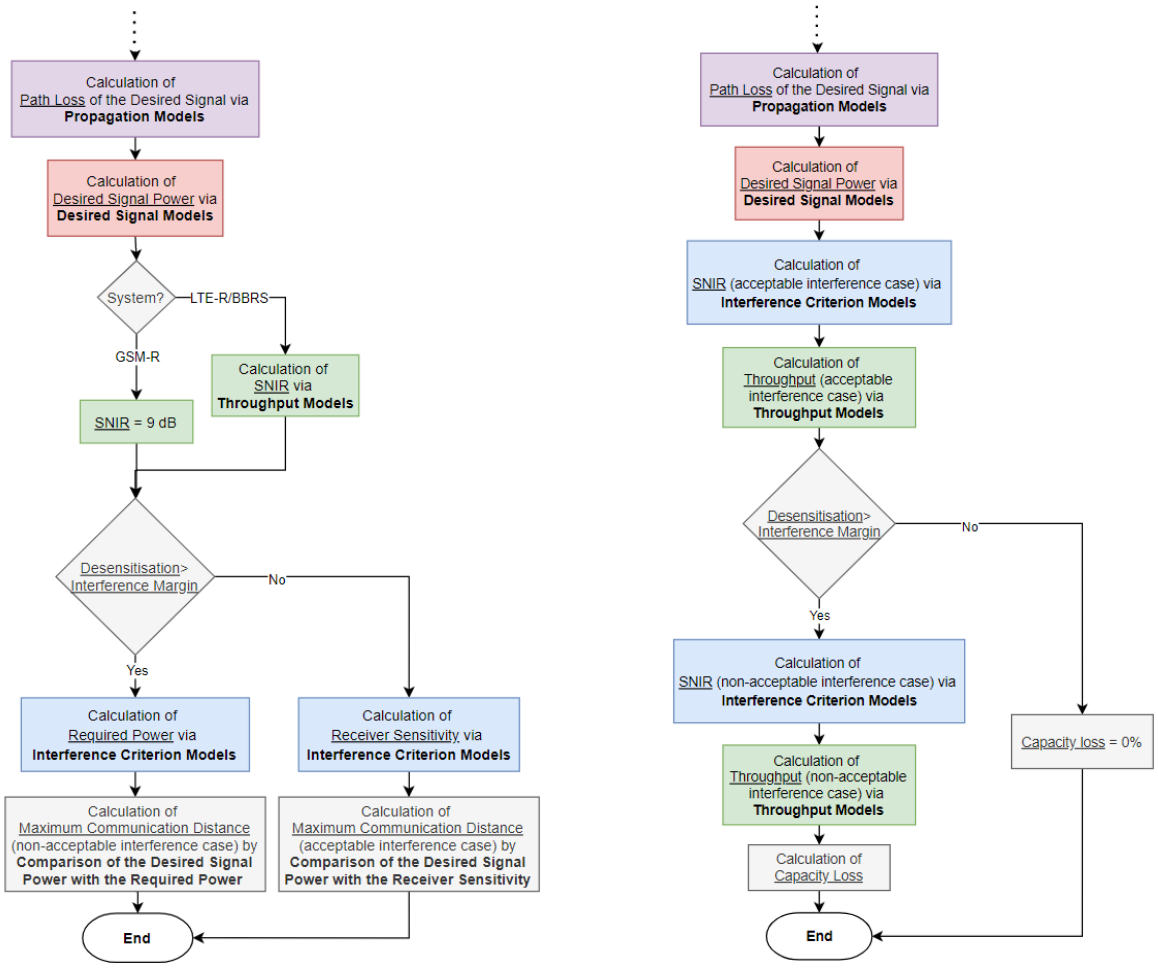

a) $d_{max.}$ b) Capacity loss.

Figure 3.10 – Flowchart of the MATLAB's script used to calculate d_{max} and capacity loss.

For the capacity loss calculation, the desired signal power is only calculated for a single maximum communication distance that is asked for input, and the throughput models are used for throughput calculations instead of SNIR calculations. If the total desensitisation is lower than the interference margin, then that interference distance being analysed leads to an acceptable interference case and there is no capacity loss; otherwise, the throughput and the corresponding capacity loss are calculated.

3.4 Model Assessment

After having implemented the model in MATLAB an assessment of the results had to be done. The various tests that one performed for the assessment of the model are presented in Table 3.2.

Table 3.2 – Model assessment tests.

Test ID	Description
1	To verify if the inputs are being correctly assigned to the variables.
2	To compare the path loss given by the different propagation models.
3	To check if the generated third-order IMPs are according to calculator ones.
4	To check if the third-order IMPs are being correctly counted.
5	To compare the interference powers of OOBI, BBI and IBI.
6	To compare the results with results from other authors.

One can see in Figure 3.11 that both the Okumura-Hata model and the Winner II model produce coherent results for the scenarios being considered. One can see that the breakpoint distance of the Okumura-Hata model is represented at a distance of 1 km, because the two slope approximation is being used. The breakpoint distance of the Winner II model is represented at a distance of around 1.7 km and is according to the frequency and heights being used for the assessment of this propagation model.

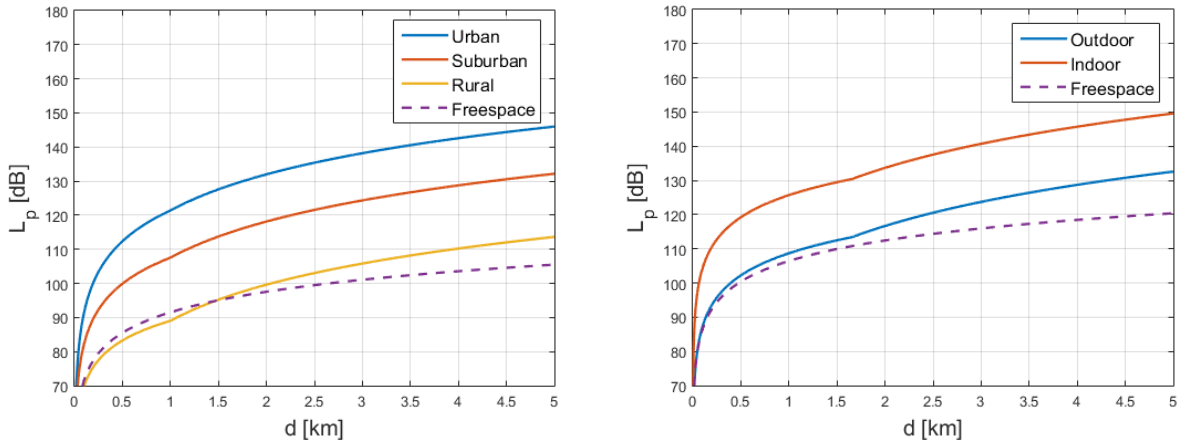

a) Okumura-Hata model (900 MHz). b) Winner II model (5 GHz).

Figure 3.11 – Propagation models.

To check if the intermodulation is being correctly performed one simulated two cases: a simple one (with few tones) and a more complex one. For the simple case, one assumed 3 equally spaced interfering tones located at 51 MHz, 52 MHz, and 53 MHz, and the victim's channel (reception band of the victim) as having 2 MHz (from 48 MHz to 50 MHz). The results are represented in Figure 3.12 and are according to calculated ones where 6 IMPs are generated, 2 of them fall within the victim's channel.

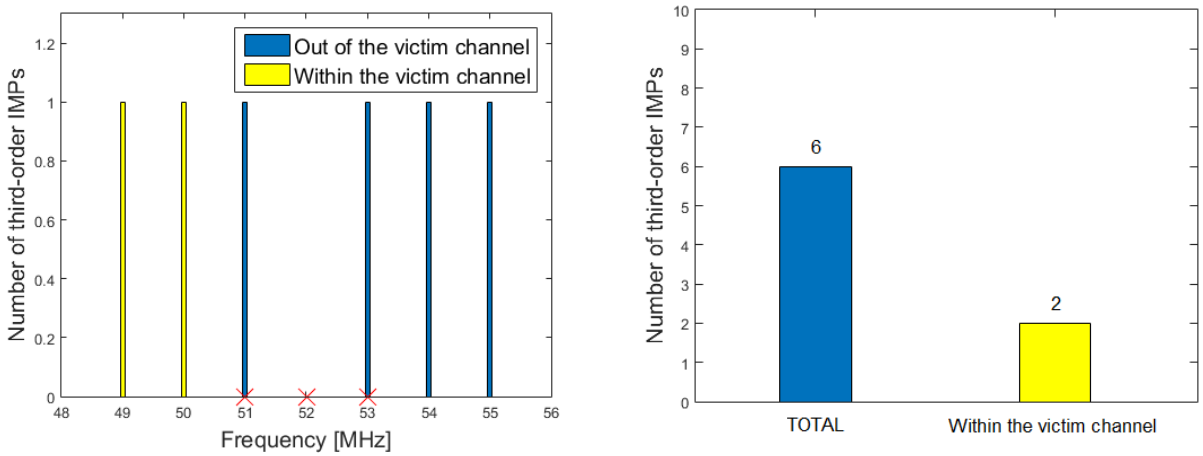

a) Location of third-order IMPs. b) Number of third-order IMPs.

Figure 3.12 – Generation of third-order IMPs by three interfering tones.

For the complex case, one assumed an interfering signal with 5 MHz bandwidth composed of 25 equally spaced tones. The red crosses represent the tones triggering the intermodulation and one can see in Figure 3.13 that the bandwidth of the resulting signal is approximately three times the bandwidth of the interfering signal, which is according to the theory of third-order IMPs.

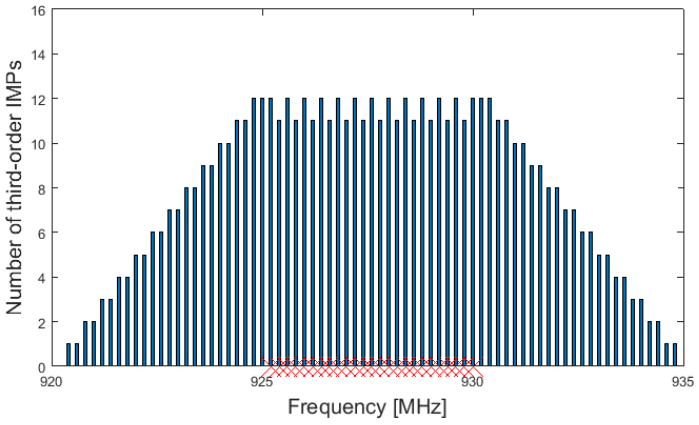

Figure 3.13 – Generation of third-order IMPs by a wideband signal.

The fifth test was to compare the interference powers referring to the different interference types. It is expected that the interference powers that are given by OOBI and BBI models increase in the same proportion. The IBI power is expected to increase faster than OOBI and BBI powers due to the characteristics of third-order IMPs. For this test one simulated a DL interference scenario of public UMTS interfering with GSM-R (2.8 MHz offset between carriers). The behaviours mentioned above were verified as represented in Figure 3.14. According to [SuMi15], interference problems due to IMPs are recorded when the public BS of UMTS is located 250 m or less from the rail track. One can see in

Figure 3.14 that for this simulation IBI starts to be the dominant interference type at an interference distance of around 200 m, a very close result. One can see also that the interference-free region distances, marked by red points, are being correctly computed for each interference type, in this case for a 3 dB interference margin, because an INR of 0 dB corresponds to a desensitisation of 3 dB.

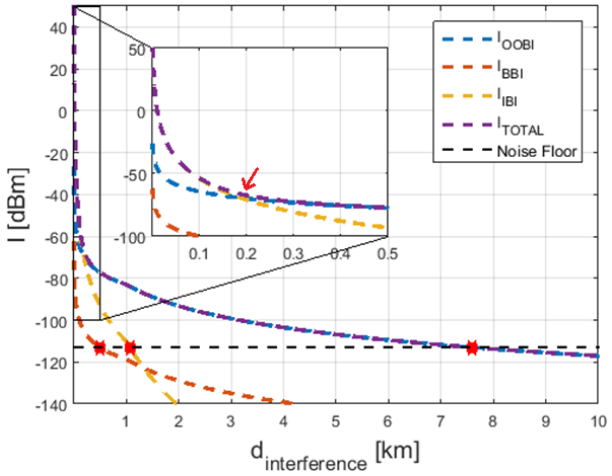

Figure 3.14 – Interference powers for the simulated interference scenario (rural scenario).

The last test was to compare the results with the ones from the ECC Report 96 [CEPT07], which allows one to assess the overall implementation of the model. The same DL interference scenario described above is analysed in [CEPT07]. The input parameters used in [CEPT07] are given in Annex A. Two interference distances are computed in [CEPT07] for two fixed maximum communication distances, and only OOBI is considered. One simulated a case considering OOBI power only and a case considering the sum of OOBI, BBI and IBI powers, which are represented in Figure 3.15 together with the results from [CEPT07]. The slight differences in the results are because in ECC Report 96 the author uses different propagation models (Okumura-Hata model quasi-open areas is used for the desired signal propagation and the free-space model is used for the interfering signal propagation) from the ones used here. One can conclude that the model produces coherent results. The assessment of the capacity loss results by comparison with results from other authors is not shown here because one could not find works that perform those calculations for either LTE-R or BBRS.

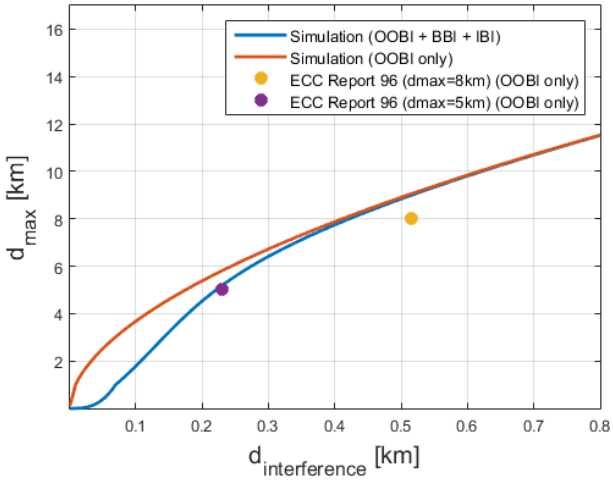

Figure 3.15 – Comparison of simulation results with results from other authors (rural scenario).

Chapter 4

Analysis of Results

In this chapter one starts by presenting the scenarios chosen for the interference analysis and the input values that one assumes to simulate those scenarios. Then, the results of the interference analysis for the three railway telecommunications systems (GSM-R, LTE-R, and BBRS) are presented.

4.1 Scenarios Description

In this section, one presents the scenarios and the values of the model input parameters for the interference analysis. An example of a real spectral analysis collected near a rail track, provided by Thales, is presented in Figure 4.1, showing interference to the DL operation of GSM-R, covering the 919 MHz to 927 MHz range, with the y-axis corresponding to the time domain. This range includes the entire DL frequency band of GSM-R (921 MHz to 925 MHz) as well as the first 2 MHz of the DL E-GSM 900 band (925 MHz to 927 MHz). One can see, in green, that a public GSM BS is using the channel centre at 926.2 MHz, and that, in certain time instants, in yellow and marked by a red rectangle, some energy of the transmission is being leaked across the entire R-GSM band. The goal is to define the scenarios (for the GSM-R analysis) around this case in order to cover not only it but also other ones related to it. Although a similar example of a real interference problem is not presented here for both LTE-R and BBRS, the scenarios for their analyses are chosen based on the worst-case scenario.

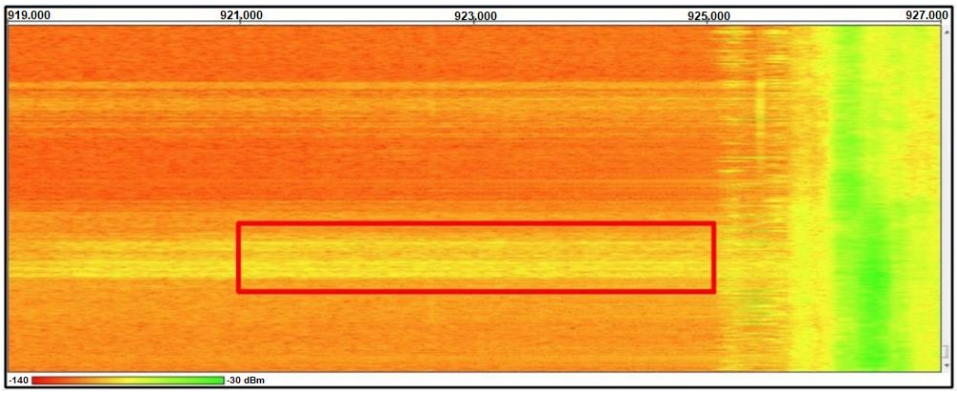

Figure 4.1 – Example of a real spectral analysis (public GSM BS interfering with GSM-R DL).

The scenarios chosen for the interference analysis are represented in Figure 4.2 from both frequency and physical perspectives. For the GSM-R analysis, one considers a public BS of either public GSM or UMTS interfering with its DL operation. According to [CEPT10b], the interference generated by public LTE is not worse than the interference caused by public UMTS to GSM-R, because the SEMs are quite similar. Due to the wideband nature of both systems, one extends the results of public UMTS to public LTE. One bases the GSM-R analysis on various frequency offsets between the channel used by the interferer and the victim, which are chosen based on the interference scenario represented in Figure 4.1. One analyses the 0.4 MHz, 1 MHz and 2 MHz offsets for the public GSM case: the 0.4 MHz is chosen to account for the worst-case scenario remembering that a 200 kHz guard band exists between the two frequency bands; the 1 MHz and 2 MHz offsets are chosen to cover a frequency offset lower and higher, respectively, than the offset represented in Figure 4.1. The offsets for the public UMTS case are chosen to represent the same separation between the edge of the interfering channel and the centre of the GSM-R channel that the 0.4 MHz, 1MHz and 2 MHz offsets represent for the public GSM case.

For the LTE-R analysis, one analyses also the public GSM and the public UMTS interfering with its DL operation, being not based on various offsets but rather on the number of RBs allocated to the user. Taking the available bandwidth considered for LTE-R into account, a user can be allocated from 1 RB to 25 RBs, these two extremes being precisely the considered scenarios. In the 1 RB case, one analyses interference into the nearest RB in frequency to the E-GSM 900 band to account for the worst-case scenario, the first channel of the E-GSM 900 band of either public GSM or public UMTS being considered. It is considered that the LTE-R BS is transmitting over the full available bandwidth in both cases of RB allocation, that is, the transmission power is equally divided per the 25 RBs.

For the BBRS analysis, one analyses two Wi-Fi devices (an AP and a Mobile Device (MD)) interfering with its UL operation (because BBRS presents higher UL throughput requirements compared to DL) [BBRS17]. For an UL interference scenario, the interfering signals interfere with the reception of the desired signals on the wayside APs of BBRS. One bases the BBRS analysis on various adjacent interfering channels (1st 20 MHz adjacent channel, 2nd 20 MHz adjacent channel and 1st 40 MHz adjacent channel) because in the 5 GHz band the Wi-Fi channels are non-overlapping channels and, therefore, they are adjacent to each other.

As already mentioned, for the GSM-R and LTE-R analyses, rural, suburban, and rural scenarios are analysed (considering the same scenario for both the desired and interfering signals). For the BBRS analysis, a rural LoS scenario is assumed for the desired signal propagation, and both an outdoor (rural LoS) and indoor scenarios are analysed for the interfering signal propagation.

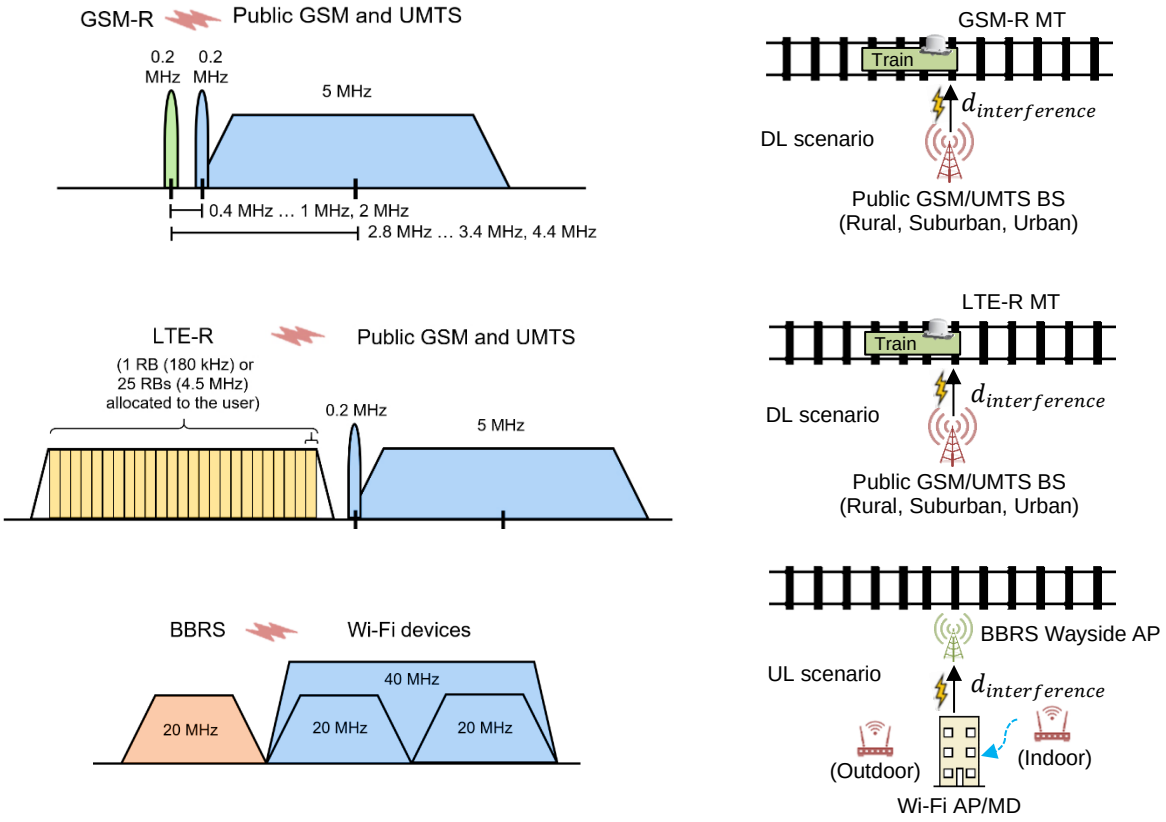

a) Frequency scenarios. b) Physical scenarios.

Figure 4.2 – Scenarios chosen for the interference analysis.

The values of the model input parameters are given in Table 4.1 and Table 4.2. The values assumed for the interfering sources are based on [CEPT11] (public GSM/UMTS) and on [CEPT19b] (Wi-Fi devices). The values assumed for GSM-R and BBRS are provided by Thales, taking real deployments into account, while the values for LTE-R were based on [ETSI19]. The IIP3 is based on [Elli16], and the SEM and selectivity attenuation values are given in Annex B and Annex C, respectively. The RF filter attenuation value is assumed to be 0 dB, but one also simulates a case where an external duplex filter is used (30 dB of RF filter attenuation and 30 dB of additional selectivity attenuation are considered in this case [MICN15]). Only one interference source is considered at a time, that is, the joint effect of two interfering sources is not considered. The worst-case scenario of antenna alignment is considered, that is, the antenna of the interfering source is considered to be pointing to the antenna of the victim.

Table 4.1 – Values of the interferer input parameters for the interference analysis.

Parameter	Public GSM BS	Public UMTS BS	Wi-Fi devices	
			AP	MD
Channel bandwidth (Δf^{int}) [MHz]	0.2	5	20, 40	
Centre frequency (f_c^{int}) [MHz]	925.2 (0.4 MHz) 925.8 (1 MHz) 926.8 (2 MHz)	927.6 (2.8 MHz) 928.2 (3.4 MHz) 929.2 (4.4 MHz)	5865 (1st 20 MHz) 5845 (2nd 20 MHz) 5855 (1st 40 MHz)	
Transmission power (P_t^{int}) [dBm]	43		20	13
Transmitter losses (L_t^{int})[dB]	3		2	
Transmitter antenna gain (G_t^{int}) [dBi]	15		5	3
Height of the base station (h_{bs}) [m]	30		1.5 (Outdoor) 5 (Indoor)	

Table 4.2 – Values of the victim input parameters for the interference analysis.

Parameter	GSM-R	LTE-R	BBRS
Channel bandwidth (Δf^{vic}) [MHz]	0.2	0.180 (1 RB), 4.5 (25 RBs)	20
Centre frequency (f_c^{vic}) [MHz]	924.8	924.55 (1 RB), 922.4 (25 RBs)	5885
Transmission power (P_t^{vic}) [dBm]	46		22
Transmitter losses (L_t^{vic}) [dB]	7.15	5	2.4
Transmitter antenna gain (G_t^{vic}) [dBi]	21	18	14
Receiver antenna gain (G_r) [dBi]	2		18
Receiver losses (L_r) [dB]	2.27	2	
Noise figure (F) [dB]	8		
System margin (M_s) [dB]	7		
Interference margin (M_I) [dB]	3		
Input third-order intercept point (P_{IIP3}) [dBm]	-10		
Height of the base station (h_{bs}) [m]	20		5
Height of the mobile station (h_{ms}) [m]	5		

In the following sections, one presents the results of the interference analysis for the previously defined scenarios and for the defined input values. The results are based on the outputs represented in Figure 3.1 which are taken as metrics for this analysis. First, the interference power at the input of the victim's receiver and the free-region distances are computed for each type of interference individually. Then, taking the sum of all types of interference into account, the maximum communication distances in the acceptable interference and non-acceptable interference cases are presented. In the LTE-R and BBRS analyses, the capacity loss (for a fixed maximum communication distance) is also addressed.

4.2 GSM-R Analysis

Figure 4.3 shows the OOBI power as a function of the interference distance at the input of the GSM-R's onboard receiver for a rural scenario, for both public UMTS and public GSM cases, and for the considered frequency offsets: the dashed black line corresponds to the noise floor of the GSM-R receiver, approximately equal to -113 dBm, and the points in red to the situation where the OOBI power is equal to the noise floor. The OOBI power for suburban and urban scenarios is given in Annex D.

When analysing OOBI, one can make the comparison between frequency offsets that represent the same frequency separation between the edge of the interfering UMTS/GSM channel and the centre of the interfered GSM-R channel. A 2.8 MHz offset between the centre frequency of UMTS and GSM-R channels corresponds to a 0.3 MHz of frequency separation between the edge of the UMTS channel to the centre of the GSM-R channel. The 0.4 MHz offset for the public GSM case also corresponds to a 0.3 MHz of frequency separation. The same match can be applied between the other considered offsets.

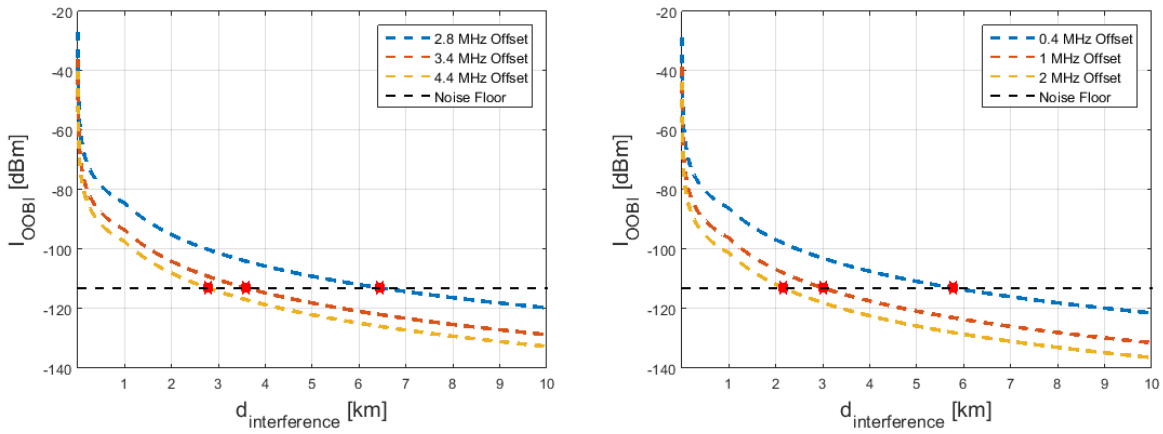

a) Public UMTS. b) Public GSM.

Figure 4.3 – OOBI power at the input of the GSM-R's receiver (rural scenario).

Making this match between frequency offsets considered for public UMTS and public GSM cases, and only by taking a look at the SEM attenuation values, one can conclude that OOBI due to UMTS emissions is more demanding than OOBI due to GSM ones. The same conclusion can be extracted from Figure 4.3, where, for the same interference distance, the OOBI power due to UMTS emissions is higher

(considering the match between frequency offsets). Because the slope of the curves is equal for all frequency offsets, this comparison can be easily performed by comparing the OOBI free-region distances (the interference distances corresponding to a desensitisation equal to the interference margin), which are approximately given by the x-coordinate of the red points in Figure 4.3 (in this case for a rural scenario), since a desensitisation of 3 dB (interference margin) is approximately equal to an INR of 0 dB. The OOBI free-region distances are given in Table 4.3, three colours being used to make data easier to read: red is used for distances higher than 1 km, yellow for distances between 300 m and 1 km, and green for distances lower than 300 m. The choice of these ranges is based on the fact that an interferer deployed at a distance higher than 300 m from a rail track is a common scenario and can still represent a problem to railway communications. Although OOBI due to UMTS emissions leads to higher free-region distances, the differences between UMTS and GSM distances are only in the order of 600 m for a rural scenario, 200 m for a suburban one and less than 100 m for an urban one. Taking the order of the OOBI free-region distances that one is dealing with into account, one can conclude that OOBI due to UMTS emissions, although more demanding, is not much worse than OOBI due to GSM ones.

By analysing the values in Table 4.3, one can see also that only for an urban scenario (due to the higher propagation losses characteristic of this scenario) the OOBI free-region distances drop to values lower than 300 m (for some offsets). For rural and suburban scenarios, these distances can be as high as 6.5 km and 1.9 km, respectively, which shows the high range of this interference type.

Another point that is worthwhile analysing is the relative decrease in the OOBI free-region distances between frequency offsets (considering the same interfering source). For the public UMTS case, the relative decreases (considering the three scenarios) are around 47% between the 2.8 MHz and 3.4 MHz offsets, and 25% between the 3.4 MHz and 4.4 MHz ones, while for the public GSM case, the relative decreases are around 51% between the 0.4 MHz and 1 MHz offsets, and 32% between the 1 MHz and 2 MHz ones. Both results for public UMTS and GSM cases reflect the less strict SEM attenuations for higher frequency offsets and the need to try to avoid the lower frequency offsets.

Table 4.3 – GSM-R's free-region distances for OOBI.

$d_{free-region}^{OOBI}$ [km]						
Scenario	**Public UMTS**			**Public GSM**		
	2.8 MHz offset	3.4 MHz offset	4.4 MHz offset	0.4 MHz offset	1 MHz offset	2 MHz offset
Rural	6.460	3.587	2.770	5.773	3.002	2.165
Suburban	1.918	1.065	0.762	1.714	0.852	0.541
Urban	0.736	0.368	0.272	0.645	0.299	0.203

Figure 4.4 shows the BBI power as a function of the interference distance at the input of the GSM-R's onboard receiver for a rural scenario, for both public UMTS and GSM cases, and for the considered frequency offsets. The BBI power for suburban and urban scenarios is given in Annex E. The BBI free-region distances are presented in Table 4.4. The same match between GSM and UMTS frequency offsets cannot be performed in the BBI analysis because it is not based on emissions into the GSM-R's

channel but rather on the ability of the receiver to block the interfering signals, which, in this case, are different (wideband UMTS vs. narrowband GSM).

The BBI free-region distances for the public UMTS case are almost all lower than 300 m, while for the GSM case, they are also almost all lower than 300 m but only for the 1 MHz and 2 MHz offsets; the distances for the 0.4 MHz offset (which can be as high as 6.5 km for a rural scenario, 1.9 km for a suburban one, and 700 m for an urban one) show the difficulty of the GSM-R receiver to block narrow-band signals in nearby frequencies not only because the total energy of the transmission is comprised in a few set of frequencies but also due to insufficient selectivity of the GSM-R's receiver. Because UMTS is a wideband signal, the energy of the transmission is spread over a wider range of frequencies and can, therefore, be easily blocked by the GSM-R receiver, which is shown by the lower BBI free-region distances.

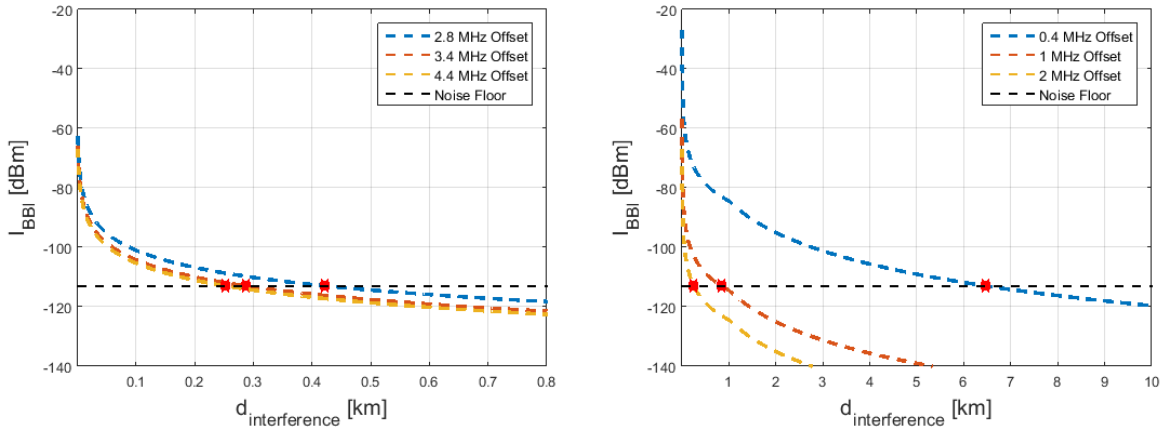

a) Public UMTS. b) Public GSM.

Figure 4.4 – BBI power at the input of the GSM-R's receiver (rural scenario).

When comparing the BBI free-region distances, Table 4.4, with the OOBI free-region ones, Table 4.3, because both types of interference are based on link budget equations, one can conclude that, except for the 0.4 MHz offset (for the public GSM case), BBI gives rise to much lower powers than OOBI (for the same interference distance). This shows that BBI will not be the dominant type of interference for any interference distance, except for the 0.4 MHz offset, for which BBI's contribution is high.

Table 4.4 – GSM-R's free-region distances for BBI.

$d_{free-region}^{BBI}$ [km]						
Scenario	**Public UMTS**			**Public GSM**		
	2.8 MHz offset	3.4 MHz offset	4.4 MHz offset	0.4 MHz offset	1 MHz offset	2 MHz offset
Rural	0.424	0.288	0.253	6.477	0.843	0.253
Suburban	0.096	0.072	0.065	1.923	0.162	0.065
Urban	0.047	0.037	0.034	0.738	0.073	0.034

To study the IBI, one has to perform first the intermodulation of the interfering signals. For the public

UMTS case, one considers a single wideband signal that generates third-order IMPs by the self-intermodulation of multiple tones as already explained. The results of the intermodulation of the UMTS signal are represented in Figure 4.5. The UMTS signal is assumed to be divided into 25 equally spaced tones, which is made under the approximation that the UMTS signal is 5 MHz wide and consequently that each tone has a bandwidth of 200 kHz, which is equal to the channel bandwidth of GSM-R. The 5 MHz bandwidth is an approximation for the bandwidth of the UMTS signal to take the leaked energy into account as a source of third-order IMPs too. According to the simulation and represented in Figure 4.5, 600 third-order IMPs are generated, 12, 10, and 8 of them fall within the GSM-R's channel if the offset is 2.8 MHz, 3.4 MHz, and 4.4 MHz, respectively.

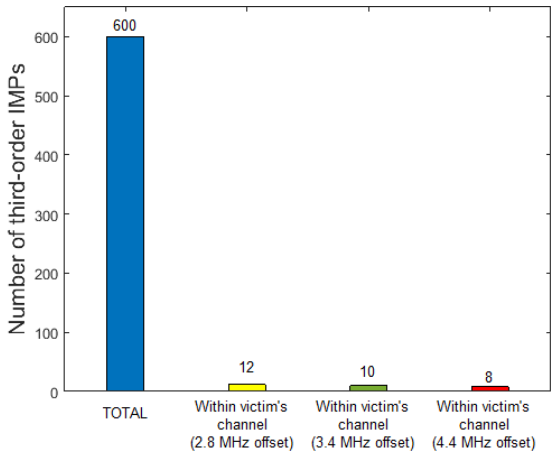

Figure 4.5 – Number of generated third-order IMPs within GSM-R's channel (single UMTS signal).

The IBI power as a function of the interference distance at the input of the GSM-R's onboard receiver for a rural scenario, for the public UMTS case, and for the considered frequency offsets is represented in Figure 4.6, together with a case where the use of an external duplex filter is simulated, which aims to provide RF filter attenuation that helps to attenuate IBI. The IBI power for suburban and urban scenarios is given in Annex F.

The variation in IBI power caused by the difference of 2 third-order IMPs between frequency offsets is highlighted by the zoom-in insert in Figure 4.6. The IBI free-region distances for the public UMTS case are presented in Table 4.5. The relative decreases in the IBI free-region distances between the 2.8 MHz and the 3.4 MHz offsets and between the 3.4 MHz and the 4.4 MHz offsets are lower than 10%, which shows that IBI, when referred to a single wideband signal, is not much dependent on the offset but more on the power of the interfering signal.

Although the IBI free-region distances in Table 4.5, for the public UMTS case, are all lower than 1 km, one can see in Figure 4.6 that for the case without filter, for a rural scenario, the IBI power reaches the value of around 50 dBm (although one has to be aware that the receiver is expected to be already overloaded at this point), which is higher than the value reached by the OOBI power, represented in Figure 4.3, which reaches only a power of around -30 dBm. The IBI power increases faster than the OOBI one with the decrease of the interference distance due to the nature of third-order IMPs and so one expects an interference distance at which the IBI starts to be the dominant type of interference when no filter is considered, which will be further analysed. For the case with filter, the IBI power reaches only

a value of -30 dBm and OOBI is expected to dominate over both BBI and IBI for all the interference distances. The use of a filter removes the possibility of IBI to dominate.

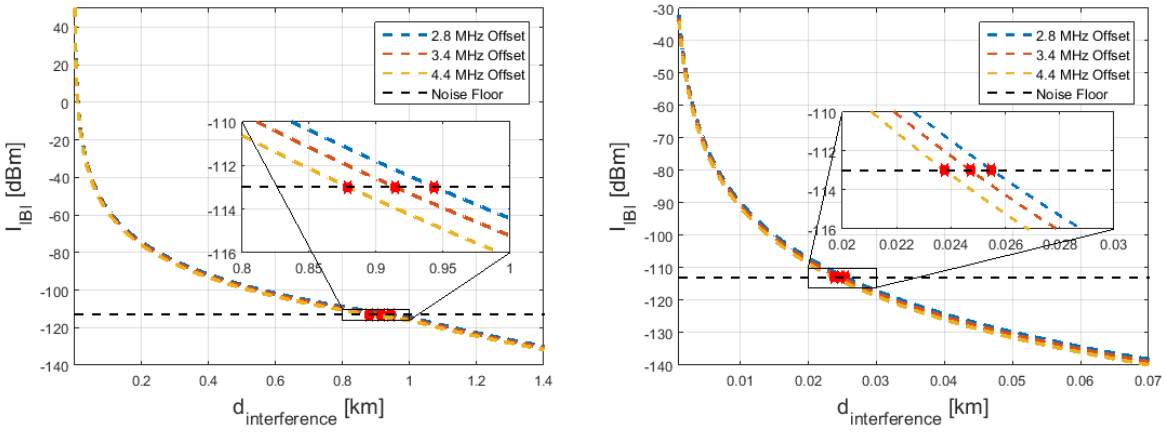

a) Without filter. b) With filter.

Figure 4.6 – IBI power at the input of the GSM-R's receiver (public UMTS in a rural scenario).

Comparing the IBI free-region distances in Table 4.5, for the public UMTS case, one obtains relative decreases of around 93% when transitioning from the case without filter to the case with one. This result shows again the huge impact of filtering the signals before the amplification stage.

Table 4.5 – GSM-R's free-region distances for IBI.

$d_{free-region}^{IBI}$ [km]								
Scenario	**Public UMTS**						**Public GSM**	
	(wo/filter)			(w/filter)			(wo/filter)	(w/filter)
	2.8 MHz offset	3.4 MHz offset	4.4 MHz offset	2.8 MHz offset	3.4 MHz offset	4.4 MHz offset		
Rural	0.944	0.914	0.880	0.026	0.025	0.024	2.326	0.127
Suburban	0.176	0.172	0.167	0.012	0.011	0.011	0.598	0.039
Urban	0.079	0.077	0.075	0.008	0.008	0.008	0.221	0.022

A single narrowband GSM signal (which is the one considered for the interference analysis) is not expected to produce IMPs but a practical GSM deployment uses normally more than one GSM carrier, either per sector or by the use of an omnidirectional arrangement [CEPT07]. To study IBI for the public GSM case, one considers the intermodulation of two equally spaced narrowband GSM signals and that one of the two resulting third-order IMPs falls within the victim's channel. It should be clear that in this case the interference does not depend on the offsets that one is analysing for public GSM. Two GSM carriers far away in frequency from the R-GSM frequency band can still generate a third-order IMP that theoretically falls into a GSM-R channel. The IBI free-region distances for the public GSM case are also given in Table 4.5, being more than two times higher compared to UMTS ones, which is a consequence of having two GSM carriers transmitted at full power. Even with the use of a filter, one gets a distance of around 127 m, which is still a high interference distance considering the behaviour of third-order IMPs. Because IBI for the public GSM case does not depend on the three frequency offsets being analysed

and because a certain combination of GSM carriers is needed, IBI is not taken into account in the following calculations for the public GSM case (only OOBI and BBI are accounted for).

The free-region distances taking the sum of the previous three types of interference (in the public GSM case only OOBI and BBI are considered) into account are given in Table 4.6. These free-region distances are almost equal to the ones given in Table 4.3 (except for the 0.4 MHz offset for the public GSM case) because OOBI is the dominant type of interference for high interference distances (IBI is negligible for high interference distances). Also, the free-region distances (referring to the sum of the interference types) for a case when the interfering source is 40 m high instead of 30 m are given in Annex G. One obtains relative increases of the free-region distances of around 18%, which shows that an interfering source of 30 m high should be probably already above the majority of the obstacles.

Table 4.6 – GSM-R's free-region distances for the sum of interference types.

$d_{free-region}^{TOTAL}$ [km]						
Scenario	**Public UMTS**			**Public GSM**		
	2.8 MHz offset	3.4 MHz offset	4.4 MHz offset	0.4 MHz offset	1 MHz offset	2 MHz offset
Rural	6.460	3.588	2.772	7.488	3.015	2.168
Suburban	1.919	1.065	0.763	2.224	0.857	0.542
Urban	0.736	0.368	0.272	0.875	0.300	0.204

The analysis performed until this point considers only the interfering signal. To assess the reduction in the maximum communication distance caused by the interfering signal one has to compute first the maximum communication distances (considering a target SNIR of 9 dB for GSM-R to be able to offer voice service) in the acceptable interference case, that is, when the desensitisation of the GSM-R's receiver is lower than the interference margin, which are presented in Table 4.7.

Table 4.7 – GSM-R's maximum communication distance (acceptable interference case).

Scenario	**Signal-to-noise Ratio** (ρ_N [dB])	**Maximum communication distance** (d_{max} [km])
Rural	9	50.546
Suburban	9	15.602
Urban	9	6.449

For interference distances lower than the free-region distances given in Table 4.6, the maximum communication distance drops below the values in Table 4.7. Because GSM-R deployments usually follow a constant maximum communication distance depending on the scenario (taken as 13 km for rural, 8 km for suburban and 5 km for urban), it is interesting to see which interference distances cause the maximum communication distance to drop below these fixed values. Figure 4.7 shows the maximum communication distance as a function of the interference distance for a rural scenario, for the public UMTS case, for the considered offsets, and for both cases without and with filter. The maximum communication

distance as a function of the interference distance for the public UMTS case but for suburban and urban scenarios is given in Annex H.

For a rural scenario and for the case without filter, the maximum communication distance drops to values lower than 13 km for interference distances lower than around 1.31 km, 0.57 km and 0.41 km for the 2.8 MHz, 3.4 MHz and 4.4 MHz offsets, respectively, as one can see in Figure 4.7 through the zoom-in insert. For a suburban scenario and for the case without filter, the maximum communication distance drops to values lower than 8 km for interference distances lower than around 0.73 km, 0.32 km and 0.23 km, for the same frequency offsets. For an urban scenario and for the case without filter, the maximum communication distance drops to values lower than 5 km for interference distances lower than around 0.46 km, 0.23 km and 0.17 km, again, for the same frequency offsets.

It is interesting to see in Figure 4.7 the interference distance from which IBI dominates (for the case without filter). When the curves in Figure 4.7 start to come together, it is where IBI starts to dominate because, as one can see in Figure 4.6, the IBI is the type of interference that presents low variations between the three frequency offsets being analysed. One can see in Figure 4.7 that this effect happens for interference distances lower than around 0.25 km for a rural scenario. For suburban and urban scenarios, the same happens for interference distances lower than around 0.10 km and 0.05 km, respectively. The use of a filter extinguishes the probability of IBI to dominate over OOBI as one can see in Figure 4.7 where the effect of the curves coming together disappears. Despite that, one has to sill account for OOBI. A filter is then, in the GSM-R case, only effective against an interfering source close deployed to the rail track. For higher interference distances, a filter does not provide any advantages because OOBI dominates and OOBI can only be attenuated by the interferer's side.

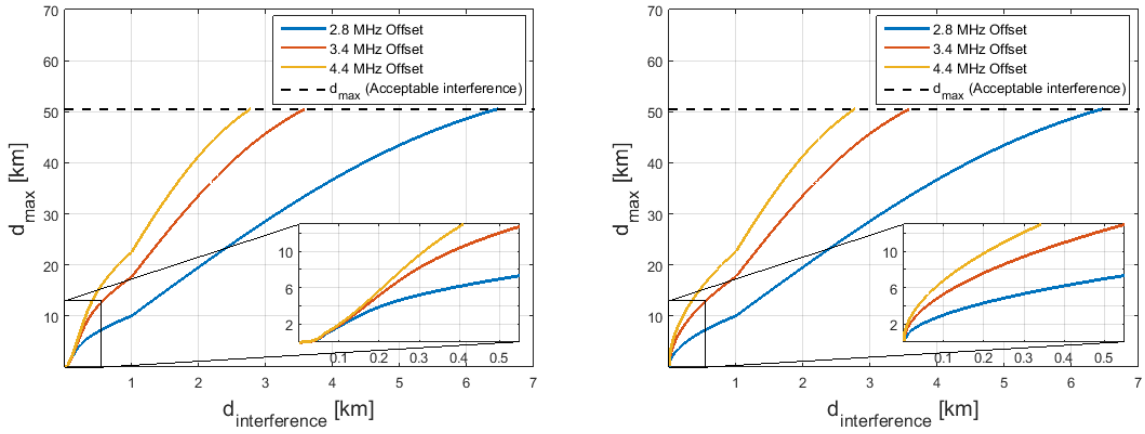

a) Without filter. b) With filter.

Figure 4.7 – GSM-R's maximum communication distance (public UMTS in a rural scenario).

The maximum communication distance as a function of the interference distance, for the public GSM case, and for the considered frequency offsets, is given Annex H. One can see that for a rural scenario the maximum communication distance drops to values lower than 13 km for interference distances lower than 1.51 km, 0.40 km and 0.22 km, for the 0.4 MHz, 1 MHz and 2 MHz offsets, respectively. For a suburban scenario, considering 8 km, these interference distances are, respectively, around 0.90 km,

0.25 km and 0.16 km. For an urban scenario, considering 5 km, these interference distances are, respectively, around 0.55 km, 0.19 km and 0.13 km. It is important to remember that one is not considering IBI in these calculations and that its effect can be even worse than for the UMTS's case.

Summing up, a UMTS/GSM BS can interfere with GSM-R if deployed at a distance from the rail track lower than around 7 km for a rural scenario, 2 km for a suburban one and 800 m for an urban one. Considering the distances followed by GSM-R deployments, the adjacent BSs of GSM-R may need only to be deployed closer to each other than usual when an interfering BS is at a distance from the rail track lower than around 1.5 km for a rural scenario and 500 m for an urban one, the recommended deployment guidelines in this thesis being useful in these cases. A filter should be used only in cases where an interfering UMTS BS is deployed at a distance from the rail track closer than 250 m for a rural scenario and 50 m for an urban one, being extremely effective in these conditions. The utility of a filter against an interfering GSM BS depends on the carriers being used by it, being highly recommended in cases where the third-order intermodulation behaviour is reported. To space the channels apart is a viable option against interference, but only when no third-order intermodulation behaviour is reported.

4.3 LTE-R Analysis

LTE-R can assign various RBs to the user depending on user requirements. As already mentioned, the LTE-R analysis is based on the number of allocated RBs to the user, that is, considering different bandwidths for the computation of the SNIR rather than frequency offsets. Figure 4.8 shows the OOBI power as a function of the interference distance at the input of the LTE-R's onboard receiver for a rural scenario, for both public UMTS and public GSM cases, and for both extreme cases of RBs allocation. The OOBI power for suburban and urban scenarios is given in Annex D. Because the SNIR is computed independently for the two bandwidths being considered, each bandwidth has its own noise floor of reference represented in Figure 4.8 (represented by a dashed black line).

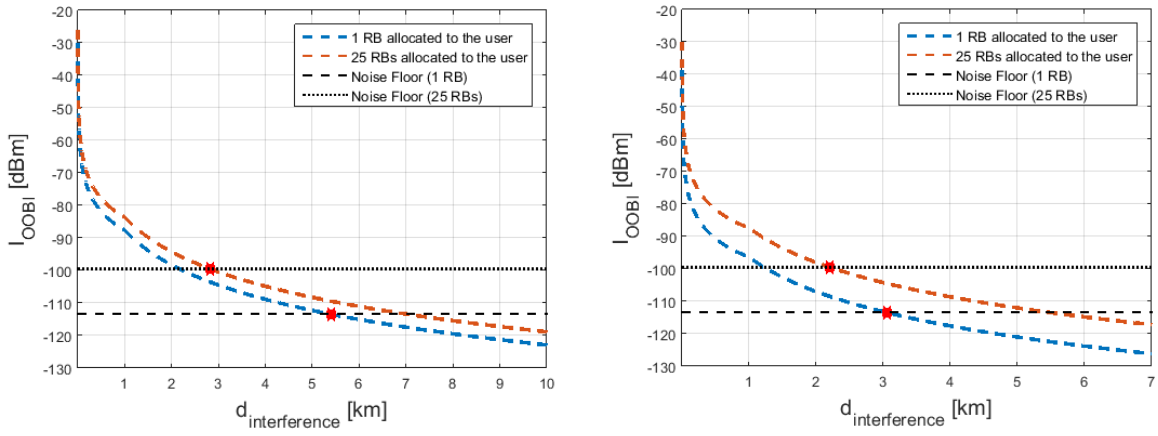

a) Public UMTS. b) Public GSM.

Figure 4.8 – OOBI power at the input of the LTE-R's receiver (rural scenario).

According to (3.5) and (3.6), the noise floor corresponding to 1 RB is equal to –113.4 dBm (aggregation of 12 subcarriers) and to 25 RBs is equal to –99.5 dBm (aggregation of 300 subcarriers). The OOBI free-region distances are approximately given by the x-coordinate of the red points in Figure 4.8 (in this case for a rural scenario) as explained in the GSM-R analysis. The OOBI free-regions are given in Table 4.8, with the same three colours code used in the GSM-R's analysis. One can see, again, that OOBI due to public UMTS emissions is more demanding than when it is produced by public GSM (for equal RB allocation). One can see also that, for the public UMTS case, the 25 RBs scenario results in OOBI free-region distances around 51% lower than the 1 RB ones. The same relative decrease is obtained for the public GSM case but only by around 32%.

Table 4.8 – LTE-R's free-region distances for OOBI.

$d_{free-region}^{OOBI}$ [km]				
Scenario	**Public UMTS**		**Public GSM**	
	1 RB allocated	25 RBs allocated	1 RB allocated	25 RBs allocated
Rural	5.404	2.820	3.056	2.204
Suburban	1.605	0.782	0.874	0.555
Urban	0.597	0.278	0.305	0.208

Because OOBI depends on frequency offsets, one can conclude that the last RB of the R-GSM band (the RB being considered for this analysis) is the RB more affected and the worst-case scenario in what concerns this interference type. Additionally, only two free-region distances in Table 4.8 are lower than 300 m, which shows again the high range of OOBI when caused by UMTS or GSM emissions.

Figure 4.9 shows the BBI power at the input of the LTE-R's onboard receiver for a rural scenario, for both public UMTS and public GSM cases, and for both RBs allocation cases. For LTE-R, the BBI power is assumed to be equally split into each of the RBs of the full bandwidth being considered, which is represented in Figure 4.9, where independently of the number of allocated RBs, the BBI free-region distances are equal. The BBI power for suburban and urban scenarios is given in Annex E.

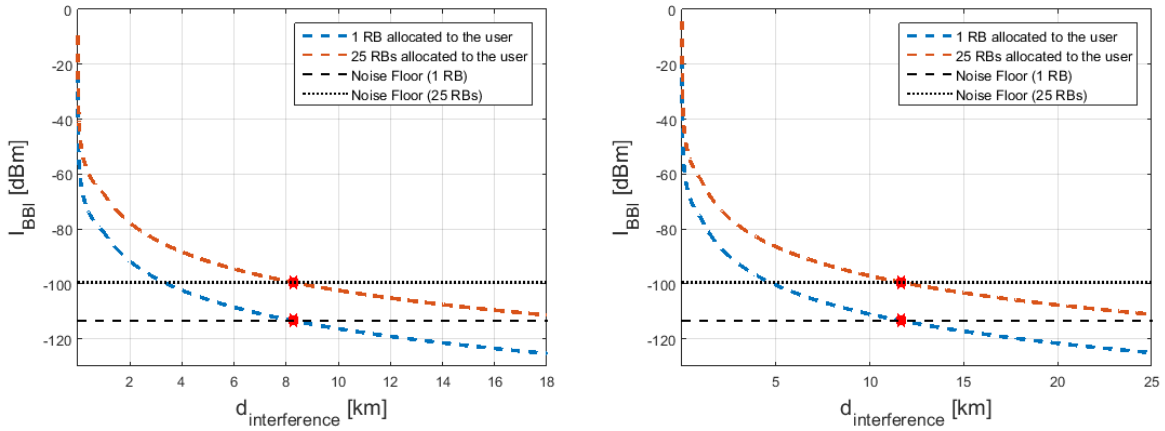

a) Public UMTS. b) Public GSM.

Figure 4.9 – BBI power at the input of the LTE-R's receiver (rural scenario).

The BBI free-region distances are presented in Table 4.9 where a case that simulates the use of a filter is also presented. As already mentioned, the filter aims to provide RF attenuation (to attenuate IBI) and to improve the selectivity attenuation (to attenuate BBI). Comparing the BBI free-region distances (for the case without filter) with the ones for OOBI in Table 4.8, one can see that the BBI free-region distances are higher than OOBI ones. This means that the lack of selectivity of the LTE-R receiver is the key factor and BBI dominates over OOBI for all the interference distances for the case without filter. The filter can reduce the BBI free-region distances by a value higher than 85% and make OOBI to dominate over BBI for all interference distances, as one can conclude by looking at the BBI free-regions distances for this case (they are now lower compared to OOBI ones).

Table 4.9 – LTE-R's free-region distances for BBI.

$d_{free-region}^{BBI}$ [km]				
Scenario	**Public UMTS**		**Public GSM**	
	(wo/filter)	(w/filter)	(wo/filter)	(w/filter)
Rural	8.275	1.164	11.702	1.647
Suburban	2.458	0.228	3.476	0.370
Urban	0.985	0.098	1.396	0.148

The study of IBI must be preceded by the intermodulation of the interfering signals as in GSM-R analysis. First, for a UMTS interfering signal, one assumes that it is divided into 25 equally spaced tones (200 kHz each tone), as in GSM-R analysis, which is close to the lowest bandwidth being considered of 1 RB (180 kHz). The results of the intermodulation of the UMTS signal are represented in Figure 4.10, where one can see that 600 third-order IMPs are generated, 11 of them fall within the victim's channel if one is considering the last RB of the band allocated the user and 132 of them fall within the victim's channel if one is considering all the available bandwidth allocated to the user.

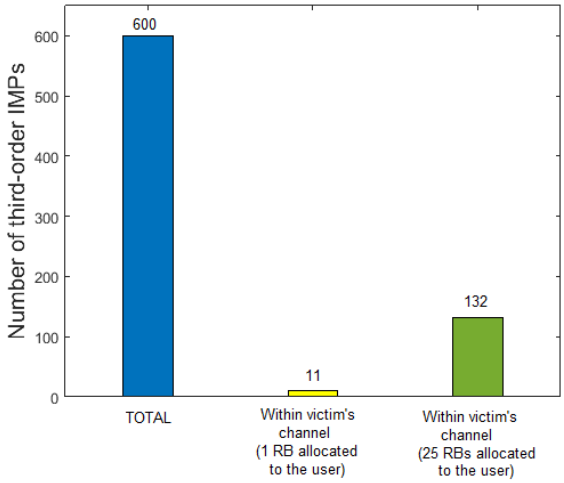

Figure 4.10 – Number of generated third-order IMPs within LTE-R's channel (single UMTS signal).

Figure 4.11 shows the IBI power at the input of the LTE-R's onboard receiver for a rural scenario, for the public UMTS case, for both RBs allocation cases, and for both cases without and with filter. As in

the GSM-R case, due to the high EIRP considered for the interfering sources, one can see that, for the public UMTS case, the IBI power can reach higher values than the BBI power (for the case without filter). One expects, therefore, an interference distance at which this interference type dominates over BBI (for the case without filter). Using a filter can make, in the LTE-R case, the IBI power to reach only values of around -30 dBm and prevent not only BBI to dominate over OOBI but also IBI to dominate over OOBI and BBI. The IBI power for suburban and urban scenarios is given in Annex F.

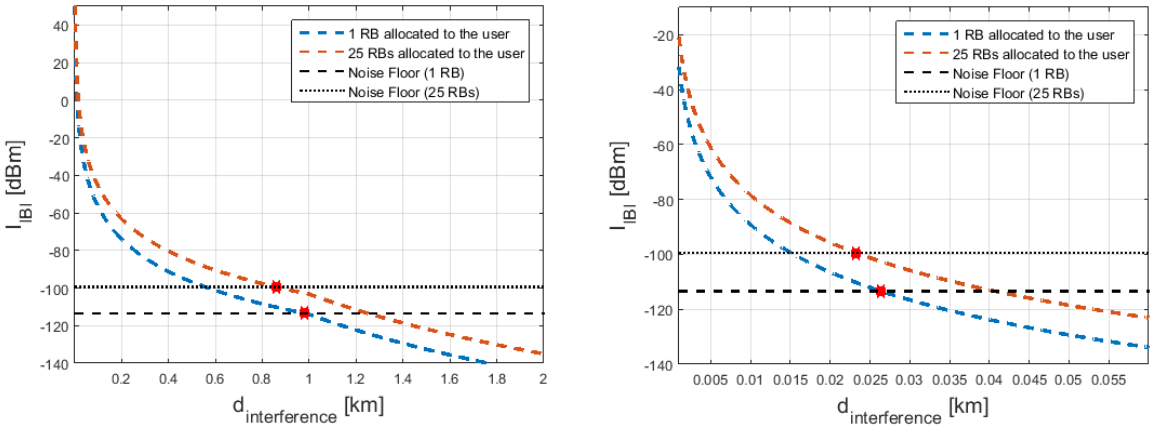

a) Without filter. b) With filter.

Figure 4.11 – IBI power at the input of the LTE-R's receiver (public UMTS in a rural scenario).

For the public UMTS case, although the third-order IMPs are expected to cover the entire R-GSM band (as one can check in Figure 3.13, where an example of a UMTS signal centred at 927.6 MHz is generating third-order IMPs), the interference to each subcarrier is not expected to be equal, because there are more third-order IMPs falling near to the E-GSM 900 band. The RBs farther away from the E-900 GSM band are less affected. Still, one considers that the overall performance of the channel, in the case of 25 RBs allocated to the user, is affected by the 132 third-order IMPs that fall within it.

The IBI free-region distances for the public UMTS case are given in Table 4.10. The IBI free-region distances for the 25 RBs case are lower than for the 1 RB case, but not much, by around 10%. This result is a consequence of having more third-order IMPs falling into the last RBs of the R-GSM band.

Table 4.10 – LTE-R's free-region distances for IBI.

$d_{interference}^{IBI}$ [km]						
Scenario	**Public UMTS**				**Public GSM**	
	(wo/filter)		(w/filter)		(wo/filter)	(w/filter)
	1 RB allocated	25 RBs allocated	1 RB allocated	25 RBs allocated	1 RB allocated	1 RB allocated
Rural	0.979	0.861	0.026	0.023	2.392	0.135
Suburban	0.182	0.165	0.012	0.011	0.622	0.041
Urban	0.081	0.075	0.008	0.007	0.229	0.023

For the public GSM case, one studies IBI in the same manner as in the GSM-R analysis. Because one is considering that only one IMP falls within the victim's channel, the interference can only be calculated

to a single RB and not to all the 25 RBs. This is precisely the case presented in Table 4.10 where the IBI free-region distances for the GSM case are given. The IBI free-region distances for public GSM are more than three times higher than UMTS ones for some of the scenarios being analysed. A filter can reduce the IBI free-region distances by more than 90%, which shows again the impact of filtering the interfering signals before the receiver's amplification stage. Due to the same reasons as explained in GSM-R's section, IBI caused by public GSM is not taken into account in the following calculations.

The free-region distances taking all the types of interference into account (in the public GSM case, only OOBI and BBI are considered) are given in Table 4.11. One can observe that for the case without filter they are almost equal to the BBI free-region distances and that for the case with filter they are almost equal to the OOBI free-region distances, which is according to the analysis above.

Table 4.11 – LTE-R's free-region distances for the sum of interference types.

$d_{interference}^{TOTAL}$ [km]								
Scenario	**Public UMTS**				**Public GSM**			
	(wo/filter)		(w/filter)		(wo/filter)		(w/filter)	
	1 RB allocated	25 RBs allocated	1 RB allocated	25 RBs allocated	1 RB allocated	25 RBs allocated	1 RB allocated	25 RBs allocated
Rural	8.762	8.328	5.411	2.855	11.731	11.712	3.150	2.404
Suburban	2.603	2.474	1.607	0.795	3.484	3.479	0.912	0.626
Urban	1.045	0.992	0.598	0.282	1.399	1.397	0.317	0.230

The free-region distances (for the sum of interference types) for an additional case of an interfering source 40 m high instead of 30 m are given in Annex G. Relative increases lower than 20% are obtained.

Independently of the number of allocated RBs, the highest throughput offered by LTE, is achieved for an SNIR of approximately 25 dB, the value where the highest MCS of LTE starts to saturate, as one can see in Figure 3.8. Figure 4.12 shows the maximum communication distance as a function of the interference distance (considering an SNIR of 25 dB) for a rural scenario, for the public UMTS case, and for both cases without and with filter. The maximum communication distance for the acceptable interference case, considering this value of SNIR, is also represented in Figure 4.12 by a dashed black line. The same figures for the public UMTS case but for suburban and urban scenarios are given in Annex H.

One of the main advantages of using the R-GSM band for the deployment of LTE-R is the possibility of reusing the masts of the GSM-R BSs (because of the frequency), which represents a huge cost saving. For an SNIR of 25 dB, the maximum communication distances for the acceptable interference case are around 8 km, 2.5 km and 1 km, for rural, suburban, and urban scenarios, respectively. This means that the deployment distances assumed for GSM-R (13 km for rural, 8 km for suburban and 5 km for urban) do not allow to extract the maximum performance of LTE-R. Lower deployment distances are needed. Additionally, one has to still account for the interfering sources causing the maximum communication distance to drop.

An interesting point to see in Figure 4.12 is the interference distance from which IBI dominates over BBI (for the case without filter). This happens when the curves start coming together as in the GSM-R case.

One can see in Figure 4.12 that this happens for interference distances lower than 0.15 km for a rural scenario, while for suburban and urban scenarios these interference distances are around 0.05 km, and 0.03 km, respectively. The inclusion of a filter attenuates the effect of both BBI and IBI and makes OOBI to dominate for all the interference distances. As one can see in Figure 4.12 the curves are now well separated for both low and high interference distances as in OOBI analysis. The maximum communication distance as a function of the interference distance for the public GSM case, is given Annex H.

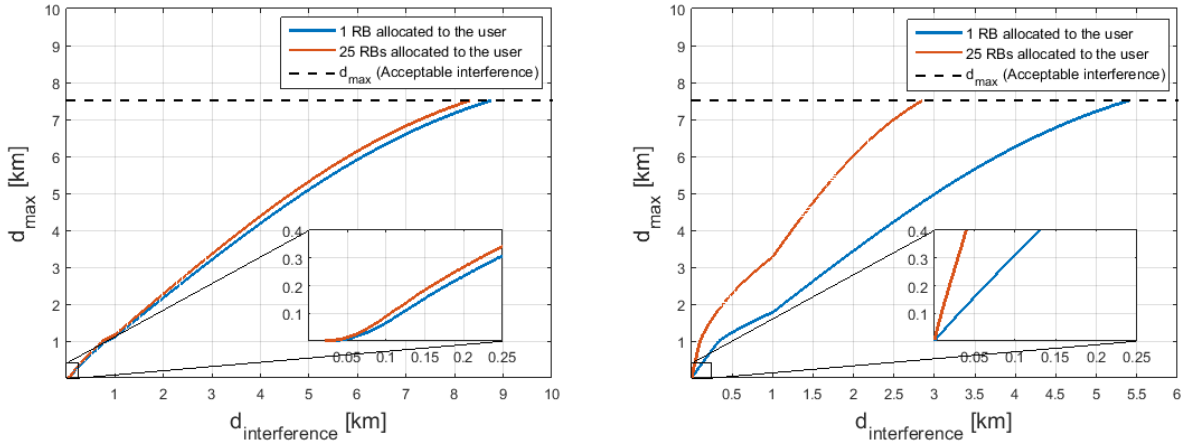

a) Without filter. b) With filter.

Figure 4.12 – LTE-R's maximum communication distance (public UMTS in a rural scenario).

The throughput offered by LTE-R (acceptable interference case), when simulating the case of a reuse of the masts of GSM-R, is given in Table 4.12 for the two RBs allocation cases being analysed. Considering that with the 1 RB allocation case LTE-R aims to provide voice service (average required throughput of 22 kbps as presented in Table 2.6) and considering that with the 25 RBs allocation case LTE-R aims to provide video and other broadband services (average required throughput of 4 Mbps as presented in Table 2.6), one can see in Table 4.12 that not all the assumed deployment distances for GSM-R provide these same throughputs (even under an acceptable interference case). A maximum communication distance of 13 km for a rural scenario is enough for LTE-R to offer both services but maximum communication distances of 8 km for a suburban scenario and of 5 km for an urban scenario are only enough for LTE-R to offer voice service.

Table 4.12 – Maximum throughput offered by LTE-R (acceptable interference case).

Communication distance (d_{max} [km])	**Signal-to-noise Ratio (ρ_N [dB])**	**Modulation and Coding Scheme**	**Maximum throughput (R_b [Mbps])**
13 (Rural)	16.4	64-QAM, r=3/4	0.328 (1 RB)
			8.201 (25 RB)
8 (Suburban)	5.5	QPSK, r=1/3	0.083 (1 RB)
			2.084 (25 RBs)
5 (Urban)	-1.1	QPSK, r=1/3	0.074 (1 RB)
			1.845 (25 RBs)

Considering now a desensitisation higher than the interference margin, for the fixed communication distances given in Table 4.12, a capacity loss occurs. The capacity loss as a function of the interference distance for a rural scenario, for the public UMTS case, for both cases of RBs allocation, and considering both cases without and with filter is given in Figure 4.13. The capacity loss as a function of the interference distance for the remaining scenarios for the UMTS case, as well as, for the public GSM case, is given in Annex I. It is interesting to calculate the interference distances that cause a capacity loss that corresponds to a throughput (after loss) of 22 kbps (for the 1 RB case) because, as one mentioned, the reuse of the masts of the GSM-R BSs should be only enough for LTE-R to provide voice service. For a rural scenario and considering the public UMTS case, these interference distances are 1.63 km and 1 km, for the case without and with filter, respectively. For the public UMTS case in a suburban scenario, these interference distances reduce to 1 km and 0.51 km, respectively. For the public UMTS case in an urban scenario, these interference distances are 0.59 km and 0.33 km, respectively.

For the public GSM case in a rural scenario, these distances are 2.18 km and 0.37 km, respectively, while in a suburban scenario, they are 1.34 km and 0.24 km, respectively, and for an urban scenario, they are 0.83 km and 0.18 km, respectively. One concludes, therefore, that there is a need for additional filtering in the LTE-R case, where not only IBI needs to be attenuated but also BBI.

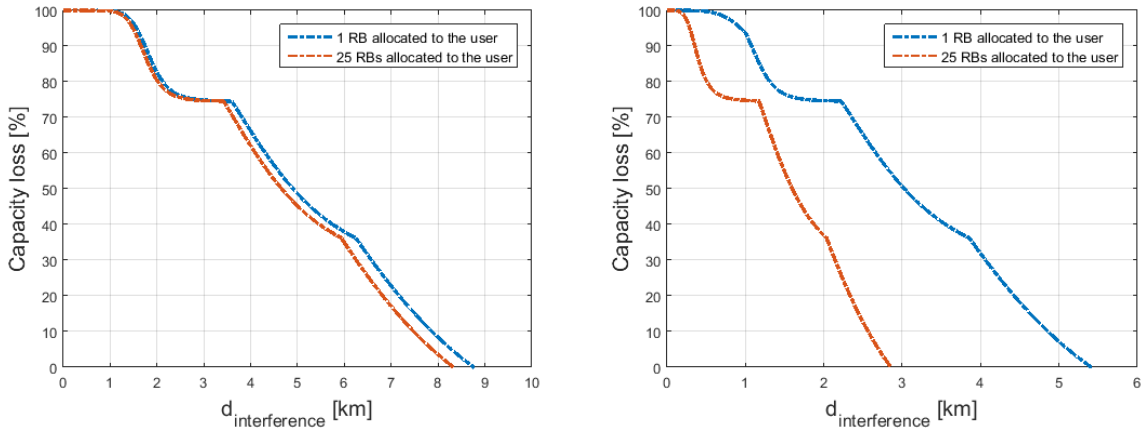

a) Without filter. b) With filter.

Figure 4.13 – LTE-R's capacity loss d_{max}=13 km (public UMTS in a rural scenario).

Summing up, a GSM BS can interfere with LTE-R if deployed at a distance from the rail track lower than around 12 km for a rural scenario, 3.5 km for a suburban one and 1.5 km for an urban one. In the case of a UMTS BS, these distances reduce to around 9 km, 2.5 km and 1 km, respectively. The reuse of the masts of the GSM-R BSs is not sufficient to extract the maximum performance of LTE-R, the deployment guidelines in this thesis being useful to extract that same performance. The reuse of the masts may not be even sufficient for LTE-R to offer video and other broadband services, a bandwidth higher than 5 MHz being required. Assuming that the masts are reused for LTE-R to offer voice service, an interfering BS deployed at a distance from the rail track closer than 2.2 km for a rural scenario and 800 m for an urban one can make the throughput to drop below 22 kbps. The use of a filter is highly recommended when the interferer is deployed at a distance from the rail track closer than these latter distances and not only when the third-order intermodulation behaviour is recorded as in GSM-R case.

4.4 BBRS Analysis

Figure 4.14 shows the OOBI power as a function of the interference distance at the input of the BBRS' receiver for the outdoor AP case and for the considered interfering channels. The noise floor of the receiver, calculated using the already defined input parameters, is approximately equal to -93 dBm and it is represented in Figure 4.14 by a black dashed line, together with the points, in red, where the OOBI power is equal to the noise floor of the receiver; as in the previous two analyses, the OOBI free-region distances are approximately given by the x-coordinates of these red points. The OOBI power for the indoor AP case as well as for both the outdoor and indoor MD cases is given in Annex D. One can see in Figure 4.14, and also based on the SEM attenuation values, that the most demanding interference scenario happens when the interferer is using the 1st 40 MHz adjacent channel. Because in the simulations, the difference of being interfered by an AP or by an MD is just the EIRP being considered, one can extend this conclusion to the MD case.

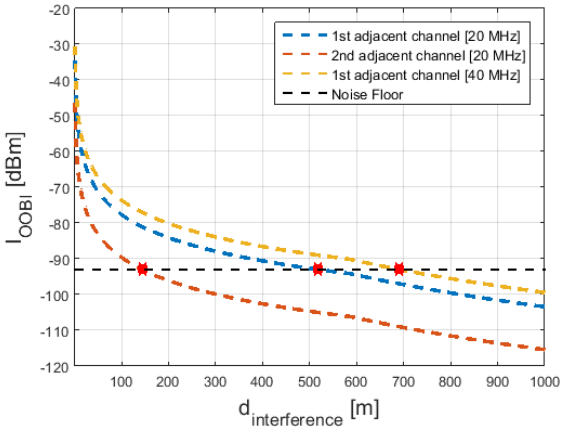

Figure 4.14 – OOBI power at the input of the BBRS' receiver (AP in an outdoor scenario).

The OOBI free-region distances are given in Table 4.13, the three colours code being used as follows: red is used for distances higher than 100 m, yellow for distances between 20 m and 100 m, and green for distances lower than 20 m. It is interesting to compare these distances between offsets (fixed outdoor/indoor scenario) and between the outdoor/indoor scenarios (fixed offset). Comparing between offsets, one obtains relative decreases in these free-region distances of around 30% when transitioning from the 1st 40 MHz adjacent channel to the 1st 20 MHz adjacent channel and of around 73% when transitioning from the 1st 20 MHz adjacent channel to the 2nd 20 MHz adjacent channel. This shows that an interferer using the 2nd 20 MHz adjacent channel has much less interference range than an interferer using either one of the two 1st (20 MHz or 40 MHz) adjacent channels being considered. When comparing the outdoor scenario with the indoor scenario, one obtains relative decreases in the OOBI free-region distances higher than 80%, which shows the huge impact that the indoor attenuation has on the OOBI free-region distances.

Because buildings are normally at a distance higher than 20 m from the rail tracks, free-region distances lower than 20 m can be considered as acceptable. The majority of OOBI free-region distances are higher than 20 m, which shows the high range of this interference type for the scenarios being considered.

Table 4.13 – BBRS' free-region distances for OOBI.

$d_{free-region}^{OOBI}$ [m]						
Scenario	**AP**			**MD**		
	1st adjacent channel (20 MHz)	2nd adjacent channel (20 MHz)	1st adjacent channel (40 MHz)	1st adjacent channel (20 MHz)	2nd adjacent channel (20 MHz)	1st adjacent channel (40 MHz)
Outdoor	518	143	691	197	54	303
Indoor	83	23	128	32	8	49

Figure 4.15 shows the BBI power as a function of the interference distance at the input of the BBRS' receiver for the outdoor AP case and for the considered interfering channels. The BBI power for the indoor AP case as well as for both the outdoor and indoor MD cases is given in Annex E. One can see in Figure 4.15 that BBI is more demanding when the interferer is using the 1st 20 MHz adjacent channel. In this case, the energy of the transmission is spread over fewer frequencies than when the interferer is using the 1st 40 MHz adjacent channel. The 1st 20 MHz adjacent channel is also well close in frequency to the victim's channel than the 2nd 20 MHz adjacent one.

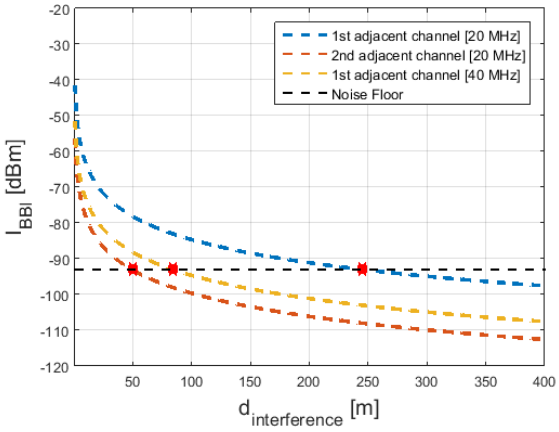

Figure 4.15 – BBI power at the input of the BBRS' receiver (AP in an outdoor scenario).

The BBI free-region distances are given in Table 4.14. One can see that all the BBI free-region distances are lower than OOBI's ones (comparing the same scenario and interfering source). One can conclude, because both interference types are based on link budget equations, that OOBI dominates over BBI for all the interference distances.

Table 4.14 – BBRS' free-region distances for BBI.

$d_{free-region}^{BBI}$ [m]						
Scenario	**AP**			**MD**		
	1st adjacent channel (20 MHz)	2nd adjacent channel (20 MHz)	1st adjacent channel (40 MHz)	1st adjacent channel (20 MHz)	2nd adjacent channel (20 MHz)	1st adjacent channel (40 MHz)
Outdoor	245	49	83	93	18	32
Indoor	39	7	13	15	3	5

To study IBI, one needs to perform first the intermodulation of the interfering signals to check if, from a theoretical point of view, there is the possibility of third-order IMPs to fall within the victim's channel. Two different intermodulation calculations are performed based on the interfering signals being considered and the results are represented in Figure 4.16. The 20 MHz and the 40 MHz interfering signals are assumed to be divided into 64 and 128 equally spaced tones, respectively, which is according to the 802.1n standard. One can see in Figure 4.16 that, according to the simulations, a 20 MHz interfering signal generates 4032 third-order IMPs, 1024 of them fall within the victim's channel in case the interferer is using the 1st 20 MHz adjacent channel. In case the interferer is using the 2nd 20 MHz adjacent channel then there is no possibility of third-order IMPs to fall within the victim's channel. A 40 MHz interfering signal generates 16256 third-order IMPs, 3072 of them fall within the victim's channel.

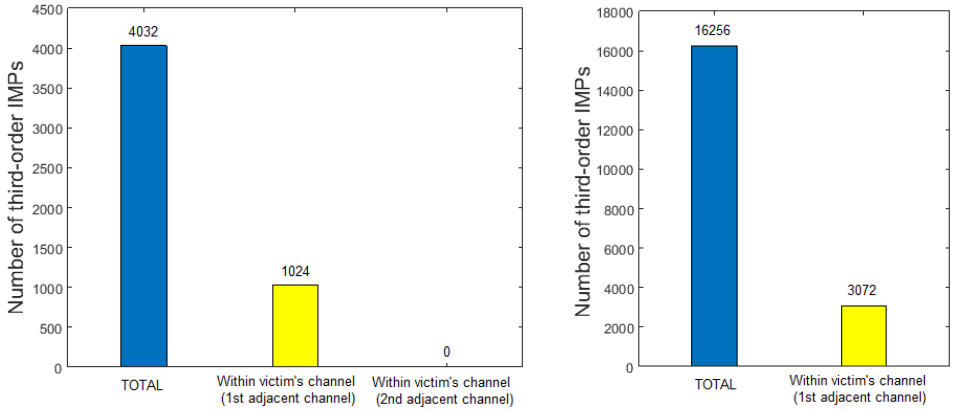

a) 20 MHz interfering signal. b) 40 MHz interfering signal.

Figure 4.16 – Number of generated third-order IMPs within BBRS' channel.

Figure 4.17 shows the IBI power at the input of the BBRS' receiver for the outdoor AP case and for the considered interfering channels. The IBI power for the indoor AP case as well as for both the outdoor and indoor MD cases is given in Annex F. Only the results for the two 1st adjacent channels (20 MHz and 40 MHz) cases are represented in Figure 4.17 because the results of the intermodulation in Figure 4.16 are such that for the 2nd 20 MHz adjacent channel case, none third-order IMPs fall within the victim's channel. One can see in Figure 4.17 that a 20 MHz interfering signal produces a higher IBI power for the same interference distance but at the same time that the results are not much different.

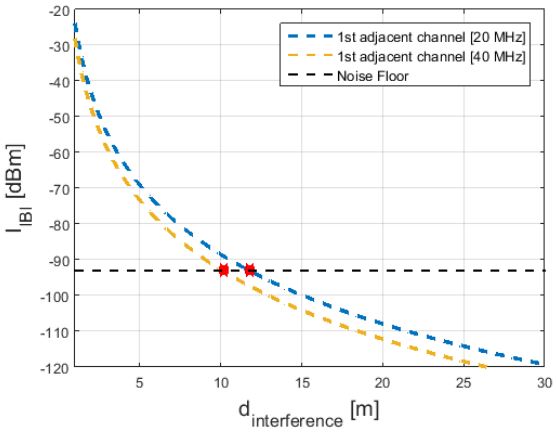

Figure 4.17 – IBI power at the input of the BBRS' receiver (AP in an outdoor scenario).

The IBI free-region distances are given in Table 4.15. All the free-region distances in Table 4.15 are well lower than 20 m. The fact that the IBI free-region distances are lower than OOBI and BBI ones does not prevent IBI to dominate for some interference distances, as one concluded in GSM-R and LTE-R analyses. As already mentioned, due to the characteristics of third-order IMPs, the IBI power increases faster with the decrease of the interference distance than OOBI and BBI powers. Because of that, one has to still check is there is any possibility of IBI to dominate for low interference distances. One can see in Figure 4.17 that an IBI power of around -30 dBm is reached for the outdoor AP case. An OOBI power of around -30 dBm is also obtained in Figure 4.14 for the same scenario (one is comparing with OOBI because, as one mentioned, OOBI dominates over BBI for all interference distances). This means that IBI does not dominate over OOBI independently of the interference distance. This also means that one does not need to use a filter to attenuate IBI. For the indoor MD case, the IBI power does not even reach values close to the noise floor of the BBRS' receiver.

Table 4.15 – BBRS' free-region distances for IBI.

$d_{free-region}^{IBI}$ [m]				
Scenario	**AP**		**MD**	
	1st adjacent channel (20 MHz)	1st adjacent channel (40 MHz)	1st adjacent channel (20 MHz)	1st adjacent channel (40 MHz)
Outdoor	12	10	5	4
Indoor	2	2	-	-

The free-region distances corresponding to the sum of the three types of interference are given in Table 4.16. One can conclude that the most demanding interference scenario is when the interferer is using the 1st 40 MHz adjacent channel which is according to the fact that OOBI is the dominant type of interference for all the interference distances.

Table 4.16 – BBRS' free-region distances for the sum of interference types.

$d_{free-region}^{TOTAL}$ [m]						
Scenario	**AP**			**MD**		
	1st adjacent channel (20 MHz)	2nd adjacent channel (20 MHz)	1st adjacent channel (40 MHz)	1st adjacent channel (20 MHz)	2nd adjacent channel (20 MHz)	1st adjacent channel (40 MHz)
Outdoor	564	149	692	215	57	304
Indoor	91	24	129	34	9	49

The wayside APs of BBRS make use of sectorial antennas and one is considering the gain of the main lobe of this antenna in the simulations to account for the worst-case scenario. One can calculate the free-region distances, referring to the sum of the three interference types, using a gain of 5 dBi instead of 18 dBi to simulate the case of interfering signals entering the antenna of the wayside APs of BBRS by a side lobe. The free-region distances referring to this case are given in Annex G and one can see relative reductions of around 75% when comparing to the case considering the main lobe gain. This

result shows that even scenarios that result in free-region distances as high as 100 m for the main lobe gain case may in practice not lead to interference problems.

All the above results are independent of the desired signal power and only take the interfering signal into account. To assess the reduction in the maximum communication distance caused by the interference source to be deployed at an interference distance lower than the free-region distances presented in Table 4.16 one has to calculate first which are the maximum communication distance (acceptable interference case) required for a certain throughput, given in Table 4.17. The MCS and the SNR corresponding to that required throughput are also given in Table 4.17.

Table 4.17 – BBRS' maximum communications distance (acceptable interference case).

Throughput (R_b [Mbps])	**Modulation and Coding Scheme**	**Signal-to-noise Ratio (ρ_N [dB])**	**Maximum communication distance (d_{max} [m])**
4	QPSK, r=1/2	5.8	3568
6	QPSK, r=1/2	7.5	3218
12	16-QAM, r=1/2	13.3	2310
24	16-QAM, r=3/4	20.3	1265
48	64-QAM, r=3/4	29.6	466

Figure 4.18 shows the maximum communication distance as a function of the interference distance for both outdoor and indoor AP cases, and considering a required throughput of 12 Mbps, which, according to [BBRS17], is the highest requirement for UL among BBRS' projects. The maximum communication distance as a function of the interference distance (for that same throughput requirement) but for both outdoor and indoor MD cases is given in Annex H. The dashed line in Figure 4.18 represents the maximum communication distance (acceptable interference case) for a 12 Mbps requirement.

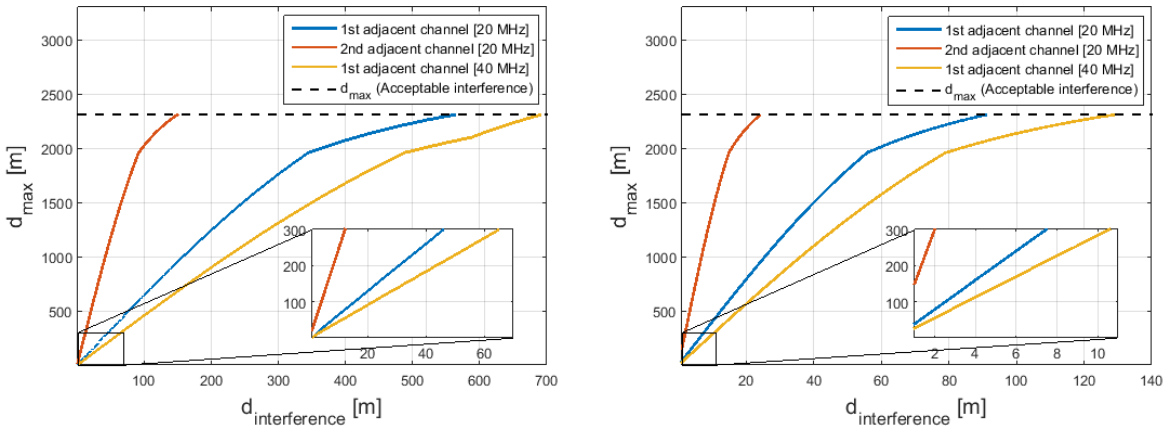

a) Outdoor. b) Indoor.

Figure 4.18 – BBRS' maximum communication distance for 12 Mbps requirement (AP).

Figure 4.18 shows the interference distances from which the maximum communication distance needs to be lower than 300 m (the typical distance in BBRS deployments). It is interesting to compare the

interference distances at which the maximum communication distance is equal to 300 m. For the outdoor AP case, these interference distances are around 46 m, 12 m, and 65 m, for the 1st 20 MHz adjacent, 2nd 20 MHz adjacent, and 1st 40 MHz adjacent interfering channels, respectively. For the outdoor MD case, these same interference distances are around 17 m, 5 m, and 25 m, respectively. For both indoor AP and MD cases, these interference distances are equal or lower than 11 m. These results show that indoor interferes (independently of the channel used) should not cause the maximum communication distance to drop below 300 m (for a 12 Mbps requirement).

In what concerns capacity loss calculations, considering a fixed maximum communication distance of 300 m, and taking a maximum desensitisation equal to the interference margin into account (acceptable interference case), BBRS can provide a throughput of around 52 Mbps according to the simulations. Figure 4.19 shows the BBRS' capacity loss as a function of the interference distance for both outdoor and indoor AP cases. The capacity loss as a function of the interference distance for both outdoor and indoor MD cases is given in Annex I.

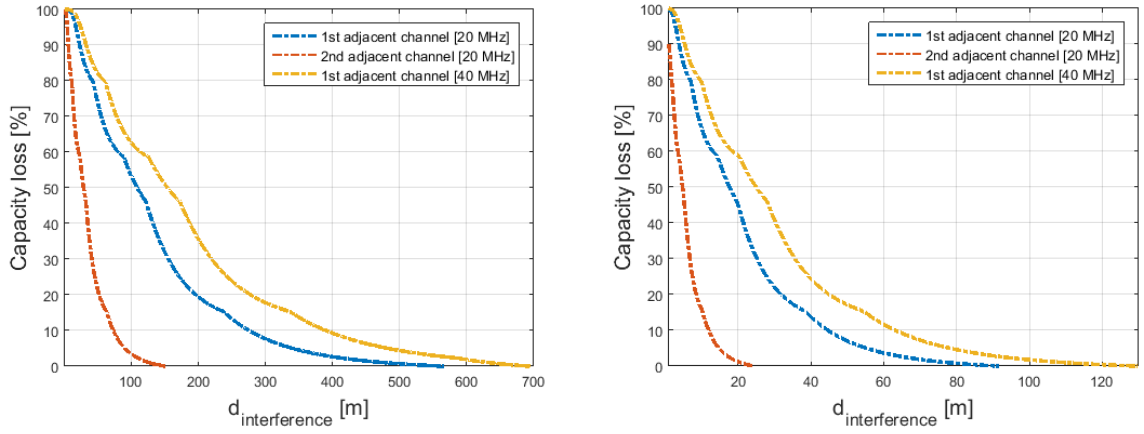

a) Outdoor. b) Indoor.

Figure 4.19 – BBRS' capacity loss for d_{max}=300 m (AP).

To analyse the capacity loss, one selects three different values (10%, 50%, and 90%) and calculates the interference distance that results in these values of capacity loss. These three values are chosen to cover the remaining throughput requirements of BBRS [BBRS17] apart from the 12 Mbps one. Capacity losses of 10%, 50%, and 90% correspond approximately to throughputs (after loss) of 47 Mbps (close to 48 Mbps), 26 Mbps (close to 24 Mbps), and 5 Mbps (close to 4 Mbps and 6 Mbps), respectively. The results of this analysis are presented in Table 4.18 and Table 4.19 for outdoor and indoor scenarios, respectively. By looking at Table 4.18 one concludes that an outdoor AP can cause a 90% capacity loss and give rise, therefore, to a throughput (after loss) of around 5 Mbps (except when using the 2nd 20 MHz adjacent channel). Also according to the simulations, if an outdoor MD is at an interference distance lower than 12 m it should be able to cause a 90% capacity loss. Although one has to be aware that a MD can get this closer to BBRS wayside APs, only rare cases of antenna alignment should in practice give rise to a capacity loss of this order.

Table 4.18 – BBRS' capacity loss d_{max}=300 m (outdoor scenario).

$d_{interference}$ [m]						
Capacity loss [%]	**AP**			**MD**		
	1st adjacent channel (20 MHz)	2nd adjacent channel (20 MHz)	1st adjacent channel (40 MHz)	1st adjacent channel (20 MHz)	2nd adjacent channel (20 MHz)	1st adjacent channel (40 MHz)
10	275	73	389	105	27	148
50	108	28	153	41	11	58
90	23	6	32	8	2	12

According to the results in Table 4.19, an indoor AP can cause a capacity loss as high as 50% and give rise, therefore, to a throughput (after loss) of around 26 Mbps (close to 24 Mbps). Also according to the results in Table 4.19, an indoor MD should only be able to cause a capacity loss as high as 10% and only in the case it is using the 1st 40 MHz adjacent channel. Concluding, throughputs (after loss) of around 26 Mbps are assured in what regards indoor interferers. Indoor interferers should only represent a problem for throughput requirements higher than 26 Mbps.

Table 4.19 – BBRS' capacity loss d_{max}=300 m (indoor scenario).

$d_{interference}$ [m]						
Capacity loss [%]	**AP**			**MD**		
	1st adjacent channel (20 MHz)	2nd adjacent channel (20 MHz)	1st adjacent channel (40 MHz)	1st adjacent channel (20 MHz)	2nd adjacent channel (20 MHz)	1st adjacent channel (40 MHz)
10	44	11	63	17	4	24
50	17	4	24	6	1	9
90	3	-	5	1	-	2

Summing up, a Wi-Fi AP can interfere with BBRS if deployed outdoors at a distance from a wayside AP lower than around 700 m and 130 m if indoors. In the case of a Wi-Fi MD, these distances reduce to 300 m and 50 m, respectively. Considering the distances followed by BBRS deployments and a 12 Mbps throughput requirement, the adjacent wayside APs of BBRS may need only to be deployed closer than usual to each other when an outdoor Wi-Fi device is at a distance from a wayside AP lower than 65 m for an AP and 25 m for an MD, the recommended deployment guidelines in this thesis being useful in these cases. Indoor Wi-Fi devices should not represent a problem in general for throughput requirements lower than 12 Mbps. There is no need to use a filter on the BBRS receiver and in the cases where there is no possibility of using lower distances between adjacent wayside APs, to deflect the antenna of the wayside AP being interfered and to use an alternate BBRS channel are viable solutions, as the results presented in this thesis suggest.

Chapter 5

Conclusions

This chapter summarises the main conclusions of this work. The structure of the work developed is described. The main results are mentioned and the points to be addressed in future works are suggested.

The goal of this thesis was to analyse the compatibility between railway telecommunications systems (GSM-R, LTE-R and BBRS) and other systems external to railway usage that use adjacent frequencies. To achieve this goal, a model for interference estimation and evaluation of interference-free regions along rail tracks was developed. Two cases were analysed: railway telecommunications systems to be deployed and railway telecommunications systems already deployed. In the first case, the interference estimation is used for a proper deployment of railway BSs / wayside APs under interference scenarios. In the second case, the interference estimation is used to calculate the capacity loss that already deployed railway telecommunications systems may be subjected to. The model was implemented in MATLAB. Several scenarios were selected for this analysis and a set of simulations were performed.

The thesis starts with Chapter 1, where the historical evolution, the current scenario, and future perspectives concerning the railway telecommunications systems are presented. The three railway telecommunications systems analysed in this thesis are introduced. The problem under study together with the most probable sources of interference are presented. The objectives of this thesis are defined. The structure of the thesis with a brief description of each chapter is provided.

In Chapter 2, the fundamental concepts required to understand the work are introduced. First, the radio interface and network architecture of each one of the three railway telecommunications systems are presented. Then, the various services and applications of railway communications together with their requirements are stated. Various scenarios and structures that can be encounter in the railway environment and that can influence the signal propagation are presented. The performance parameters to be taken as metrics for the interference analysis are introduced. A subsection is dedicated to introducing the types of interference that one is going to study (OOBI, BBI, and IBI). The state of the art is presented where relevant works to the topic dealt are mentioned and their main differences to this work are stated.

In Chapter 3, the model developed to analyse the problem under study is fully described. The chapter starts by providing a high-level overview of the model where the main inputs and outputs are presented. On the input side, one defines interferer parameters, victim parameters, infrastructure parameters and scenario parameters. The interferer parameters refer to parameters of the interferer's transmitter. The victim parameters refer to parameters of both the victim's transmitter and receiver. The infrastructure parameters and the scenario parameters are related to, respectively, the heights of the infrastructure involved and to the corrections factors to apply to the propagation models used. On the output side, one defines interference power, interference-free region distance, maximum communication distance and capacity loss. The first two are related to interference estimation calculations. The latter two outputs relate to, respectively, the distance for a proper deployment of railway BSs / wayside APs and to the decrease in throughput that railway telecommunications systems already deployed may be subject to.

After the model being overviewed, the various equations that compose the model are presented. Seven sub-models are defined: desired signal models, interference criterion models, out-of-band interference models, blocking-based interference models, intermodulation-based interference models, propagation models and throughput models. The desired-signal models define equations to calculate the desired signal power at the input of the victim's receiver. The interference criterion models define equations related to the classification of acceptable and non-acceptable interference cases. The three mentioned

interference models are used to calculate the interference power (referred to each interference type) at the input of the victim's receiver. The propagation models are chosen based on the scenarios that one selects for the interference analysis and are used to calculate the path loss of both desired and interfering signals. The throughput models define equations that relate throughput and SNIR. After having defined all the equations, the steps needed to implement the model in MATLAB are explained and an assessment of that same implementation is performing by comparing the results with results from other authors for a set of well-known inputs. The results of the simulation prove the correct implementation of the model, where the obtained small deviations in the results are justified by the use of different propagation models from those used in this work.

At the beginning of Chapter 4, the scenarios chosen for the interference analysis are described. For the GSM-R and LTE-R analyses, one analyses both a public GSM and UMTS BSs as being the interfering sources. For the BBRS analysis, one analyses both a Wi-Fi AP and a Wi-Fi MD as being the interfering sources. The interfering sources are selected based on the frequencies used by each system. Also, one defines the interference scenarios from both frequency and physical perspectives.

From a frequency perspective and for the GSM-R analysis, one selects three different frequency offsets between the centre of the GSM-R channel (being interfered) and the centre of the public GSM/UMTS channel (causing the interference). The chosen offsets between public GSM and GSM-R channels are 0.4 MHz, 1 MHz and 2 MHz. The chosen offsets between public UMTS and GSM-R channels are 2.8 MHz, 3.4 MHz and 4.4 MHz. The 0.4 MHz (public GSM) and 2.8 MHz (public UMTS) offsets are chosen to study the worst-case scenario and the other two to assess the effect of spacing the channels apart. For the LTE-R analysis, the closest channels of public GSM/UMTS to the R-GSM band are assumed for this analysis (worst-case scenario) and, because of the use of OFDMA by LTE-R, one considers interference to two extreme cases of RB allocation (1 RB and 25 RBs). For the BBRS analysis, one chooses to focus on three cases of adjacent interference: the 1st 20 MHz adjacent channel, the 2nd 20 MHz adjacent channel, and the 1st 40 MHz adjacent channel as being used by the considered Wi-Fi devices (AP and MD).

From a physical perspective, for both GSM-R and LTE-R analyses, one focuses on a DL interference scenario (a public GSM/UMTS BS interfering with the reception of the desired signal on a railway MT) according to the reported cases of interference. For the BBRS analysis, one focuses on an UL interference scenario (a Wi-Fi AP/MD interfering with the reception of the desired signal on a wayside AP of BBRS) according to the higher throughput requirements that BBRS presents in UL. Also from a physical perspective, one defines the scenarios considered for signal propagation. For both the GSM-R and LTE-R analyses, one considers three different scenarios: rural, suburban, and urban. The same scenario is considered for both the desired and interfering signals propagation. For the BBRS analysis, one considers a rural LoS scenario for the desired signal propagation according to the usual low distances in play, and both an outdoor (rural LoS) and indoor scenarios for the interfering signal propagation.

The worst-case of antenna alignment between the interferer and victim antenna is analysed. For the GSM-R and LTE-R analyses, a case that simulates the use of an external duplex filter is considered. The filter not only provides RF filter attenuation (IBI) but also additional selectivity attenuation (BBI).

Starting with the GSM-R's results, one concludes that OOBI is more demanding for the public UMTS case than for the public GSM case (comparing between offsets that represent the same frequency separation between the edge of the interfering channel and the centre of the GSM-R channel). The differences in the OOBI free-region distances between the two cases are, nevertheless, low (around 600 m for a rural scenario, 200 m for a suburban one, and less than 100 m for an urban one) considering that they can be as high as 6.5 km for a rural scenario, 1.9 km for a suburban one and 700 m for an urban one. An interesting point is the relative reductions in the OOBI free-region distances between frequency offsets. One obtains relative reductions from 47% to 51% when transitioning from the 0.4 MHz/2.8 MHz pair to the 1 MHz/3.4 MHz pair and from 25% to 32% when transitioning from this last pair to the 2 MHz/4.4 MHz pair. This shows the advantage to at least trying to avoid the 0.4 MHz/2.8 MHz pair by either using a different GSM-R channel or by asking the public operator to shift frequencies.

The obtained BBI free-regions are almost all lower than 300 m (for both cases) where the only exception is the 0.4 MHz offset (public GSM case) where one obtains BBI free-region distances in the same order as OOBI ones. This implies that, except for the 0.4 MHz offset, BBI has almost no contribution.

In what concerns IBI, when caused by a wideband signal like UMTS, it is not much dependent on the offsets being analysed (where one obtains just a 10% relative decrease in the IBI free-region distances when spacing apart the UMTS and GSM-R channels). This means that spacing the channels apart might not attenuate IBI unless the spacing is high enough so that no third-order IMPs fall within the victim's channel. The simulation for the public UMTS case shows that IBI dominates over OOBI for interference distances lower than 0.25 km, 0.10 km, and 0.05 km, for rural, suburban, and urban scenarios, respectively. For interference distances higher than these, OOBI dominates as mentioned above. The use of a filter excludes any probability of IBI to dominate. The simulations for the public GSM case result in IBI free-region distances more than two times higher than UMTS ones which shows that although not so probable due to the need for a certain combination of carriers, it can be much more severe.

Summing up and taking into account the sum of the three types of interference (in public GSM case only OOBI and BBI are taken into account due to the lower probability of IBI to occur), a UMTS/GSM BS can interfere with GSM-R if deployed at a distance from the rail track lower than around 7 km for a rural scenario, 2 km for a suburban one and 800 m for an urban one. Considering the distances followed by GSM-R deployments, the adjacent BSs of GSM-R may need only to be deployed closer to each other than usual when an interfering BS is at a distance from the rail track lower than around 1.5 km for a rural scenario and 500 m for an urban one, the recommended deployment guidelines in this thesis being useful in these cases. The highest frequency offsets being analysed reduce these latter interference distances to values lower than around 400 m for a rural scenario and 170 m for an urban one. A filter should be used only in cases where an interfering UMTS BS is deployed at a distance from the rail track closer than 250 m for a rural scenario and 50 m for an urban one, being extremely effective in these conditions. The utility of a filter against an interfering GSM BS depends on the carriers being used by it, being highly recommended in cases where the third-order intermodulation behaviour is reported. To space the channels apart is a viable option against interference, but only when no third-order intermodulation behaviour is reported.

For LTE-R, one obtains higher OOBI free-region distances for the 1 RB case than for the 25 RBs case. For the 1 RB case they can be as high as 5.4 km, 1.6 km, and 0.6 km, for rural, suburban, and urban scenarios, respectively. Considering the 25 RBs case, the OOBI free-region distances decrease around 51% for the UMTS case and around 32% for the GSM case.

In what concerns BBI, the interference power is assumed to be equally divided by all RBs so this interference type is independent of the number of allocated RBs. One obtains BBI free-region distances as high as 11.7 km for a rural scenario, 3.5 km for a suburban one and 1.4 km for an urban one. One concludes that BBI dominates over OOBI. The use of a filter can reduce these distances by a value higher than 85% and make BBI to have almost no contribution.

For IBI, the results for LTE-R are very similar to GSM-R ones. The simulations for the public UMTS case allow one to conclude that IBI dominates over BBI for interference distances lower than 0.15 km, 0.05 km, and 0.03 km, for rural, suburban and urban scenarios, respectively. For interference distances higher than these, BBI dominates as mentioned above. The inclusion of a filter can prevent not only BBI to dominate over OOBI as concluded above but also to prevent IBI to dominate over BBI. It is therefore highly recommended the use of a filter.

Summing up and taking into account the sum of the three types of interference (in public GSM case only OOBI and BBI are taken into account due to the lower probability of IBI to occur), a GSM BS can interfere with LTE-R if deployed at a distance from the rail track lower than around 12 km for a rural scenario, 3.5 km for a suburban one and 1.5 km for an urban one. In the case of a UMTS BS, these distances reduce to around 9 km, 2.5 km and 1 km, respectively. The reuse of the masts of the GSM-R BSs is not sufficient to extract the maximum performance of LTE-R even under acceptable interference cases, the deployment guidelines in this thesis being useful to extract that same performance. The reuse of the masts may not be even sufficient for LTE-R to offer video and other broadband services in suburban and urban scenarios, a bandwidth higher than 5 MHz being required. To offer the voice service, the reuse of the masts of GSM-R BSs is viable but only under acceptable interference cases. Assuming that the masts are reused for LTE-R to offer the voice service, an interfering BS deployed at a distance from the rail track closer than 2.2 km for a rural scenario and 800 m for an urban one can make the throughput at the handover point to drop below 22 kbps. The use of a filter is highly recommended when the interferer is deployed at a distance from the rail track closer than these latter distances and not only when third-order intermodulation behaviour is recorded as in GSM-R case, where the latter distances are reduced to values lower than 1 km for a rural scenario and 0.33 km for an urban scenario.

For BBRS, the highest OOBI free-region distances are obtained for the 1st 40 MHz adjacent channel case, where they can be as high as 700 m for an outdoor scenario and 130 m for an indoor one. When the interferer is using the 1st 20 MHz adjacent channel, the OOBI free-region distances decrease 35% relative to this previous case. From the 1st 20 MHz adjacent channel to the 2nd one, a relative decrease of around 73% is obtained. This shows the much lower impact that an interferer using the 2nd adjacent channel has. Also, one obtains relative reductions of around 75% from the outdoor to the indoor scenario which shows the high impact that indoor attenuation has. In what concerns BBI, all the free-region distances obtained are well lower than OOBI ones, so OOBI dominates over BBI.

In what concerns IBI, one concludes that only for two 1st adjacent channels (20 MHz and 40 MHz) cases there is a possibility of third-order to fall within the BBRS' channel. Even in these two cases, the IBI power is lower than the OOBI one, no matter the interference distance. This means that OOBI dominates also over IBI and that there is not a need for a filter to be used on the BBRS' receiver.

The wayside APs of BBRS make use of sectorial antennas and so the interfering signals might not enter the antenna by its main lobe. Considering a gain of 5 dBi (instead of 18 dBi) to simulate this case, one obtains relative reductions in the total free-region distances of around 75%, which shows the huge impact that deflecting the BBRS antenna can have in alleviating the interference effects.

Summing up and taking into account the sum of the three types of interference, a Wi-Fi AP can interfere with BBRS if deployed outdoors at a distance from a wayside AP lower than around 700 m and 130 m if indoors. In the case of a Wi-Fi MD, these distances reduce to 300 m and 50 m, respectively. Considering the distances followed by BBRS deployments and a 12 Mbps throughput requirement, the adjacent wayside APs of BBRS may need only to be deployed closer than usual to each other when an outdoor Wi-Fi device is at a distance from a wayside AP lower than 65 m for an AP and 25 m for an MD, the recommended deployment guidelines in this thesis being useful in these cases. Indoor Wi-Fi devices should not represent a problem in general for throughput requirements lower than 12 Mbps. According to the capacity loss calculations, a Wi-Fi AP can limit the throughput (at the handover point) to around 5 Mbps. An indoor Wi-Fi AP can only limit at most the throughput (at the handover point) to around 26 Mbps. This shows that indoor interferers should only represent a problem for throughputs requirements higher than 26 Mbps. There is no need to use a filter on the BBRS receiver and in the cases where there is no possibility of using lower distances between adjacent wayside APs, to deflect the antenna of the wayside AP being interfered and to use an alternate BBRS channel are viable solutions, as the results presented in this thesis suggest.

For future works, one recommends several points to be covered. MIMO can reduce the interference effects in both LTE-R and BBRS cases, where it is usually employed, and its effect needs to be addressed. Also, different configurations for both the antenna of the victim and of the interfering source need to be studied. The Okumura-Hata model is used in this work for the desired signal propagation in GSM-R and LTE-R analyses, but, mainly for suburban and urban scenarios, it may lead to higher path losses than the real ones. A propagation model suitable for HSR that takes into account these two scenarios (based on real measurement) may produce better results. The use of data based on real measurements rather than specifications of systems may also produce better results. Finally, one would like to mention that a system based on 5G can be the future of railway communications and that the choice of LTE-R as the next railway telecommunications system can facilitate this transition because 5G is backward compatible with 4G. A point that aggregates even more value to this work.

Annex A

Model Assessment Input Values

This annex gives the input values that are used in [CEPT07] for the analysis of interference from UMTS to the DL operation of GSM-R. These values are used in this thesis for the assessment of the model.

Table C.1 and Table C.2 give the input values used for the model assessment. Only two values in these tables are not used in [CEPT07]. Those are the IIP3 and the selectivity attenuation. This is because in [CEPT07] only OOBI is considered. Because one is simulating the case of the sum of OOBI, BBI, and IBI, one has to define values for these two input parameters. A value of -10 dBm is assumed for the IIP3. According to [Elli16], the IIP3 of a typical receiver varies between -30 dBm and 10 dBm. The selectivity attenuation value is calculated based on the same estimation method as in [CEPT11], where the corresponding wideband blocking power level (for wideband interfering systems) is derived from the narrowband blocking power level.

Table A.1 – Model assessment input values for the interferer system (public UMTS).

Parameter	Public UMTS BS
Channel bandwidth (Δf^{int}) [MHz]	5
Centre frequency $\left(f_c{}^{int}\right)$ [MHz]	927.6
Transmission power $\left(P_t{}^{int}\right)$ [dBm]	43
Transmitter losses $(L_t{}^{int})$[dB]	3
Transmitter antenna gain $\left(G_t{}^{int}\right)$ [dBi]	15
Height of the base station (h_{bs}) [m]	45
Spectrum emission mask attenuation (A_{mask}) [dB]	50.04

Table A.2 – Model assessment input values for the victim system (GSM-R).

Parameter	GSM-R
Channel bandwidth (Δf^{vic}) [MHz]	0.2
Centre frequency $\left(f_c{}^{vic}\right)$ [MHz]	924.8
Transmission power $\left(P_t{}^{vic}\right)$ [dBm]	45
Transmitter losses $\left(L_t{}^{vic}\right)$ [dB]	3
Transmitter antenna gain $\left(G_t{}^{vic}\right)$ [dBi]	18
Receiver antenna gain (G_r) [dBi]	2
Receiver losses (L_r) [dB]	3
Noise figure (F) [dB]	7
System margin (M_s) [dB]	8
Interference Margin (M_I) [dB]	0
Input third-order intercept point (P_{IIP3}) [dBm]	-10
Height of the base station (h_{bs}) [m]	45
Height of the mobile station (h_{ms}) [m]	4.5
Selectivity attenuation (A_{sel}) [dB]	85.71

Annex B

Spectrum Emission Mask Attenuation Values

This annex gives the input values of the SEM attenuation input parameter. The assumptions made are explained and the references from where these values are taken from are given.

The input values of the SEM attenuation parameter are given in Table D.1. All the values in Table D.1 are derived from the SEMs given in the specifications of the systems. The SEM that applies to a BS of public GSM can be found in [ETSI17]. The SEM for a BS of public UMTS is given in [ETSI15]. The SEM for Wi-Fi (802.11n), considering both 20 MHz and 40 MHz channels can be found in [ITUR14]. As already mentioned, one picks the SEM attenuation value corresponding to the centre frequency of the reception band of the victim. The attenuation values given in Table D.1 are already converted to the channel's bandwidth of the victim.

Table B.1 – Spectrum emission mask attenuation values for the considered interference scenarios.

Parameter	**Public GSM BS**	**Public UMTS BS**	**Wi-Fi devices**	
			Access point	**Mobile device**
Spectrum emission mask attenuation (A_{mask}) $[\mathrm{dB/victim's\ channel\ bandwidth}]$	51.76 dB/(200 kHz) (0.4 MHz offset [GSM-R]) 61.76 dB/(200 kHz) (1 MHz offset [GSM-R]) 66.76 dB/(200 kHz) (2 MHz offset [GSM-R]) 62.22 dB/(180 kHz) (0.6 MHz offset [LTE-R]) 53.24 dB/(4.5 MHz) (2.8 MHz offset [LTE-R])	50.04 dB/(200 kHz) (2.8 MHz offset [GSM-R]) 59.04 dB/(200 kHz) (3.4 MHz offset [GSM-R]) 62.99 dB/(200 kHz) (4.4 MHz offset [GSM-R]) 53.50 dB/(180 kHz) (3 MHz offset [LTE-R]) 49.47 dB/(4.5 MHz) (5.2 MHz offset [LTE-R])	28 dB/(20 MHz) (20 MHz offset - 1st 20 MHz adjacent channel [BBRS]) 40 dB/(20 MHz) (40 MHz offset – 2nd 20 MHz adjacent channel [BBRS]) 24 dB/(20 MHz) (30 MHz offset – 1st 40 MHz adjacent channel [BBRS])	

Annex C

Selectivity Attenuation Values

This annex gives the input values of the selectivity attenuation input parameter. The assumptions made are explained and the references from where these values are taken from are given.

The input values of the selectivity attenuation parameter are given in Table D.2. These values, contrary to the SEM attenuation ones which are derived from the specifications of the systems, are highly dependent on the equipment being used. With this said, the values presented here, although also extracted from documents that provide specifications of the systems, can only be taken as a reference value. The selectivity values for GSM-R are obtained in different ways depending on the interfering system being considered. For a public GSM BS as interfering source, the values are extracted from [ETSI17]. The selectivity value for the 0.4 MHz offset is referent to ACS and the value for the 1 MHz and 2 MHz are derived from the blocking power levels. For a public UMTS as interfering source, the values are deduced using the same estimation method as in [CEPT11], where the corresponding wideband blocking power level is derived from the narrowband blocking ones. The selectivity values for LTE-R are extracted from [CEPT10c]. The selectivity value corresponding to the first 20 MHz adjacent channel are derived from [Zhan05]. The other two values for BBRS are assumed based on this latter selectivity value.

Table C.1 – Selectivity attenuation values for the considered interference scenarios.

Parameter	**GSM-R**	**LTE-R**	**BBRS**
Selectivity attenuation (A_{sel}) [dB]	50 dB (0.4 MHz offset) [Public GSM] 80 dB (1 MHz offset) [Public GSM] 90 dB (2 MHz offset) [Public GSM] 85.71 dB (2.8 MHz offset [Public UMTS]) 88.92 dB (3.4 MHz offset) [Public UMTS] 90 dB (4.4 MHz offset) [Public UMTS]	27.7 dB [Public GSM] 33 dB [Public UMTS]	35 dB [1st 20 MHz adjacent channel) 50 dB [2nd 20 MHz adjacent channel] 45 dB [1st 40 MHz adjacent channel]

Annex D

Out-of-band Interference Power

OOBI power as a function of the interference distance at the input of the victim’s receiver for the scenarios being considered.

D.1 GSM-R

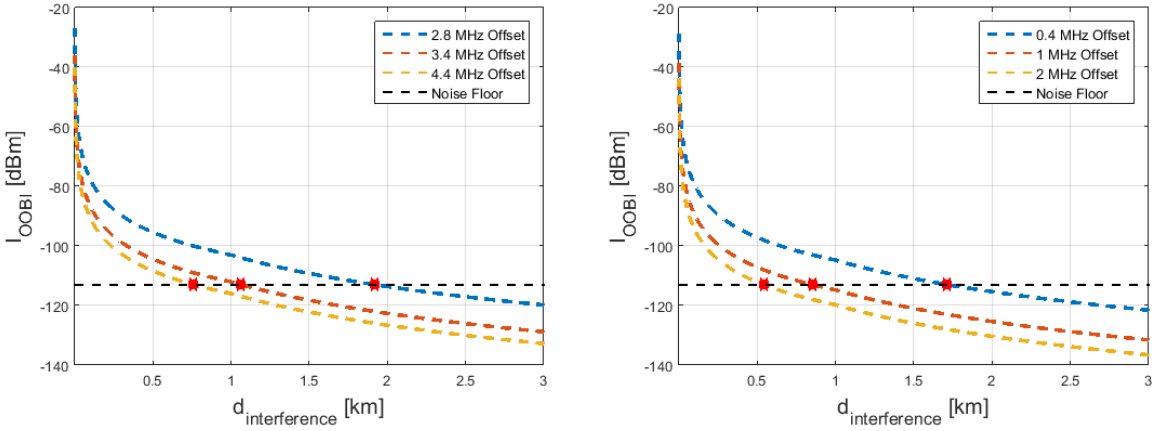

a) Public UMTS. b) Public GSM.

Figure D.1 – OOBI power at the input of the GSM-R's receiver (suburban scenario).

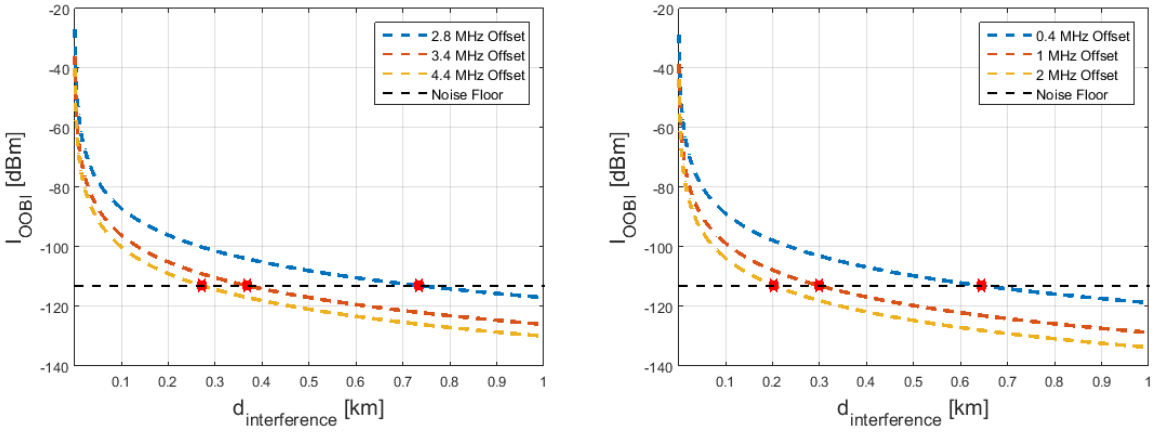

a) Public UMTS. b) Public GSM.

Figure D.2 – OOBI power at the input of the GSM-R's receiver (urban scenario).

D.2 LTE-R

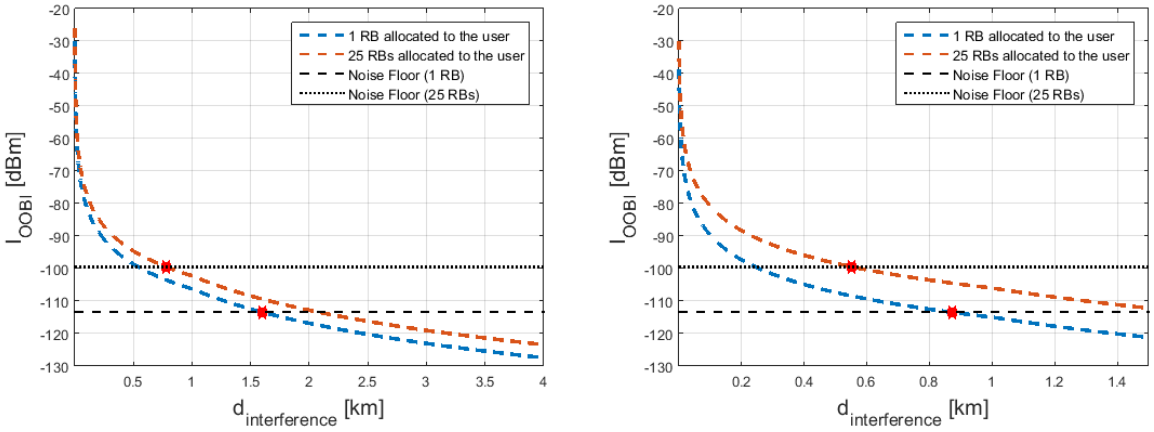

a) Public UMTS. b) Public GSM.

Figure D.3 – OOBI power at the input of the LTE-R's receiver (suburban scenario).

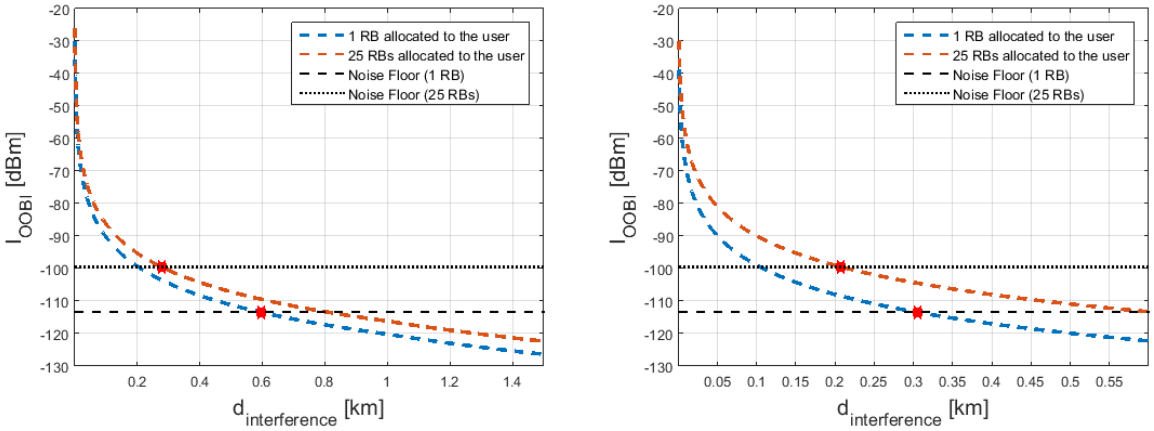

a) Public UMTS. b) Public GSM.

Figure D.4 – OOBI power at the input of the LTE-R's receiver (urban scenario).

D.3 BBRS

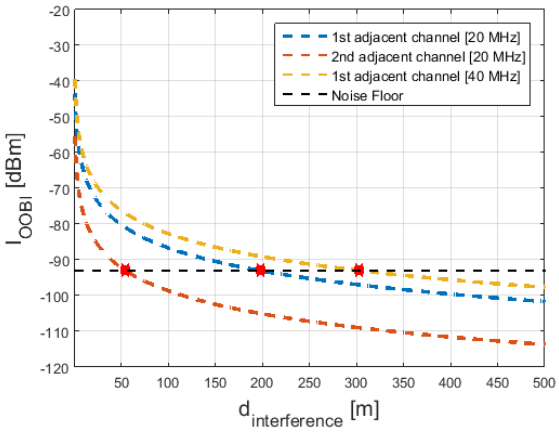

Figure D.5 – OOBI power at the input of the BBRS' receiver (MD in an outdoor scenario).

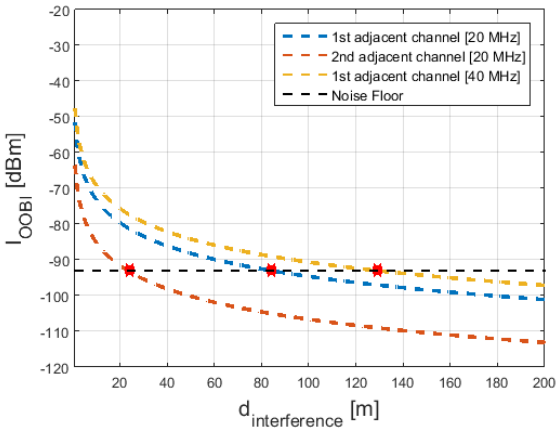

Figure D.6 – OOBI power at the input of the BBRS' receiver (AP in an indoor scenario).

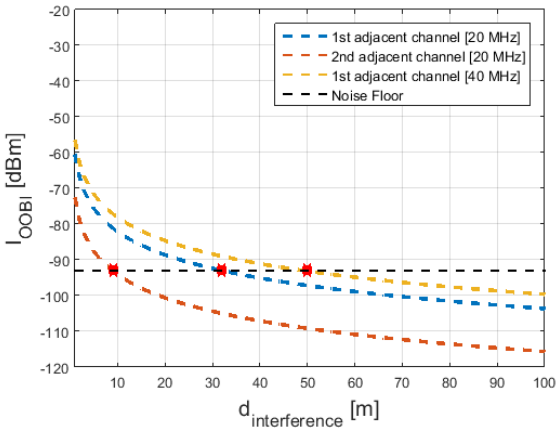

Figure D.7 – OOBI power at the input of the BBRS' receiver (MD in an indoor scenario).

Annex E

Blocking-based Interference Power

BBI power as a function of the interference distance at the input of the victim’s receiver for the scenarios being considered.

E.1 GSM-R

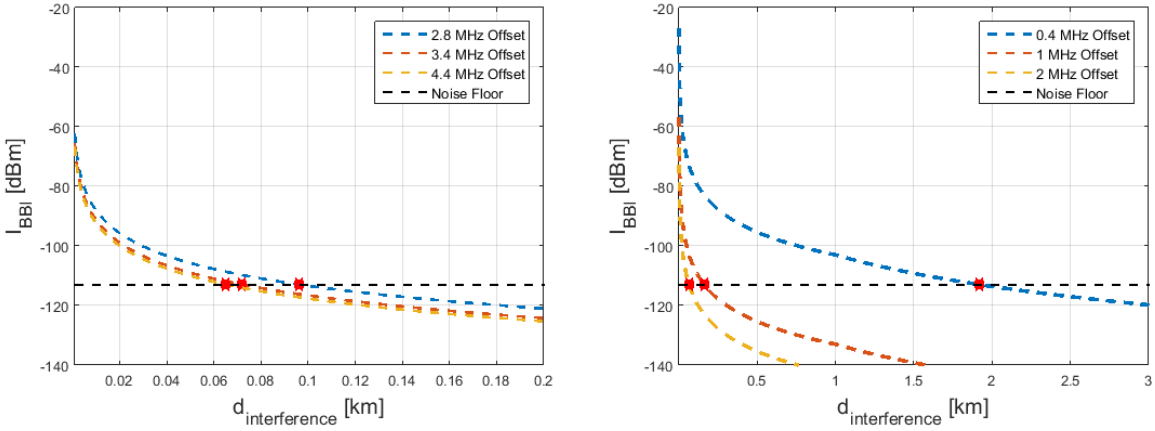

a) Public UMTS. b) Public GSM.

Figure E.1 – BBI power at the input of the GSM-R's receiver (suburban scenario).

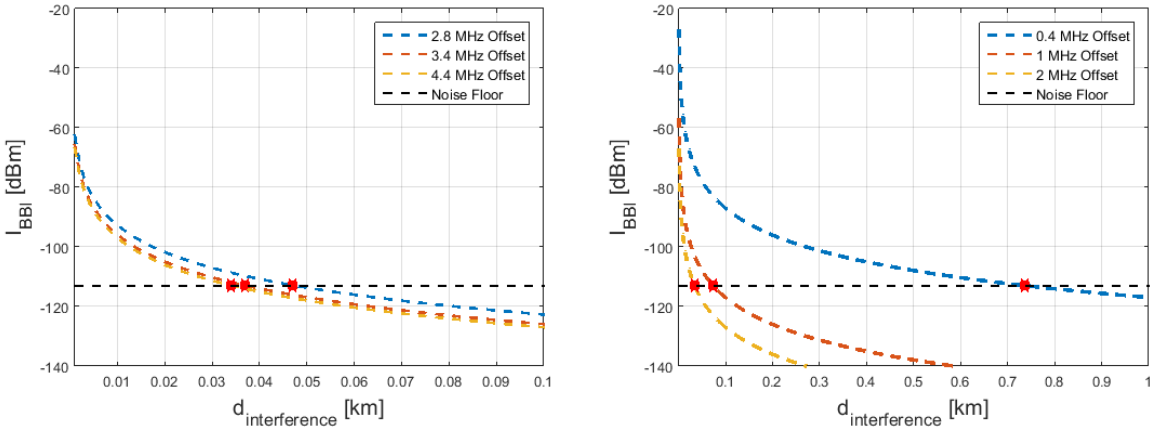

a) Public UMTS. b) Public GSM.

Figure E.2 – BBI power at the input of the GSM-R's receiver (urban scenario).

E.2 LTE-R

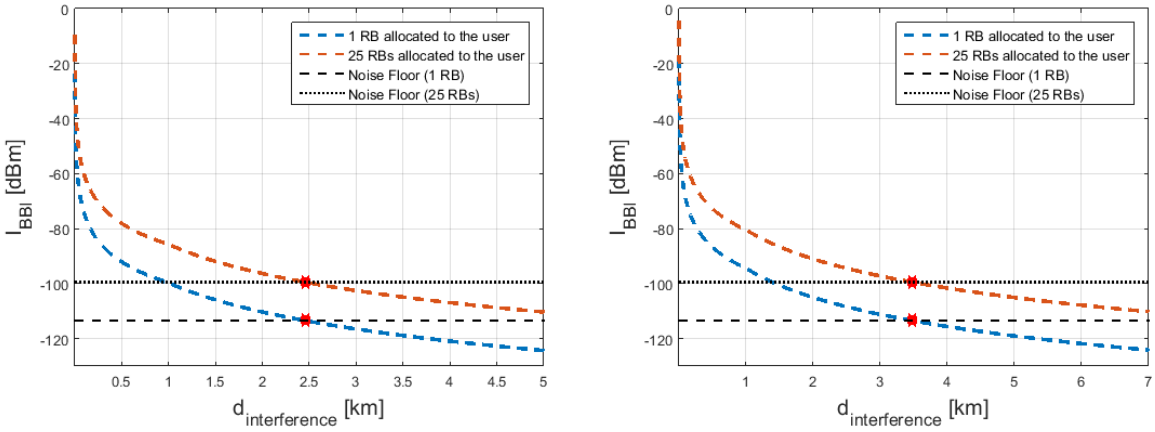

a) Public UMTS. b) Public GSM.

Figure E.3 – BBI power at the input of the LTE-R's receiver (suburban scenario).

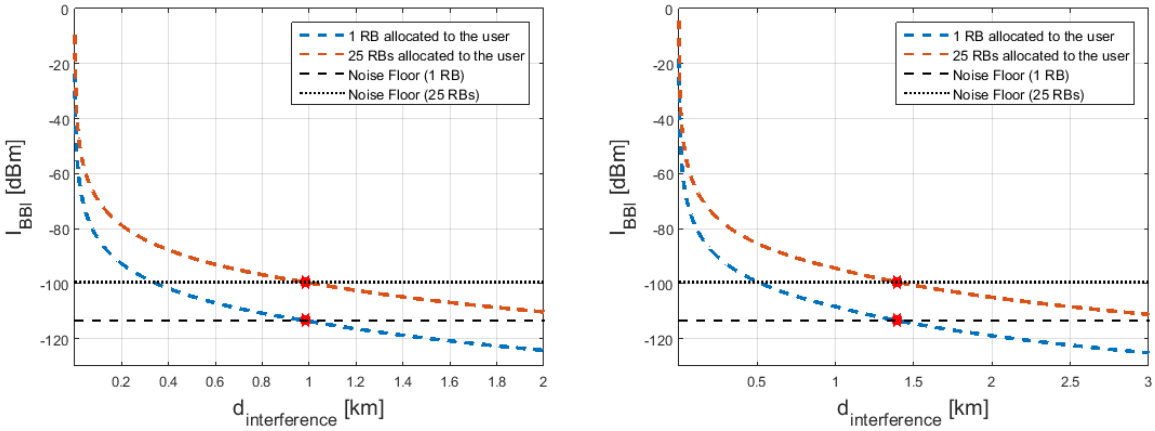

a) Public UMTS. b) Public GSM.

Figure E.4 – BBI power at the input of the LTE-R's receiver (urban scenario).

E.3 BBRS

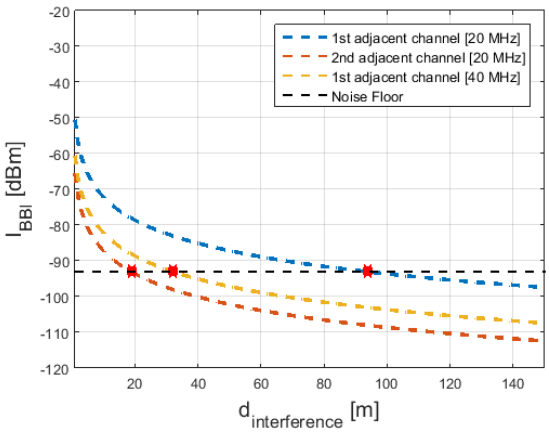

Figure E.5 – BBI power at the input of the BBRS' receiver (MD in an outdoor scenario).

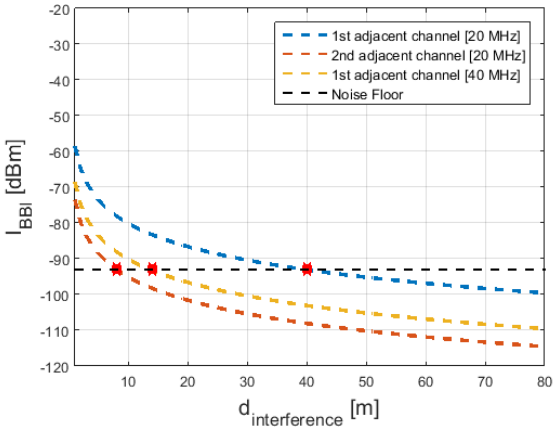

Figure E.6 – BBI power at the input of the BBRS' receiver (AP in an indoor scenario).

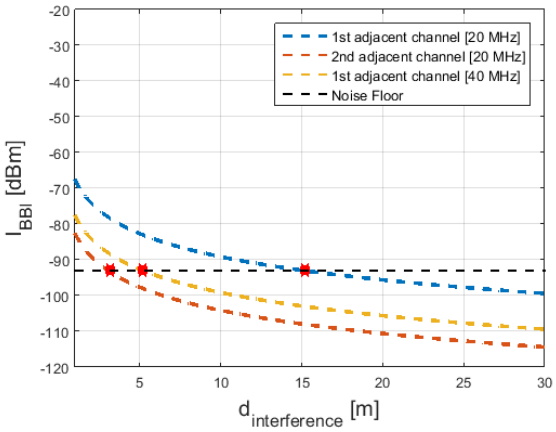

Figure E.7 – BBI power at the input of the BBRS' receiver (MD in an indoor scenario).

Annex F

Intermodulation-based Interference Power

IBI power as a function of the interference distance at the input of the victim’s receiver for the scenarios being considered.

F.1 GSM-R

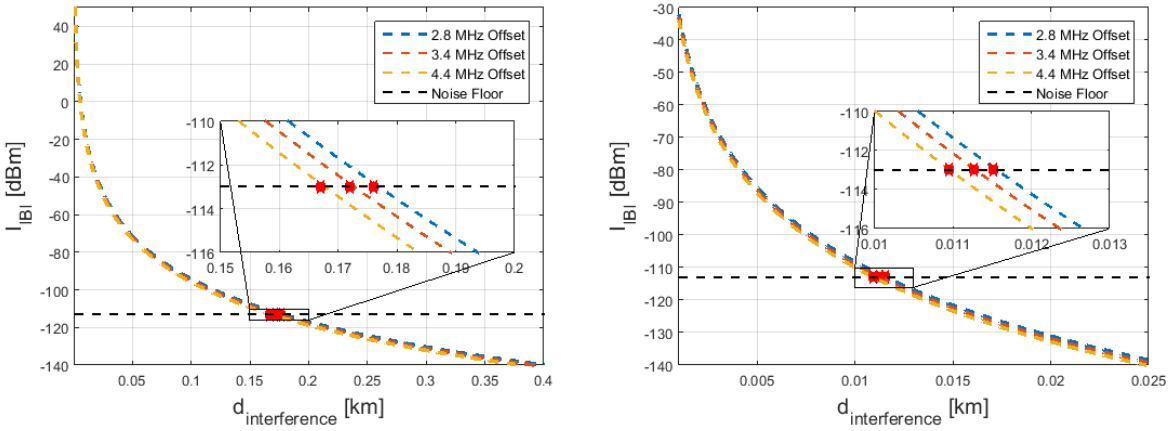

a) Without filter. b) With filter.

Figure F.1 – IBI power at the input of the GSM-R's receiver (public UMTS in a suburban scenario).

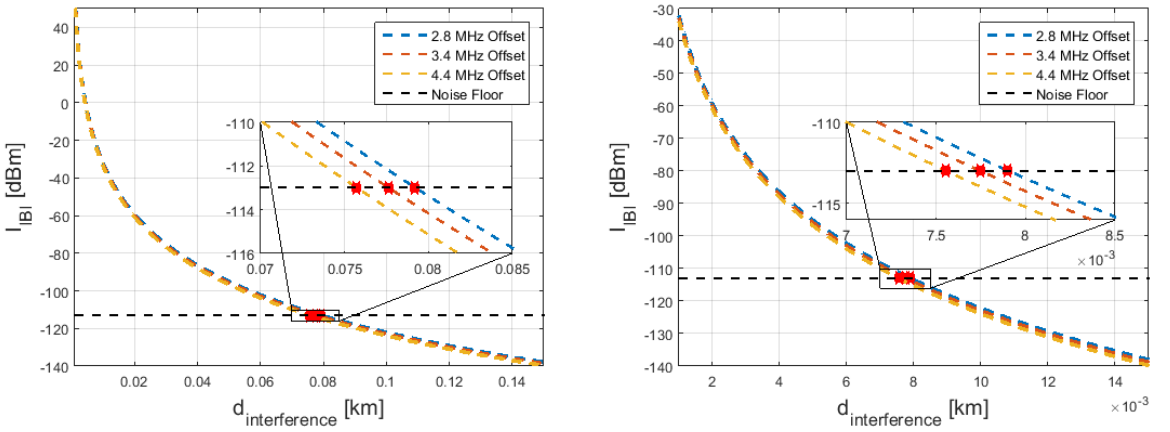

a) Without filter. b) With filter.

Figure F.2 – IBI power at the input of the GSM-R's receiver (public UMTS in an urban scenario).

F.2 LTE-R

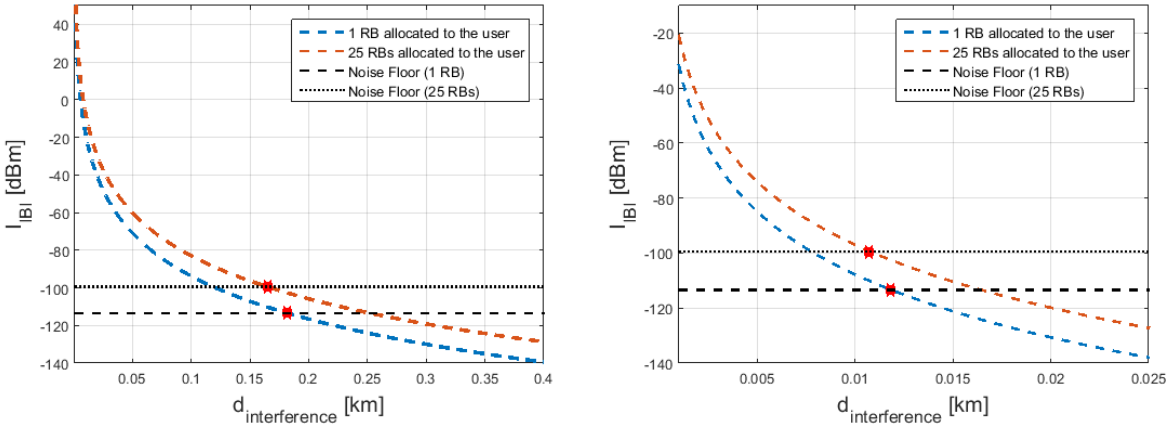

a) Without filter. b) With filter.

Figure F.3 – IBI power at the input of the LTE-R's receiver (public UMTS in a suburban scenario).

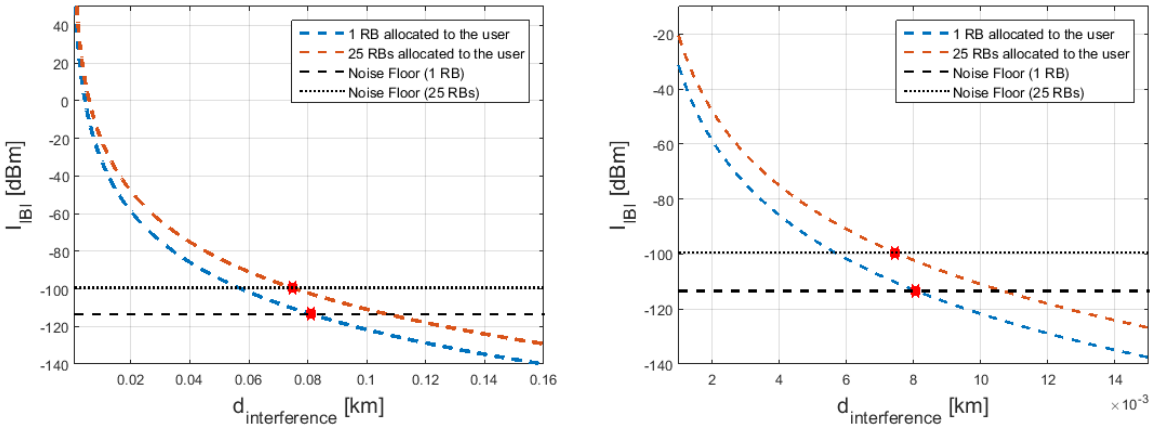

a) Without filter. b) With filter.

Figure F.4 – IBI power at the input of the LTE-R's receiver (public UMTS in an urban scenario).

F.3 BBRS

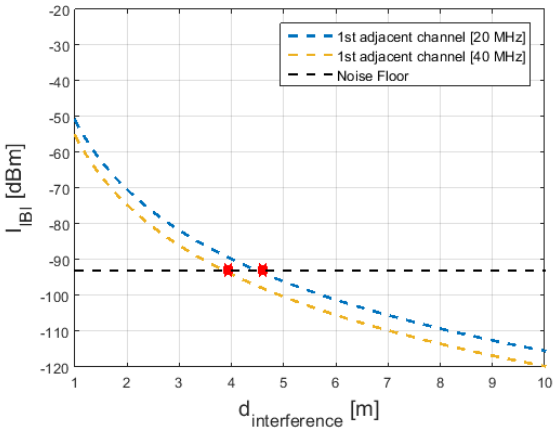

Figure F.5 – IBI power at the input of the BBRS' receiver (MD in an outdoor scenario).

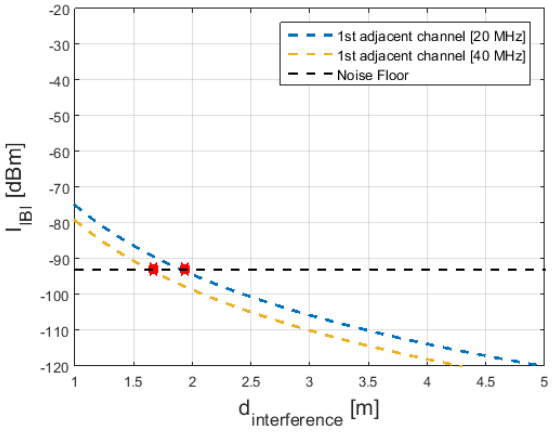

Figure F.6 – IBI power at the input of the BBRS' receiver (AP in an indoor scenario).

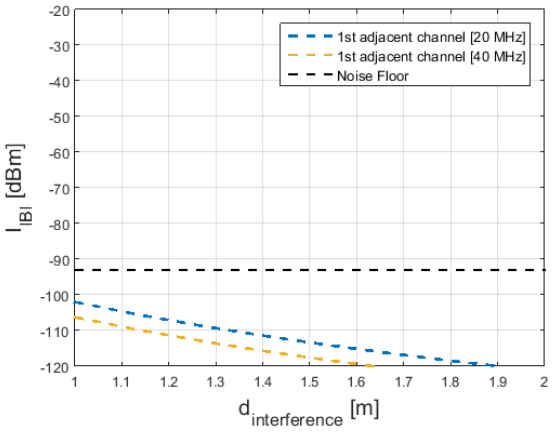

Figure F.7 – IBI power at the input of the BBRS' receiver (MD in an indoor scenario).

Annex G

Interference-free Region Distance

Interference-free region distances for supplementary scenarios taking the sum of interference types into account.

G.1 GSM-R

Table G.1 – GSM-R's free-region distances for the sum of interference types (${h_{bs}}^{int}$=40 m).

$d_{free-region}^{TOTAL}$ [km]						
Scenario	**Public UMTS**			**Public GSM**		
	2.8 MHz offset	3.4 MHz offset	4.4 MHz offset	0.4 MHz offset	1 MHz offset	2 MHz offset
Rural	7.581	4.152	3.188	8.817	3.475	2.479
Suburban	2.187	1.198	0.890	2.544	1.002	0.627
Urban	0.837	0.414	0.304	0.999	0.336	0.226

G.2 LTE-R

Table G.2 – LTE-R's free-region distances for the sum of interference types (${h_{bs}}^{int}$=40 m).

$d_{interference}^{TOTAL}$ [km]								
Scenario	**Public UMTS**				**Public GSM**			
	(wo/filter)		(w/filter)		(wo/filter)		(w/filter)	
	1 RB allocated	25 RBs allocated	1 RB allocated	25 RBs allocated	1 RB allocated	25 RBs allocated	1 RB allocated	25 RBs allocated
Rural	10.354	9.831	6.321	3.284	13.961	13.936	3.634	2.754
Suburban	2.986	2.836	1.824	0.929	4.029	4.021	1.049	0.726
Urban	1.174	1.114	0.676	0.314	1.581	1.579	0.354	0.256

G.3 BBRS

Table G.3 – BBRS' free-region distances for the sum of interference types (G_r=5 dBi).

$d_{free-region}^{TOTAL}$ [m]						
Scenario	**AP**			**MD**		
	1st adjacent channel (20 MHz)	2nd adjacent channel (20 MHz)	1st adjacent channel (40 MHz)	1st adjacent channel (20 MHz)	2nd adjacent channel (20 MHz)	1st adjacent channel (40 MHz)
Outdoor	140	37	198	53	14	75
Indoor	22	6	32	8	2	12

Annex H

Maximum Communication Distance

Maximum communication distance as a function of the interference distance for the scenarios being considered.

H.1 GSM-R

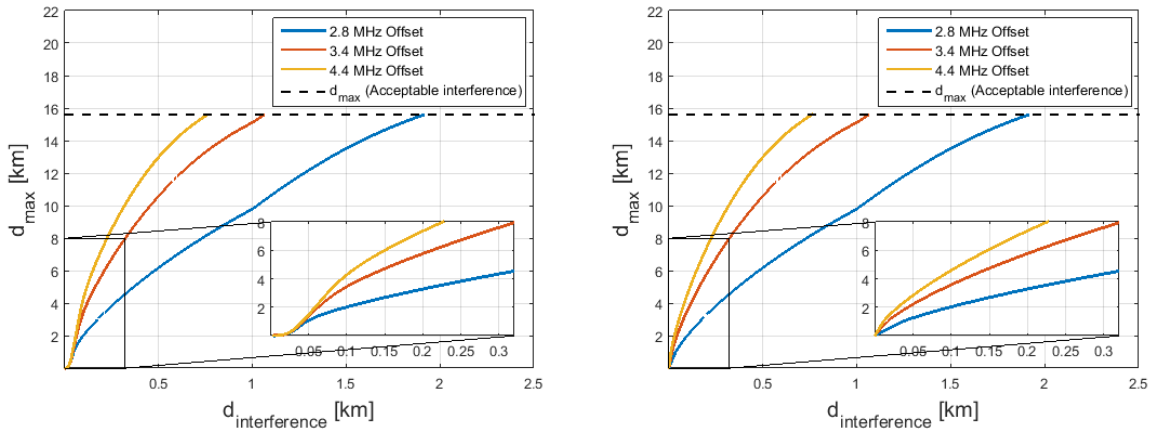

a) Without filter. b) With filter.

Figure H.1 – GSM-R's maximum communication distance (public UMTS in a suburban scenario).

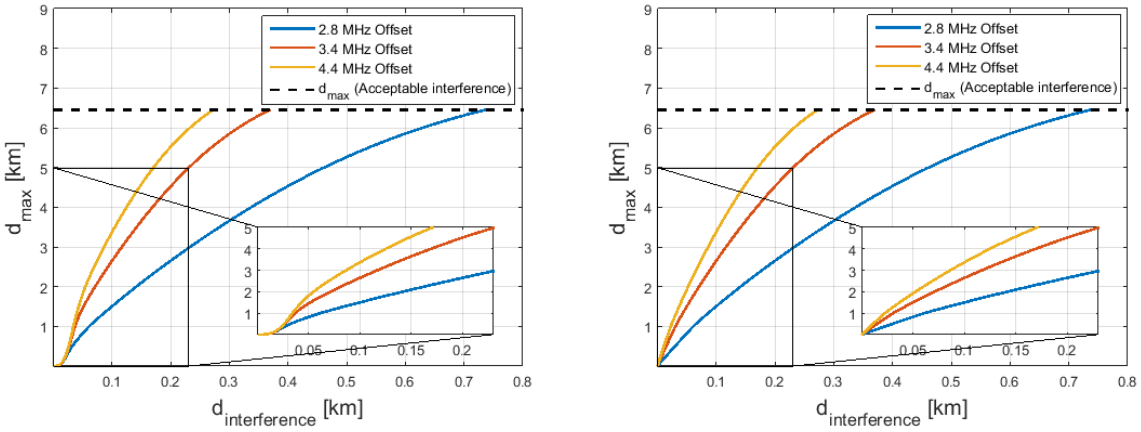

a) Without filter. b) With filter.

Figure H.2 – GSM-R's maximum communication distance (public UMTS in an urban scenario).

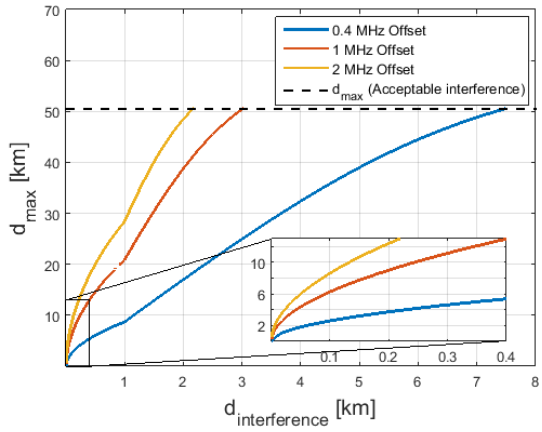

Figure H.3 – GSM-R's maximum communication distance (public GSM in a rural scenario).

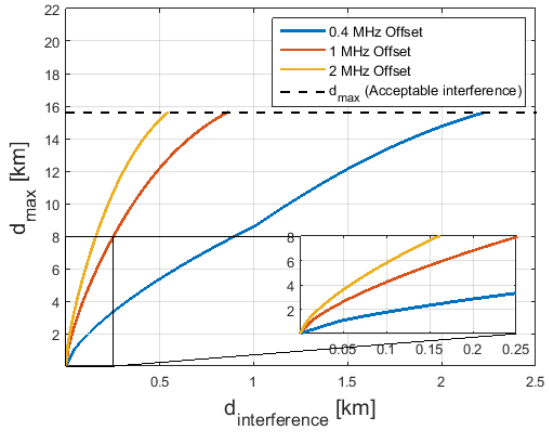

Figure H.4 – GSM-R's maximum communication distance (public GSM in a suburban scenario).

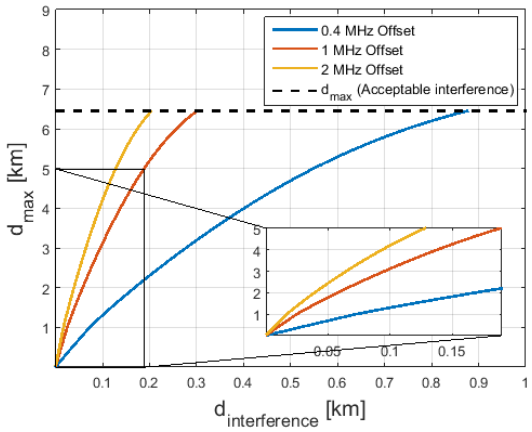

Figure H.5 – GSM-R's maximum communication distance (public GSM in an urban scenario).

H.2 LTE-R

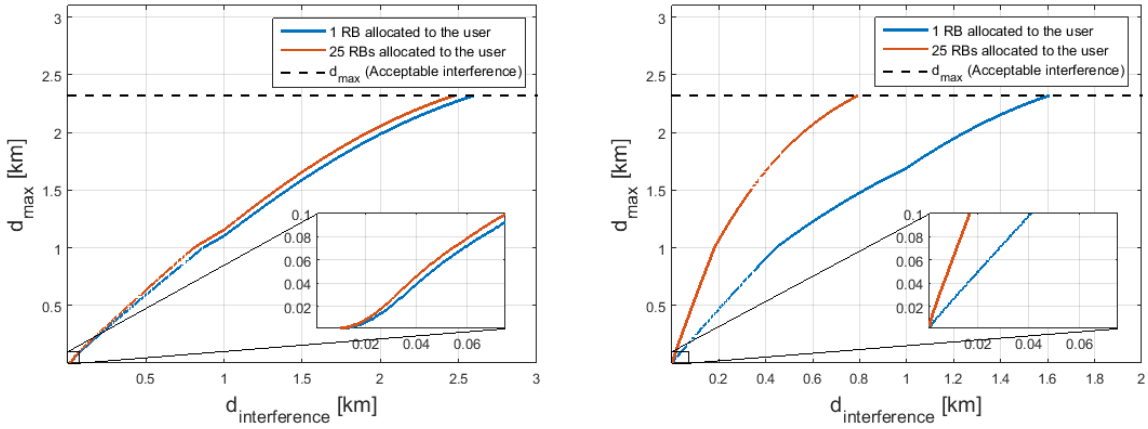

a) Without filter. b) With filter.

Figure H.6 – LTE-R's maximum communication distance (public UMTS in a suburban scenario).

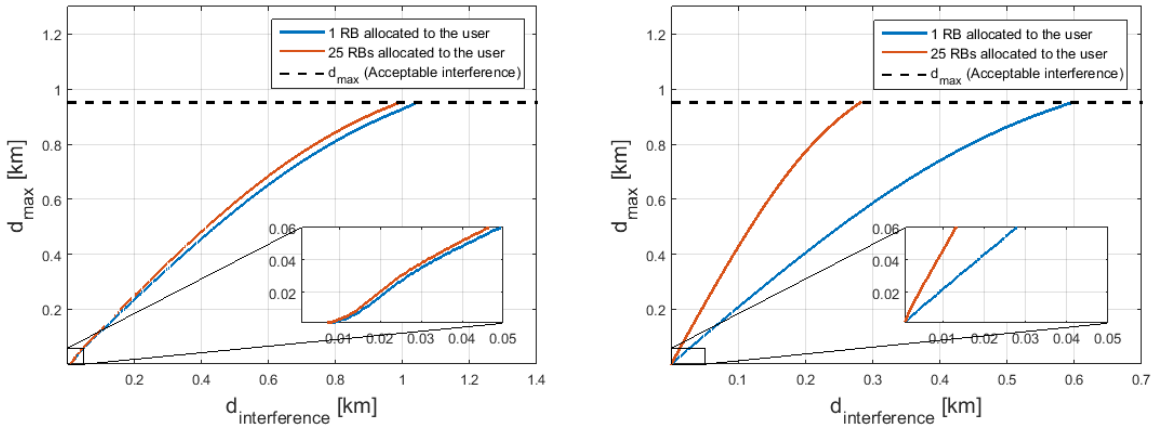

a) Without filter. b) With filter.

Figure H.7 – LTE-R's maximum communication distance (public UMTS in an urban scenario).

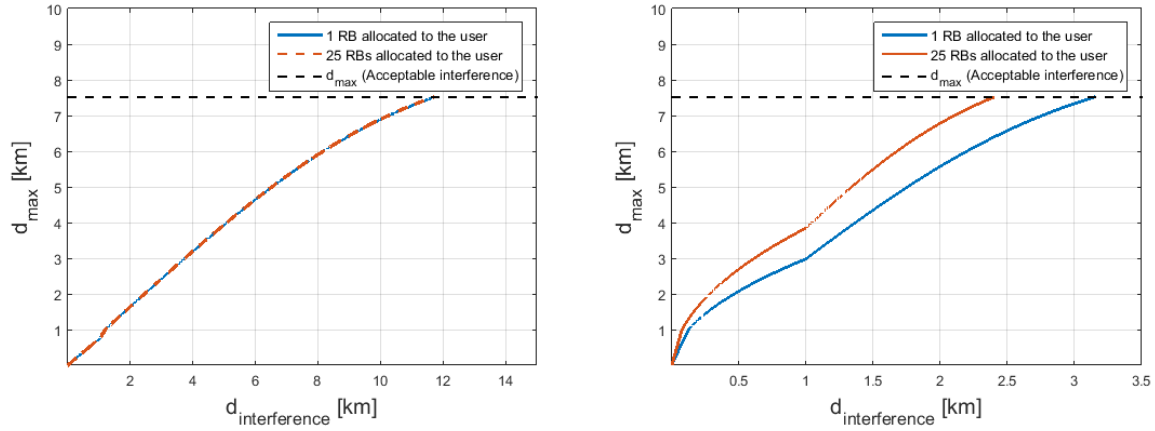

a) Without filter. b) With filter.

Figure H.8 – LTE-R's maximum communication distance (public GSM in a rural scenario).

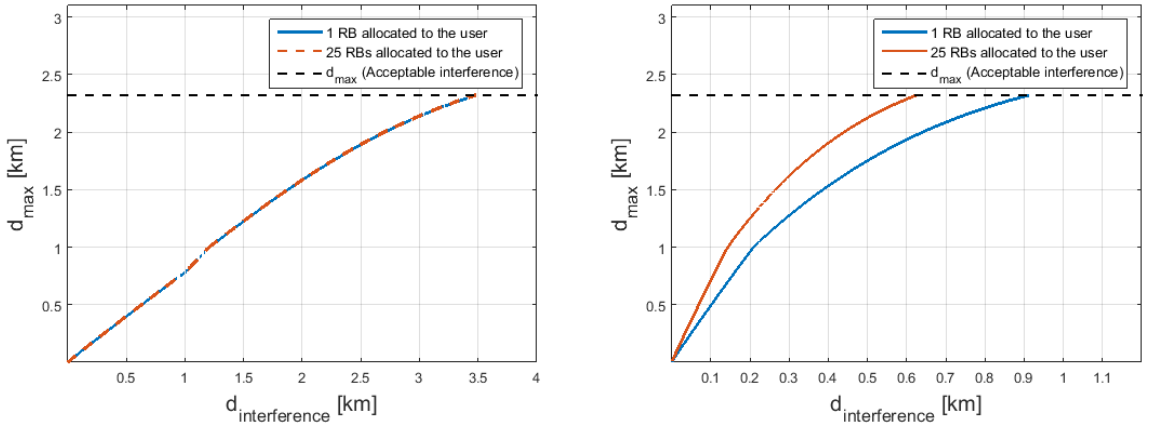

a) Without filter. b) With filter.

Figure H.9 – LTE-R's maximum communication distance (public GSM in a suburban scenario).

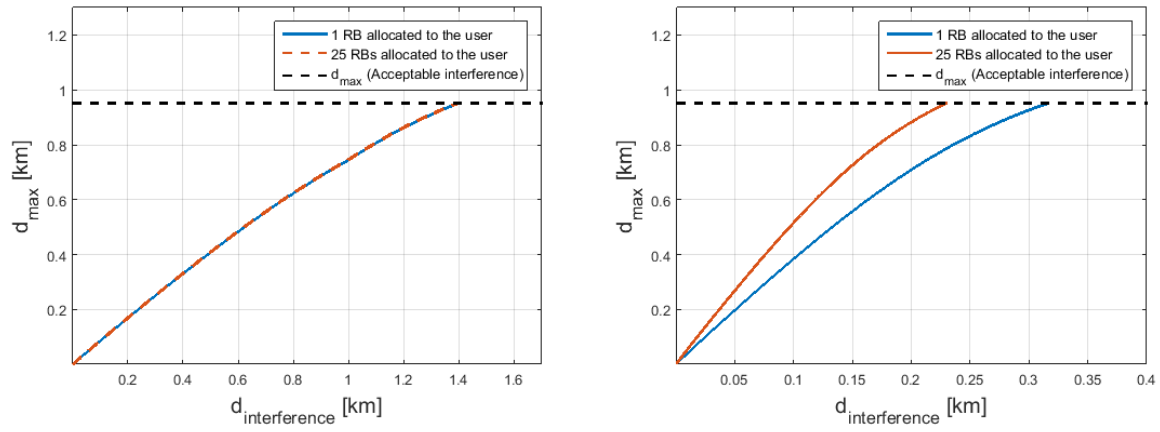

a) Without filter. b) With filter.

Figure H.10 – LTE-R's maximum communication distance (public GSM in an urban scenario).

H.3 BBRS

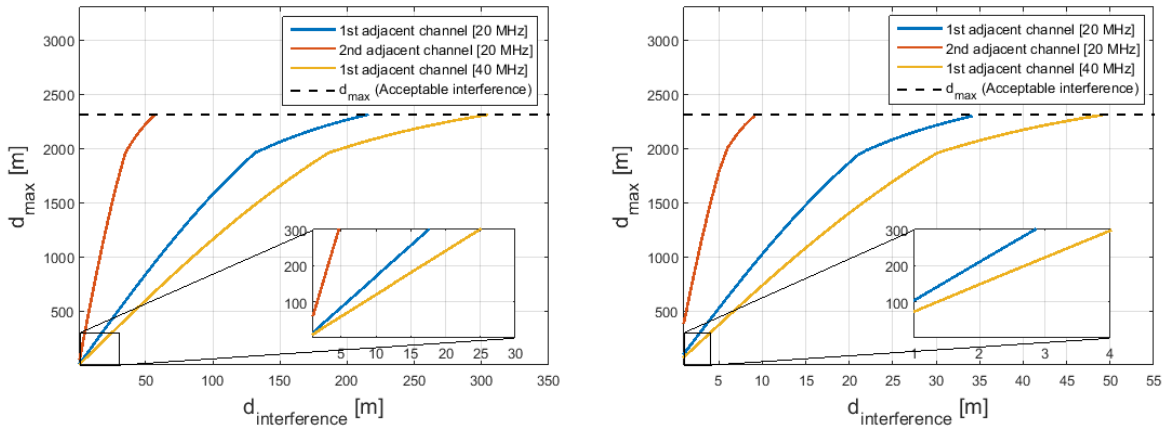

a) Outdoor. b) Indoor.

Figure H.11 – BBRS' maximum communication distance for 12 Mbps requirement (MD).

Annex I

Capacity Loss

Capacity loss as a function of the interference distance for the scenarios being considered.

I.1 LTE-R

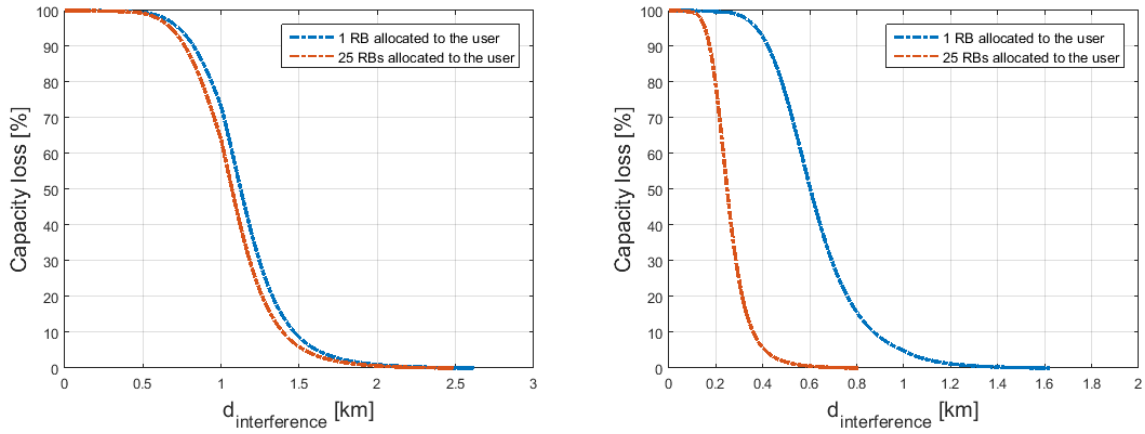

a) Without filter. b) With filter.

Figure I.1 – LTE-R's capacity loss d_{max}=8 km (public UMTS in a suburban scenario).

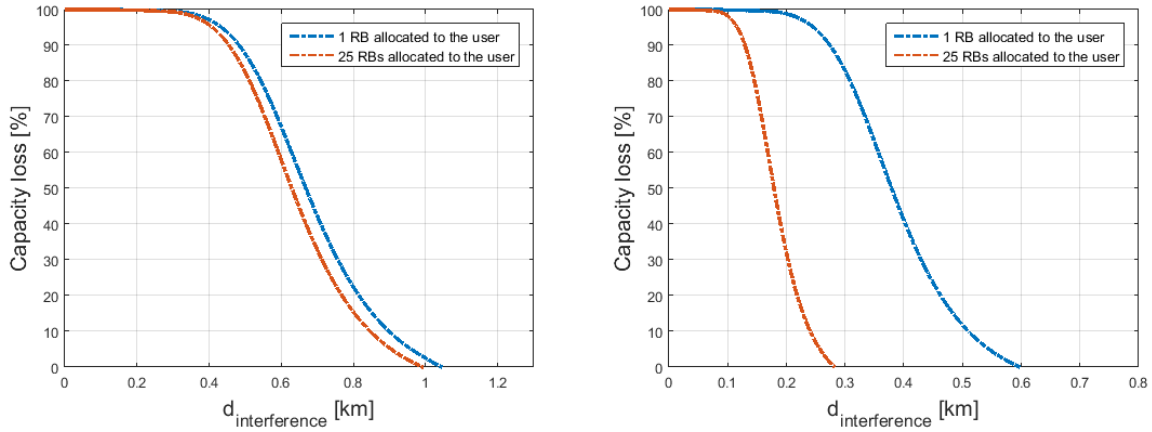

a) Without filter. b) With filter.

Figure I.2 – LTE-R's capacity loss d_{max}=5 km (public UMTS in an urban scenario).

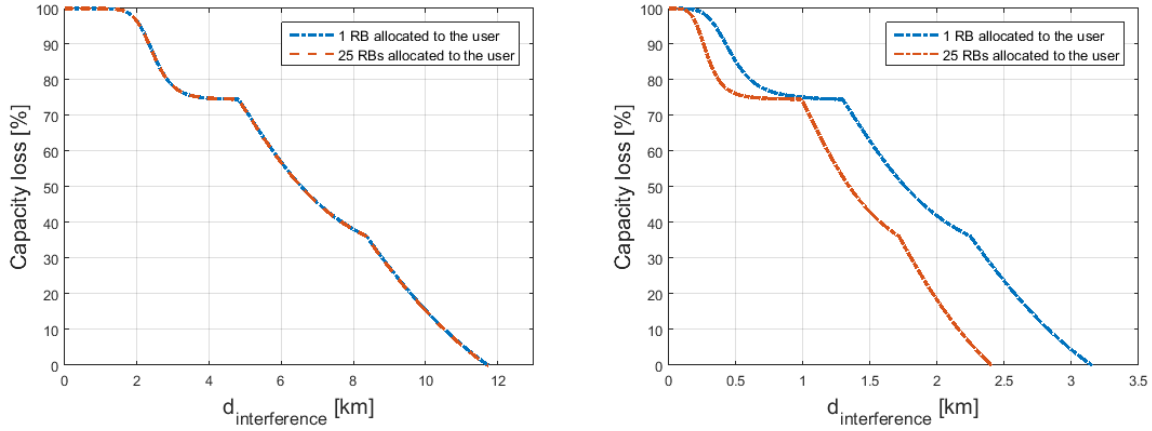

a) Without filter. b) With filter.

Figure I.3 – LTE-R's capacity loss d_{max}=13 km (public GSM in a rural scenario).

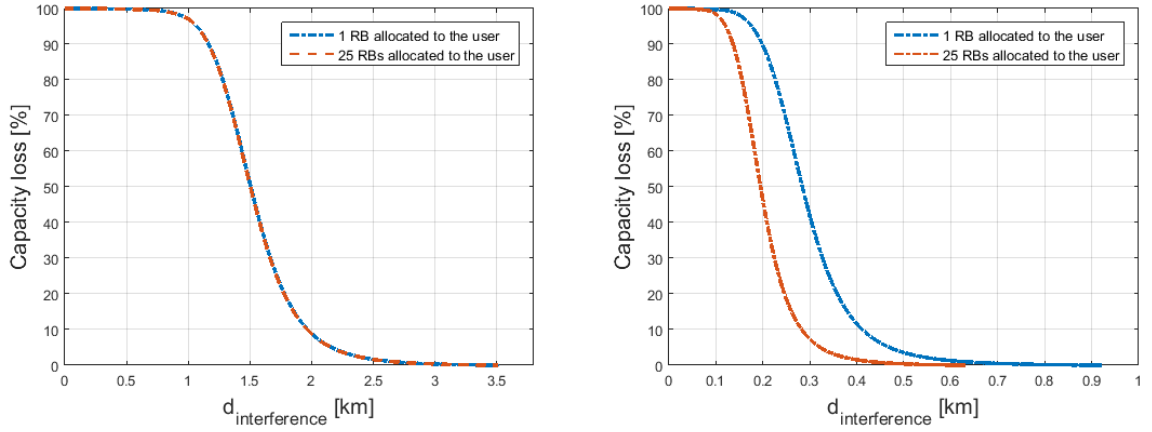

a) Without filter. b) With filter.

Figure I.4 – LTE-R's capacity loss d_{max}=8 km (public GSM in a suburban scenario).

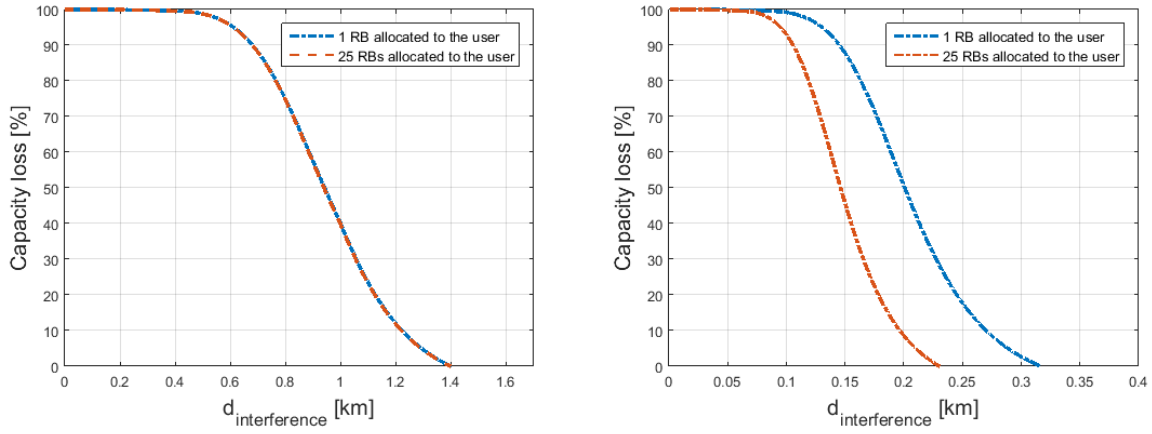

a) Without filter. b) With filter.

Figure I.5 – LTE-R's capacity loss d_{max}=5 km (public GSM in an urban scenario).

I.2 BBRS

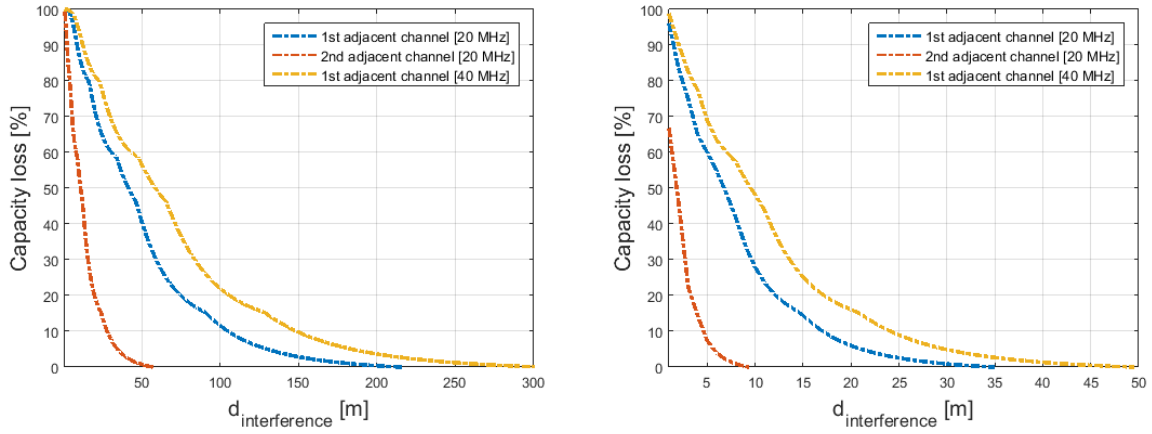

a) Outdoor. b) Indoor.

Figure I.6 – BBRS' capacity loss d_{max}=300 m (MD).

References

[3GPP11] 3GPP – Technical Specification Group – RAN WG4, *Summary of alignment and impairments results for eDL-MIMO demodulation requirements*, Report R4-112713, May 2011. Available in: (http://3gpp.org).

[AHZG12] B. Ai, R. He, Z. Zhong, K. Guan, B. Chen, P. Liu and Y. Li, "Radio Wave Propagation Scene Partitioning for High-Speed Rails", *International Journal of Antennas and Propagation*, Vol. 2012, Sep. 2012. Available in: (https://new.hindawi.com/journals/ijap/2012/815232/).

[BBRS17] Broad Band Radio System (BBRS), Thales Group, Portugal, 2017.

[BJHS03] B. Bangerter, E. Jacobsen, M. Ho, A. Stephens, A. Maltsev, A. Rubtsov, A. Sadri, "High-Throughput Wireless LAN Air Interface", *Intel Technology Journal*, Vol. 7, Issue 3, Aug. 2003, pp. 47-57. Available in: (https://pdfs.semanticscholar.org/8690/4ffa0f4b933731b0cde4a6609841cf908207.pdf).

[CaPe99] N. B. Carvalho, J. C. Pedro, "Multi-Tone Intermodulation Distortion Performance of 3rd Order Microwave Circuits", in *1999 IEEE MTT-S International Microwave Symposium*, Anaheim, USA, Jun. 1999. Available in: (https://ieeexplore.ieee.org/document/779871).

[CEPT07] CEPT ECC Electronic Communications Committee, *Compatibility between UMTS 900/1800 and systems operating in adjacent bands,* ECC Report 96, Mar. 2007. Available in: (https://www.ecodocdb.dk/download/815bc8b3-2614/ECCREP096.PDF).

[CEPT10a] CEPT ECC Electronic Communications Committee, *Compatibility between GSM MCBTS and other services (TRR, RDBN/PRMG, HC-SDMA, GSM-R, DME, MIDS, DECT) operating in the 900 and 1800 MHz frequency bands,* ECC Report 146, Jun. 2010. Available in: (https://www.ecodocdb.dk/download/5086e2b6-45c8/ECCREP146.PDF).

[CEPT10b] CEPT ECC Electronic Communications Committee, *Compatibility between LTE and WiMAX operating within the bands 880-915 MHz / 925-960 MHz and 1710-1785 MHz / 1805-1880 MHz (900/1800 MHz bands) and systems operating in adjacent bands,* CEPT Report 41, Nov. 2010. Available in: (https://www.ecodocdb.dk/download/7f9af1a2-5806/CEPTREP041.PDF).

[CEPT10c] CEPT ECC Electronic Communications Committee, *"Compatibility study for LTE and WiMAX operating within the bands 880-915 MHz / 925-960 MHz and 1710-1785 MHz /1805-1880 MHz (900/1800 MHz bands)",* CEPT Report 40, Nov. 2010. Available in: (https://www.ecodocdb.dk/download/4ce187bc-3569/CEPTREP040.PDF).

[CEPT11] CEPT ECC Electronic Communications Committee, *Practical mechanism to improve compatibility between GSM-R and public mobile networks and guidance on practical coordination,* ECC Report 162*,* Montegrotto Terme, Italy, May. 2011. Available in: (https://www.ecodocdb.dk/download/1ac09063-352f/ECCREP162.PDF).

[CEPT15] CEPT ECC Electronic Communications Committee, *Guidance for improving coexistence between GSM-R and MFCN in the 900 MHz band,* ECC Report 229*,* May. 2015. Available in: (https://www.ecodocdb.dk/download/42bc81c7-22bc/ECCREP229.PDF).

[CEPT19a] CEPT ECC Electronic Communications Committee, *The European table of frequency allocations and applications in the frequency range 8.3 kHz to 3000 GHz (ECA table)*, ERC Report 25, Mar. 2019. Available in: (https://www.ecodocdb.dk/download/2ca5fcbd-4090/ERCREP025.pdf).

[CEPT19b] CEPT ECC Electronic Communications Committee, *Sharing and compatibility studies related to Wireless Access Systems including Radio Local Area Networks (WAS/RLAN) in the frequency band 5925-6425 MHz,* ECC Report 302*,* May. 2019. Available in: (https://www.ecodocdb.dk/download/cc03c766-35f8/ECC%20Report%20302.pdf).

[CISC07] CISCO, *802.11n Wireless Technology Overview*, White Paper, 2007. Available in: (https://www.ventevinfra.com/pdf/802.11n%20Wireless%20Technology%20Overview.pdf).

[CMAF13] J. Calle-Sánchez, M. Molina-García, J. I. Alonso, and A. Fernández-Durán, “Long Term Evolution in High Speed Railway Environments: Feasibility and Challenges”, *Bell Labs Technical Journal*, Vol.18, No.2, Sep. 2013, pp.237-253. Available in: (http://ieeexplore.ieee.org/document/6772145/).

[Corr18] L. M. Correia, *Mobile Communication Systems*, Lecture Notes, Instituto Superior Técnico (IST), Lisbon, Portugal, 2018.

[Delg18] P. Delgado, *Evaluation of Train Communications in Bridges and other Metallic Structures*, M.Sc. thesis, Instituto Superior Técnico, Lisbon, Portugal, Nov. 2018. Available in: (https://fenix.tecnico.ulisboa.pt/downloadFile/563345090416553/Thesis_PedroD_final.pdf).

[ECMT19a] European Commission – Mobility and Transport (ERTMS - What is ERTMS?). Available in: (https://ec.europa.eu/transport/modes/rail/ertms/what-is-ertms_en). [Accessed in Nov. 2019].

[ECMT19b] European Commission – Mobility and Transport (ERTMS - Subsystems and Constituents of the ERTMS). Available in: (https://ec.europa.eu/transport/modes/rail/ertms/what-is-ertms/subsystems_and_constituents_of_the_ertms_mt). [Accessed in Nov. 2019].

[Elli16] S. Ellingson, *Radio Systems Engineering*, Cambridge University Press, Virginia, USA, 2016.

[ERTM19] ERTMS – The European Rail Traffic Management System (ERTMS Deployment Statistics

- Overview). Available in: (http://www.ertms.net/?page_id=58). [Accessed in Dec. 2019].

[ETSI15] ETSI Technical Committee Railway Telecommunications, Universal Mobile Telecommunications System (UMTS); Base Station (BS) radio transmission and reception (FDD), ETSI TS 125 104 V12.5.0, France, Jan. 2015. Available in: (https://www.etsi.org/deliver/etsi_ts/125100_125199/125104/12.05.00_60/ts_125104v120500p.pdf).

[ETSI17] ETSI Technical Committee Railway Telecommunications, *Digital cellular telecommunications system (Phase 2+) (GSM); GSM/EDGE Radio Transmission and Reception,* ETSI TS 145 005 V13.3.0, France, Jan. 2017. Available in: (https://www.etsi.org/deliver/etsi_ts/145000_145099/145005/13.03.00_60/ts_145005v130300p.pdf).

[ETSI19] ETSI Technical Committee Railway Telecommunications, *Radio performance simulations and evaluations in rail environment Part 1: Long Term Evolution (LTE)*, ETSI TR 103 554-1 V1.2.1, France, 2019. Available in: (https://www.etsi.org/deliver/etsi_tr/103500_103599/10355401/01.02.01_60/tr_10355401v010201p.pdf).

[EuCO16] European Communications Office (ECO), *SEAMCAT Handbook Edition 2,* ECC Report 252, Apr. 2016. Available in: (https://www.ecodocdb.dk/download/5b8f9726-04a6/ECCRep252.pdf).

[EUSE19a] Eurostat Statistics Explained (Railway freight transport statistics). Available in: (https://ec.europa.eu/eurostat/statistics-explained/index.php/Railway_freight_transport_statistics). [Accessed in Dec. 2019].

[EUSE19b] Eurostat Statistics Explained (Railway passenger transport statistics - quarterly and annual data). Available in: (https://ec.europa.eu/eurostat/statistics-explained/index.php/Railway_passenger_transport_statistics_-_quarterly_and_annual_data#Number_of_passengers_transported_by_rail_increased_in_2018). [Accessed in Dec. 2019].

[FICS12] A. Ferrari, M. Itria, S. Chiaradonna, G. Spagnolo, “Model-Based Evaluation of the Availability of a CBTC System”, in *4th International Workshop on Software Engineering for Resilient Systems,* Pisa, Italy, Sep. 2012. Available in: (https://www.researchgate.net/publication/262164828_Model-Based_Evaluation_of_the_Availability_of_a_CBTC_System).

[FMST12] R. Folkesson, D. Martens, D. Schattschneider, K. Tuominen, *GSM-R MS Interference measurements at Ispra*, GSM-R Frequency Management Working Group, Document No. O-8725, Union International Des Chemins De Fer (UIC), Ispra, Italy, Apr. 2012. Available in: (https://www.efis.dk/documents/11893).

[FrFC17] P. Fraga-Lamas, T.M. Fernández-Caramés and L. Castedo, “Towards the Internet of Smart Trains: A Review on Industrial IoT-Connected Railways”, *Sensors*, Vol.17, No.6, June. 2017, pp.1457(1-44). Available in: (http://www.mdpi.com/1424-8220/17/6/1457/pdf).

[GeRK12] C. Gessner, A. Roessler, and M. Kottkamp, *UMTS Long Term Evolution (LTE) Technology Introduction*, Note 1MA111, July 2012. Available in: (https://cdn.rohde-

schwarz.com/pws/dl_downloads/dl_application/application_notes/1ma111/1MA111_4E_LTE_technology_introduction.pdf).

[Ghaz14] M. Ghazel, “Formalizing a subset of ERTMS/ETCS specifications for verification purposes”, *Transportation Research Part C Emerging Technologies*, Vol. 42, Mar. 2014. Available in: (https://www.researchgate.net/publication/260065898_Formalizing_a_subset_of_ERTMSETCS_specifications_for_verification_purposes).

[GLCI19] GL Communications Inc – Telecommunications Products & Consulting Services, *2G Networks Test Solutions*, Brochure, Gaithersburg, Maryland, EUA, Apr. 2019. Available in: (https://www.gl.com/Brochures/Brochures/2G-Networks-Test-Solutions-Combined-Brochure.pdf).

[GSMR15a] GSM-R Operations Group, *EIRENE – System Requirements Specification Version 16.0.0, UIC*, Paris, France, 2015. Available in: (https://uic.org/IMG/pdf/srs-16.0.0_uic_951-0.0.2_final.pdf).

[GSMR15b] GSM-R Operations Group, *EIRENE – Functional Requirements Specification Version 8.0.0*, UIC, Paris, France, 2015. Available in: (https://uic.org/IMG/pdf/frs-8.0.0_uic_950_0.0.2_final.pdf).

[GSMR19] GSMR – INFO (GSM-R Technology At A Glance). Available in: (http://gsmr-info.com/gsm-r_history.cfm). [Accessed in Dec. 2019].

[HAWG16] R. He, B. Ai, G. Wang, K. Guan, Z. Zhong, A. F. Molisch, C. Briso-Rodriguez and C. P. Oestges, “High-speed railways communications: From GSM-R to LTE-R”, *IEEE Vehicular Technology Magazine*, Vol. 11, No. 3, Sep. 2016, pp. 49-58. Available in: (http://ieeexplore.ieee.org/document/7553613/).

[HSDR09] T. Hammi, N.B. Slimen, V. Deniau, J. Rioult and S. Dudoyer, “Comparison between GSM-R coverage level and EM noise level in railway environment”, in *9th International Conference on Intelligent Transport Systems Telecommunications*, Lille, France, Oct. 2009. Available in: (https://ieeexplore.ieee.org/document/5399370).

[HUAW12] HUAWEI, *Future-Oriented LTE for Rail Solution,* 2012. Available in: (https://www.huawei.com/minisite/Innotrans/download/LTE%20Solution.pdf).

[Isab14] J. Isabona, “Maximising Coverage and Capacity with QOS Guarantee in GSM Network by Means of Cell Cluster Optimization”, *International Journal of Advanced Research in Physical Science (IJARPS)*, Vol. 1, Issue 6, Oct. 2014, pp. 44-55. Available in: (https://www.researchgate.net/publication/303985068_Maximising_Coverage_and_Capacity_with_QOS_Guarantee_in_GSM_Network_by_Means_of_Cell_Cluster_Optimization).

[ITUR07] ITU-R, *Intermodulation interference calculations in the land-mobile service,* Recommendation ITU-R SM.1134-1, Feb. 2007. Available in: (https://www.itu.int/dms_pubrec/itu-r/rec/sm/R-REC-SM.1134-1-200702-I!!PDF-E.pdf).

[ITUR14] ITU-R, *Characteristics of broadband radio local area networks,* Recommendation ITU-R

M.1450-5 (M Series Mobile, radiodetermination, amateur and related satellite services), Geneva, Switzerland, Feb. 2014. Available in: (https://www.itu.int/dms_pubrec/itu-r/rec/m/R-REC-M.1450-5-201404-I!!PDF-E.pdf).

[ITUR19] ITU-R, *Prediction of building entry loss,* Recommendation ITU-R P.2109-1, Aug. 2019. Available in: (https://www.itu.int/dms_pubrec/itu-r/rec/p/R-REC-P.2109-1-201908-I!!PDF-E.pdf).

[KMHZ07] P. Kyösty, J. Meinilä, L. Hentilä, X. Zhao, T. Jämsä, C. Schneider, M. Narandzić, M. Milojević, A. Hong, J. Ylitalo, V. Holappa, M. Alatossava, R. Bultitude, Y. Jong, T. Rautiainen, *Winner II Channel Models*, IST-4-027756 WINNER II, Deliverable D1.1.2 V1.2, Sep. 2007. Available in: (https://cept.org/files/8339/winner2%20-%20final%20report.pdf).

[LSTA16] LS Telcom AG, *Coexistence of GSM-R with other Communication Systems / ERA 2015 04 2 SC,* D5 FINAL REPORT*,* Jul. 2016. Available in: (https://www.era.europa.eu/sites/default/files/library/docs/studies/ls_telcom_study_on_co-existence_of_gsm-r_and_other_radio_technologies_in_the_current_railway_radio_spectrum_en.pdf).

[MERA07] MERAKI, *802.11n Technology*, White Paper, Feb. 2007. Available in: (https://www.skyloft-networks.com/pdf/meraki_whitepaper_802_11n.pdf).

[MICN15] MIC Nordic, *GSM-R Protection Filter (Advanced world class RF-filter),* 2015. Available in: (http://www.micnordic.se/wp-content/uploads/2016/05/GSM-R-Filter-2.pdf).

[NAIN19] National Instruments – NI (Introduction to 802.11ax High-Efficiency Wireless). Available in: (https://www.ni.com/pt-pt/innovations/white-papers/16/introduction-to-802-11ax-high-efficiency-wireless.html). [Accessed in Oct. 2019].

[PaGG14] S. Patel, S. Gupta, D. Ghodgaonkar, “Analysis of Nonlinear Effects on Operation of Low Noise Amplifier for Satellite Scatterometer”, in *2014 International Conference on Computational Intelligence and Communication Networks*, Bhopal, India, 2014. Available in: (https://ieeexplore.ieee.org/document/7065452).

[PALA15] C. Pinedo, M. Aguado, I. Lopez, J. Astorga, “Modelling and Simulation of ERTMS for Current and Future Mobile Technologies”, *International Journal of Vehicular Technology*, Vol.15, Article ID 912417, Nov. 2015. Available in: (https://www.researchgate.net/publication/287215000_Modelling_and_Simulation_of_ERTMS_for_Current_and_Future_Mobile_Technologies).

[Palu13] M. Palumbo, *Railway Signalling since the birth to ERTMS*, Italy, Nov. 2013. Available in: (http://www.railwaysignalling.eu/wp-content/uploads/2014/06/Railway_Signalling_since_birth_to_ERTMS.pdf).

[PuTa09] L. Pushparatnam, T. Taylor, *Overview of GSM-R*, GSM-R Implementation and Procurement Guide, UIC, Paris, France, 2009. Available in: (https://uic.org/IMG/pdf/2009gsm-r_guide.pdf).

[Rahn08] M. Rahnema, *UMTS Network Planning, Optimization, and Inter-Operation with GSM*,

Wiley-IEEE Press, USA, 2008. Available in: (hhttps://books.google.pt/books?id=qVhf1rElNe4C&pg=PA53&lpg=PA53&dq=two+slope+model+hata&source=bl&ots=-J_v5J-pzU&sig=ACfU3U3c-GrdoqiWZF2rbqDRCWCMkCalzw&hl=pt-PT&sa=X&ved=2ahUKEwiX_tr2hq7qAhWKDmMBHbIFAnYQ6AEwCnoECAsQAQ#v=onepage&q=two%20slope%20model%20hata&f=false).

[RGIN19] Railway Gazette International (EU invites proposals for next round of Connecting Europe Facility funding). Available in: (https://www.railwaygazette.com/policy/eu-invites-proposals-for-next-round-of-connecting-europe-facility-funding/41601.article). [Accessed in Dec. 2019].

[SAMS19] SAMSUNG - World's First LTE-Railway Service on High-speed Train Goes Live in Korea, Supplied by Samsung and KT. Available in: (https://www.samsung.com/global/business/networks/insights/press-release/worlds-first-lte-railway-service-on-high-speed-train-goes-live-in-korea-supplied-by-samsung-and-kt/). [Accessed in Dec. 2019].

[Sarf08] R. Sarfati, *Achieving a successful GSM-R radio plan*, Issue 4 2008, Aug. 2008. Available in: (https://www.globalrailwayreview.com/article/648/achieving-a-successful-gsm-r-radio-plan/).

[Smit17] K. Smith, “Beyond GSM-R: the future of railway radio”, *IRJ - International Railway Journal*, Mar. 2017. Available in: (https://www.railjournal.com/in_depth/beyond-gsm-r-the-future-of-railway-radio).

[SnSo12] A. Sniady, J. Soler, “An overview of GSM-R technology and its shortcomings”, *in 12th International Conference on ITS Telecommunications*, Taipei, Taiwan, Nov. 2012. Available in: (https://ieeexplore.ieee.org/document/6425256).

[Sour13] J.A.F. Soure, *Implementation of GSM-R system in the national railway network – Pilot-project* (Portuguese), M.Sc. thesis, Instituto Superior de Engenharia de Coimbra, Coimbra, Portugal, Oct. 2013. Available in: (https://comum.rcaap.pt/handle/10400.26/13547).

[SuMi15] M. Sumila, A. Miszkiewicz, “Analysis of the Problem of Interference of the Public Network Operators to GSM-R”, J. Mikulski (ed.), *Tools of Transport Telematics: 15th International Conference on Transport Systems Telematics*, TST 2015, Wrocław, Poland, 2015. Available in: (https://link.springer.com/chapter/10.1007/978-3-319-24577-5_25).

[Sumi16a] M. Sumila, “Risk Analysis of Interference Railway GSM-R System in Polish Conditions”, in W. Zamojski, J. Mazurkiewicz, J. Sugier., T. Walkowiak, and J. Kacprzyk (ed.), *Dependability Engineering and Complex Systems: Proceedings of the Eleventh International Conference on Dependability and Complex Systems DepCoS-RELCOMEX*., Brunów, Poland, 2016. Available in: (https://link.springer.com/chapter/10.1007/978-3-319-39639-2_41).

[Sumi16b] M. Sumila, “Risk Analysis of Railway Workers Due to Interference into GSM-R System by

MFCN", in J. Mikulski (ed.), *Challenge of Transport Telematics: 16th International Conference on Transport Systems Telematics, TST 2016,* Katowice-Ustroń, Poland, 2016. Available in: (https://link.springer.com/chapter/10.1007/978-3-319-49646-7_18).

[THAL19] Thales (European Train Control System (ETCS)). Available in: (https://www.thales-group.com/en/european-train-control-system-etcs). [Accessed in Nov. 2019].

[TrSK18] Trafikverket, SNCF Réseau, Kapsch CarrierCom, *FRMCS coexistence with GSM-R in the UIC/E-UIC band*, Future Railway Mobile Communication System UIC Group for Frequency Aspects (UGFA), Document No. O-8789, Jan. 2018. Available in: (https://docplayer.net/81713457-Future-railway-mobile-communication-system-uic-group-for-frequency-aspects-ugfa.html).

[UICG19] UIC - International Union of Railways (GSM-R). Available in: (https://uic.org/rail-system/gsm-r/). [Accessed in Oct. 2019].

[UICF19] UIC - International Union of Railways (FRMCS). Available in: (https://uic.org/rail-system/frmcs/). [Accessed in Dec. 2019].

[Vere18] U. Vered, *Intersystem EMC Analysis, Interference, and Solutions*, Artech House Publishers, Norwood, USA, 2018. Available in: (https://books.google.pt/books?id=SfF5DwAAQBAJ&pg=PA35&hl=pt-PT&source=gbs_toc_r&cad=3#v=onepage&q&f=false).

[Wolf18] A. Wolf, *D4.1 Technological Forces and Railway Performance Conditions,* Technical Viability Analysis*,* Mistral – Communication Systems For Next-Generation Railways, Apr. 2018. Available in: (https://projects.shift2rail.org/download.aspx?id=a2d32c6b-b31e-4de8-b484-ccfaf32d7f8c).

[Zhan05] M. Zhang, *System and Circuit Design Techniques For WLAN-Enabled Multi-Standard Receiver*, Ph.D. thesis, The Ohio State University, USA, 2005. Available in: (https://etd.ohiolink.edu/!etd.send_file%3Faccession%3Dosu1131432639%26disposition%3Dinline).